

7-65

**INDUSTRIAL PREPAREDNESS MEASURE:  
STUDY OF IMPROVED METHODS OF  
DRYING CASTING POWDER**

**25 MARCH 1965**

STAYING POWER OF THE ... FROM ...

**U. S. NAVAL PROPELLANT PLANT · INDIAN HEAD, MARYLAND**

4 6 4 5 7 4

PRODUCTION DEPARTMENT

INDUSTRIAL PREPAREDNESS MEASURE:  
STUDY OF IMPROVED METHODS OF DRYING CASTING POWDER

By  
J. E. Geist

25 March 1965

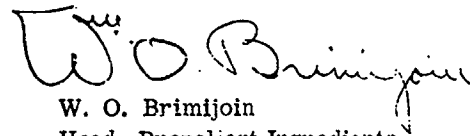
U. S. NAVAL PROPELLANT PLANT  
Indian Head, Maryland

O. F. DREYER  
Captain, USNavy  
Commanding Officer

JOE L. BROWNING  
Technical Director

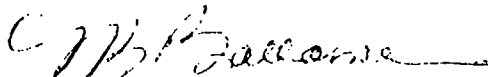
## FOREWORD

This report is a summary of the results obtained in accomplishing the objectives of the Improvement Study of Casting-Powder Drying Methods. Funds for this program were provided by the Bureau of Naval Weapons on Project Order 2-0010, Subhead . 1925, dated 11 January 1962.



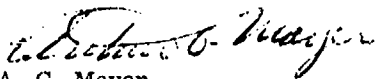
W. O. Brimjoin  
Head, Propellant Ingredients  
Division

Approved by:



N. B. Ballance  
Chief, Production Engineer

Released by:



A. G. Mayer  
Director, Production Department

## CONTENTS

<u>Headings</u>	<u>Page</u>
Foreword _____	iii
Abstract _____	vii
Summary _____	1
Introduction _____	3
Background _____	3
Discussion _____	5
Appendix _____	23

## FIGURES

1. Flow Diagram for Manufacturing Casting Powder _____	4
2. Schematic of Equipment for Sweetie Barrel Studies _____	5
3. Drying Rate Curve for Sweetie Barrel Drying Studies With ABL 2056D Casting Powder (Studies 2 and 3) _____	7
4. Drying Rate Curve for Sweetie Barrel Drying Studies With ABL 2056D Casting Powder (Studies 6 and 7) _____	8
5. Drying Rate Curve for Sweetie Barrel Drying Studies With ABI, 2056D Casting Powder (Study 12) _____	9
6. Schematic of Equipment for Bed-Drying Studies _____	10
7. Drying Rate Curves for Bed-Drying Studies (Studies 13, 15, and 16) _____	12
8. Drying Rate Curves for Bed-Drying Studies With ABL 2523 Casting Powder (Studies 14 and 17) _____	13
9. Schematic of Equipment for Roto-Louvre Dryer Studies _____	14
10. Drying Rate Curves for Roto-Louvre Dryer Studies With ABL 2434 Casting Powder (Studies 18 and 19) _____	16
11. Drying Rate Curves for Roto-Louvre Dryer Studies With ABL 1362 Casting Powder (Studies 20 and 21) _____	17
12. Drying Rate Curves for Roto-Louvre Dryer Studies With ABL 2423 Casting Powder (Studies 22 and 23) _____	18
13. Drying Rate Curves for Roto-Louvre Dryer Studies With ABL 2523 Casting Powder (Studies 24 and 25) _____	19
14. Recommended Dielectric Dryer (Pilot Plant Unit) _____	21

TABLES

I. Data From Sweetie Barrel Drying Studies With ABL 2056D Casting Powder _____	6
II. Data From Bed-Drying Studies _____	11
III. Data From Roto-Louvre Dryer Studies _____	15
IV. Economic Study for Dielectric Drying of Casting Powder _____	20

## ABSTRACT

Four methods of drying casting powder were studied, namely "sweetie" barrel, bed drying, Roto-louvre, and dielectric. Of the methods studied, the dielectric drying offers the most advantages in regard to safety, adaptability to remote and continuous processing, drying time, and operating cost. Estimated annual savings of \$178,260 may be obtained by using dielectric drying in place of the present dryhouse method.

## SUMMARY

Initial studies were made of a method by which the glazing and drying of casting powder could be accomplished simultaneously. Heated air at 160° F was directed into a "sweetie" barrel and onto 24 pounds of ABL 2056D casting powder while the barrel rotated. During the process, graphite was added in an attempt to glaze and dry the powder in one operation. This effort was abandoned, since the required drying time was estimated to be more than doubled. During part of this study a sonic generator was used to break down the molecular attraction between the moisture and the powder. The sonic generator reduced the required drying time by 33%. Drying was accomplished under optimum conditions within 7 hours as compared to 40 hours in a dryhouse.

Studies were conducted on casting powder dried by the bed-drying method. Graphical extrapolation of test data indicated more than 18 hours would be required to dry ABL 705 casting powder with 150° F air circulated through a boiling bed, 4 inches deep, whereas 14 days would be required to dry this powder in a dryhouse. A 13-inch bed of 2056D casting powder was dried within 6 hours by the bed-drying method.

A bench-model Roto-louvre dryer, rented from the Link Belt Company, was evaluated for drying casting powder. More than 18 hours were estimated to be required to dry a double-base formulation, ABL 2434, with 145° F air circulated through a bed tumbling at 5 rpm. The sonic generator was again found to increase the drying rate by 33%. ABL 2523 casting powder was satisfactorily dried within 5 hours with the generator on and with 150° F air circulated through the bed at 18 c.m. With air circulated at 30 cfm, more rapid drying was obtained, but the nitroglycerin content of the powder was reduced below the specified minimum. Based on the data obtained, the Link Belt Company recommended a batch-type dryer for drying the ABL 2523 casting powder because of the difficulty in controlling the removal of moisture at a slow speed and the long retention time required of powder in a continuous dryer (4 to 8 hours).

Studies on dielectric drying of ABL 705 double-base casting powder were conducted by contract with Pratt and Whitney. Their report shows that dielectric heating is a feasible technique for drying casting powder and that it gives drying times as short as 5 hours. ABL 705 powder requires up to 14 days in a dryhouse. An estimated \$178,260 in annual savings in handling and personnel costs can be realized by using dielectric drying in place of the present dryhouse method. Calculations were based on figures from the Pratt and Whitney report and the projected production for 1969.

The results of these studies to improve the method of drying of casting powder led to the following conclusions and recommendations.

### Conclusions:

Glazing casting powder while drying with heated air more than doubles the required drying time. The use of a sonic generator increases the drying rate by 33%.

ABL 2523 casting powder was satisfactorily dried in a bench model Link Belt Company Roto-louvre dryer within 5 hours as compared to 40 hours in a conventional dryhouse. The Link Belt Company recommends a batch dryer for drying ABL 2523 powder because of the difficulty in controlling the removal of moisture at a slow speed and the long retention time required of powder in a continuous dryer.

A study contracted with Pratt and Whitney proves the feasibility of drying double-base casting powder by dielectric heating. ABL 705 casting powder, which requires up to 14 days to dry in a dryhouse, was dielectrically dried in 5 hours. An economic study based on the Pratt and Whitney findings estimates an annual savings of \$178,260 may be obtained by using dielectric drying in place of the present dryhouse method. Dielectric drying can be done remotely and continuously. It would reduce handling of powder and eliminate the hazardous dryhouse operations.

### Recommendations:

Further development work on the dielectric-drying method is recommended. Of the methods studied, it offers the most advantages in regard to safety, adaptability to remote and continuous processing, drying time, and operating cost. A dielectric-drying pilot plant is therefore recommended to permit gathering information on drying temperatures, power programming cycle, electrode configuration, etc. The basic equipment would consist of a series of independent electrodes positioned along movable beds of powder. The power to the electrodes would be programmed to give the highest power input to the greenest powder in order to bring it to the desired drying temperature in the shortest possible time. Downstream electrodes would be programmed at lower power levels to maintain the partially dried powder at the desired drying temperature.

To control the dielectric-drying process and to provide adequate safety interlocks, instruments must be provided. A study of existing instruments and their adaptability for use in explosive processing is therefore recommended. As an example, onstream analysis to measure and control the final moisture in paper is a routine procedure today. The end item of the study would be a remote monitoring system for a dielectric-drying facility.

The estimated cost to construct and evaluate a dielectric-drying pilot plant is \$31,844. Approximately 17 months from the date of funding would be required to complete the evaluation.

## INTRODUCTION

The objectives of this study were to improve the present method of drying casting powder, investigate the feasibility of glazing the powder concurrently with drying, and to analyze the improved drying process in order to specify the type of processing equipment necessary for continuous drying of casting powder.

Four methods of drying casting powder were studied, namely, "sweetie" barrel, bed drying, Roto-louvre, and dielectric. The methods studied were conducted at NPP with the exception of the dielectric method which was contracted with the Pratt and Whitney Division of Fairbanks Whitney Corporation.

## BACKGROUND

A flow diagram of the operations for manufacturing casting powder is shown in Figure 1. In the powder mixing operation, solvents such as ether, alcohol, and acetone are dispersed into the matrix resulting in a gel-like structure. The powder is then blocked and extruded through dies which form strands. These strands are cut to a desired length to produce uniform grains. The grains are placed on trays in drying carts which are transported to a dryhouse. Heated air at 140° F is passed through the dryhouse and about the trays of grains for a period of 2 to 14 days. The required time varies with the various powder formulations and size of the grain.

During the drying process, evaporation commences on the surface of the grains where the temperature is highest. The surface skin then shrinks and hardens causing a drop in diffusivity. This sets up a barrier against removal of the interior solvent, which is known as case-hardening, and accounts for the required long drying times. After drying, the grains are emptied manually from the trays into containers and stored in magazines while waiting to be glazed. Manual handling is dangerous because of the buildup of electrostatic charge on the grains.

The casting powder is glazed with graphite to form a conductive coating which prevents accumulation of static charge and improves its burning characteristics. The operation is conducted in a sweetie barrel where graphite is added to the casting powder and tumbled for 2 to 3 hours. The operation is controlled remotely and monitored by closed-circuit television.

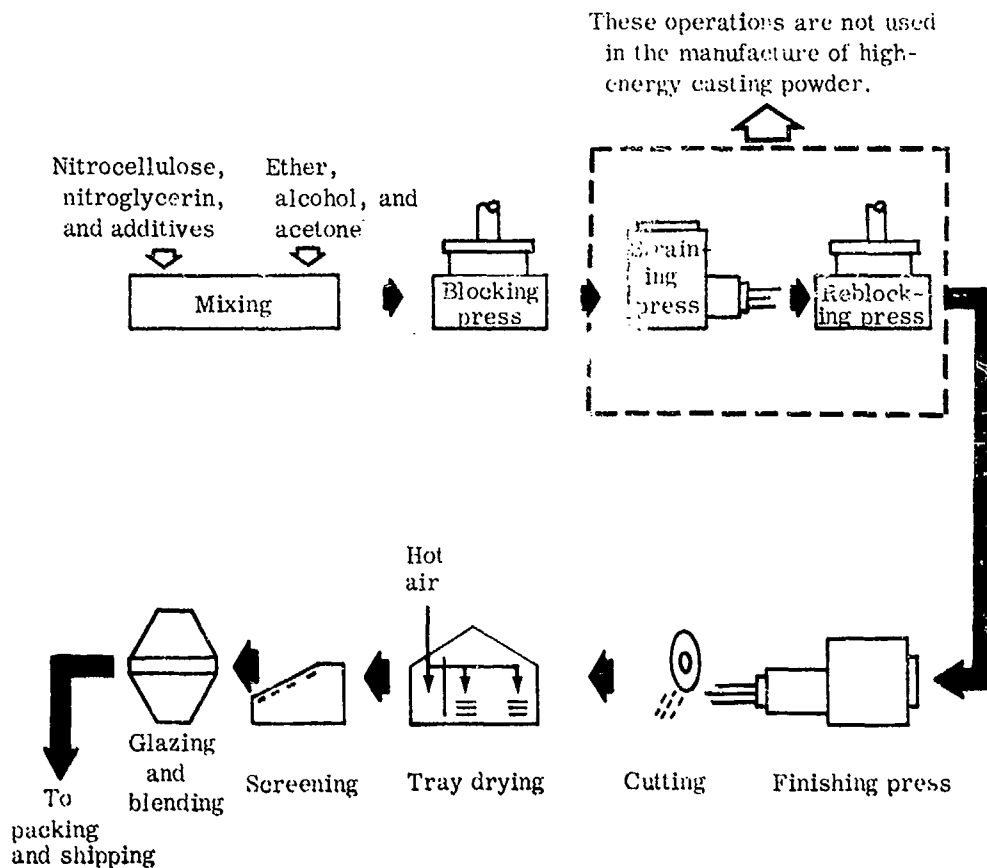


FIGURE 1. FLOW DIAGRAM FOR MANUFACTURING CASTING POWDER

After the grains are glazed, they are transferred pneumatically to the screening house where dust and oversize grains are removed. The proper size grains are collected and placed in magazine storage while waiting to be blended. Blending is performed in a double-conical blender. Next the grains are packed automatically into 125-pound shipping containers.

When processing ABL 2523 casting powder (for second-stage A3 Polaris), the grains are green-tumbled in a sweetie barrel before being dried. The tumbling increases the screen-loading density of the grains and makes them more uniform.

## DISCUSSION

### Sweetie Barrel Drying Method:

Initial studies were conducted of a method for drying casting powder in a sweetie barrel since glazing therein could be readily conducted concurrently with drying. As shown in Figure 2, heated air was directed onto approximately 24 pounds of ABL 2056D casting powder while the barrel was rotated. The variables and data of the studies are given in Table I.

The procedures for studies 2 and 3 were identical except for the addition of 4 grams of graphite during study 3. As shown in Figure 3, the required drying time was estimated to be more than doubled by the addition of the graphite; therefore, further effort to combine the drying and glazing processes was discontinued. For these two studies the casting powder was allowed to dry for 3 hours. For later studies the drying time was increased to 4, 5, and, finally, 6 and 7 hours as it became apparent that longer drying times were required.

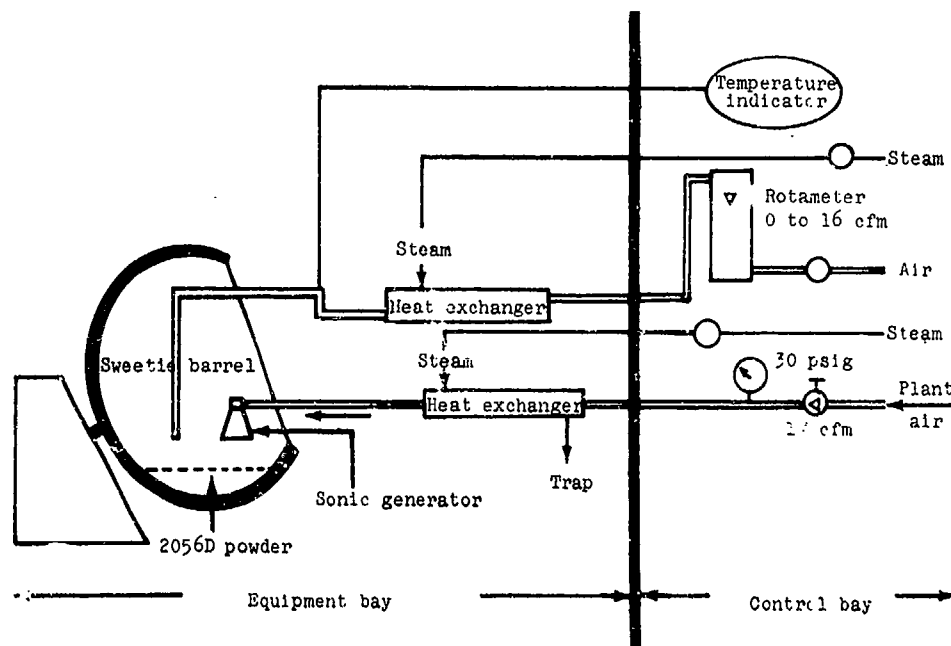


FIGURE 2. SCHEMATIC OF EQUIPMENT FOR SWEETIE BARREL STUDIES

Table I  
DATA FROM SWEETIE BARREL DRYING STUDIES WITH ABL 2056D CASTING POWDER

Study no.	Jacket temperature (°F)	Casting powder (lb)	Barrel speed (rpm)	Air flow (cfm)	Average temperature (°F)	Sonic generator	Total volatiles (%)								Remarks		
							0 hr	1 hr	2 hr	3 hr	4 hr	5 hr	6 hr	7 hr			
1	80	24	8	8	126	Off	9.33	7.18	6.10	5.32	-	-	-	-	-	-	-
2	120	24	8	16	158	Off	9.66	4.21	3.41	2.37	-	-	-	-	-	-	-
3	120	24	8	16	159	Off	9.41	6.69	5.68	4.40	-	-	-	-	-	-	4 Grams graphite added
4	140	24	8	16	155	Off	10.16	4.06	3.32	2.38	1.56	1.76	-	-	-	-	-
5	105	24	16	15	160	Off	9.95	6.29	4.32	3.21	2.83	1.92	-	-	-	-	Poor control jacket temperature
6	140	24	24	16	160	Off	9.53	3.53	2.36	1.92	1.57	1.44	-	-	-	-	-
7	140	25	24	16	160	On <sup>1</sup>	8.55	3.45	2.27	1.64	1.29	0.76	-	-	-	-	-
8	140	25	24	16	160	On <sup>1</sup>	8.70	3.23	1.89	1.22	0.64	0.78	0.96	-	-	-	-
9	140	25	24	15	160	On <sup>1</sup>	6.88	2.93	1.99	1.57	1.51	0.95	1.09	-	-	-	Baffle added
10	140	25	24	15	160	On <sup>2</sup>	8.11	4.17	2.39	1.47	1.22	0.59	-	-	-	-	Baffle added
11	140	25	24	16	165	On <sup>2</sup>	10.25	2.72	1.50	1.02	0.80	0.67	0.57	-	-	-	Baffle added
12	140	25	24	16	160	On <sup>2</sup>	8.01	3.09	1.80	1.40	1.25	0.87	0.55	0.32	-	-	Baffle added

<sup>1</sup> Air unheated.

<sup>2</sup> Air heated.

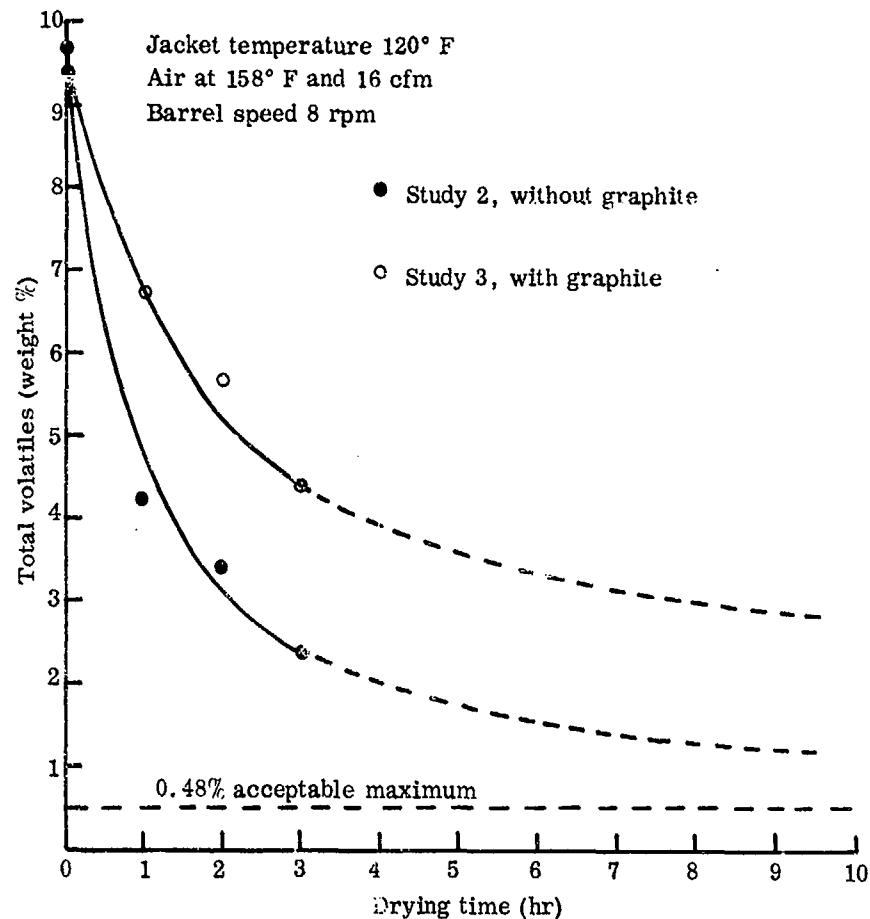


FIGURE 3. DRYING RATE CURVE FOR SWEETIE BARREL DRYING STUDIES WITH ABL 2056D CASTING POWDER (STUDIES 2 AND 3)

The jacket temperature of the barrel was increased to 140° F in study 4, and the rotational speed was increased to 24 rpm in study 6. In each case the drying rate was increased. Studies 7 through 12 were made with the use of a sonic generator operated approximately 10 inches above the surface of the powder. The generator, which was purchased from Branson Instruments Inc., produced sound waves at 11.6 kilocycles and 161 decibels to break down molecular attraction between the moisture and the powder. The procedures for studies 6 and 7 were identical except for the use of the sonic generator. As shown in Figure 4, 8 hours would be required for satisfactory drying with the sonic generator as compared to over 12 hours without it.

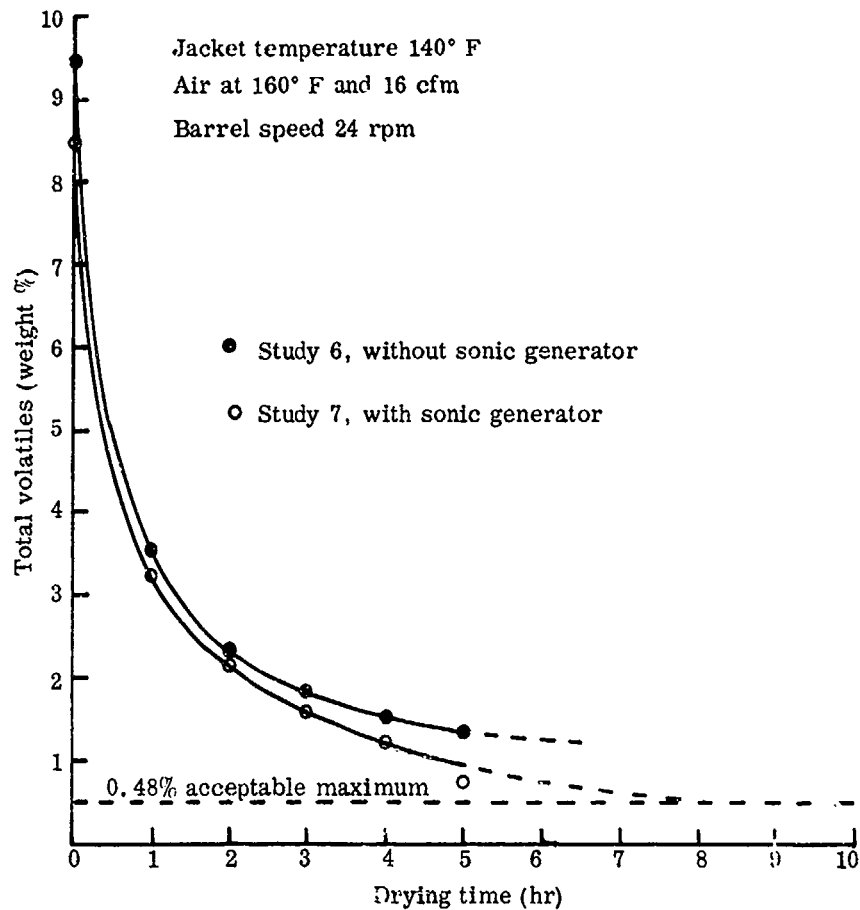


FIGURE 4. DRYING RATE CURVE FOR SWEETIE BARREL DRYING STUDIES WITH ABL 2056D CASTING POWDER (STUDIES 6 AND 7)

A baffle was placed in the barrel to increase the agitation of the powder for studies 9 to 12. However, this decreased the drying rate, which was probably due to decreased contact between the powder and the heated jacket.

Heated air (approximately 150° F) was used to operate the sonic generator starting with study 10. This increased the drying rate. ABL 2056D casting powder was dried below the acceptable maximum volatile content within 7 hours during study 12. The drying curve for study 12 is shown in Figure 5.

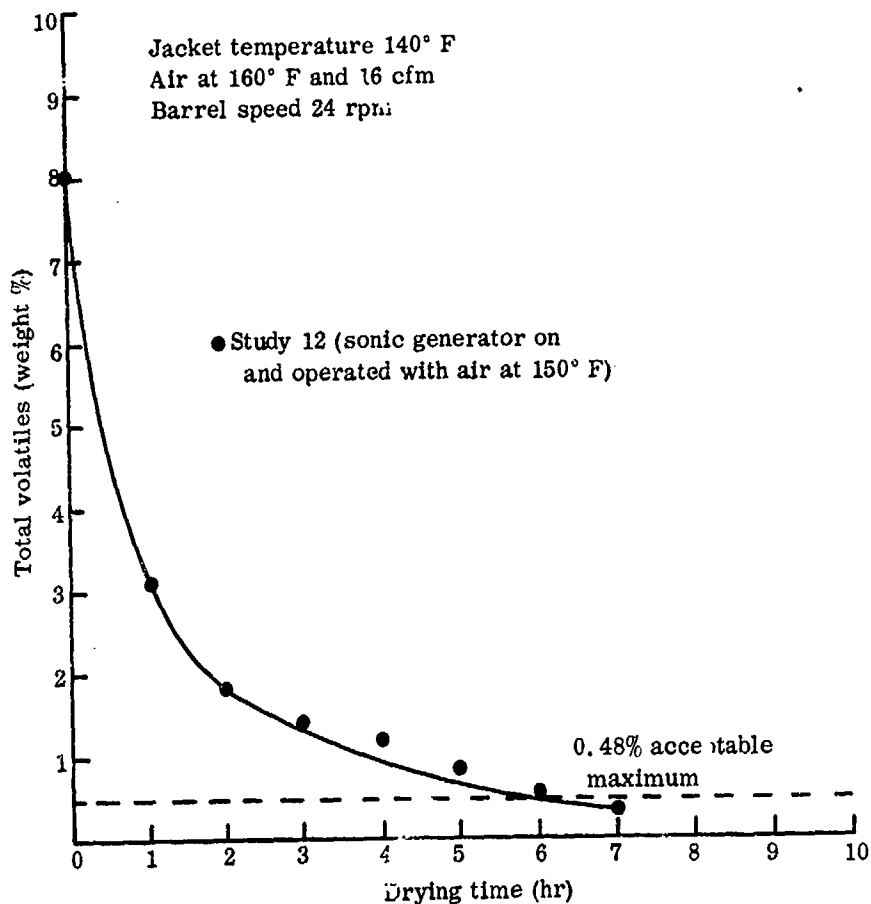


FIGURE 5. DRYING RATE CURVE FOR SWEETIE BARREL DRYING STUDIES WITH ABL 2056D CASTING POWDER (STUDY 12)

The data from these sweetie barrel studies were reviewed with the Patterson-Kelley Company, East Stroudsburg, Pennsylvania. The use of a jacketed Patterson-Kelley continuous solids-solids blender, which has a tumbling action somewhat similar to that of the sweetie barrel, was considered. However, this blender could not be used as it has a material residence time of only a few minutes and the ABL 2056D casting powder required 7 hours to dry in the sweetie barrel studies. This casting powder is one of the more rapid drying formulations and requires approximately 40 hours in a dryhouse.

Bed-Drying Method:

A series of studies was conducted on casting powder dried by the bed-drying method. Heated air was circulated through a bed of casting powder lying on a porous stainless steel disc. Since the bed was contained within a 4-inch-diameter pipe, only a limited number of samples could be taken for analysis in each study. A schematic of the equipment is shown in Figure 6, and the data are given in Table II.

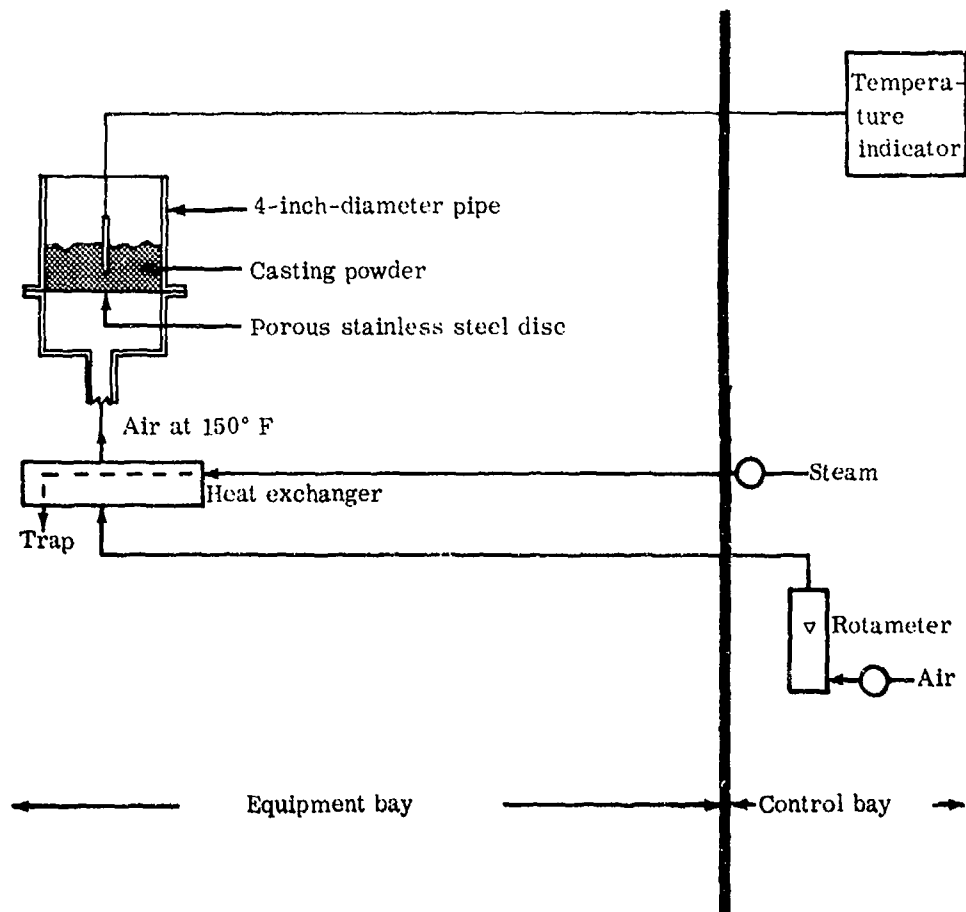


FIGURE 6. SCHEMATIC OF EQUIPMENT FOR BED-DRYING STUDIES

Table II  
DATA FROM BED-DRYING STUDIES

Study no.	Casting powder	Air (cfm)	Air (°F)	Initial bed height (in.)	Bed condition	Total volatiles (%)								
						0 hr	1 hr	2 hr	3 hr	4 hr	5 hr	6 hr	7 hr	
13	ABL 1362	5	150	4	Static	26.85	-	-	-	-	-	-	2.70	-
14	ABL 2523	5	150	4	Static	9.61	-	-	-	0.31	-	-	0.20	-
15	ABL 705	6	147	4	Boiling	24.27	-	-	-	4.47	-	-	3.86	-
16	ABL 705	7	152	4	Boiling	25.91	-	-	-	-	3.86	-	-	3.40
17	ABL 2523	5	150	13	Static	6.00	-	-	-	0.77	-	-	0.27	-

The results with double-base formulations, ABL 1362 and ABL 705 (studies 13, 15, and 16) were not encouraging as shown in Figure 7. By extrapolation, over 18 hours would be required to dry ABL 705 casting powder by circulating air at 152° F through a boiling bed 4 inches high. Up to 14 days are required to dry these formulations in a dryhouse.

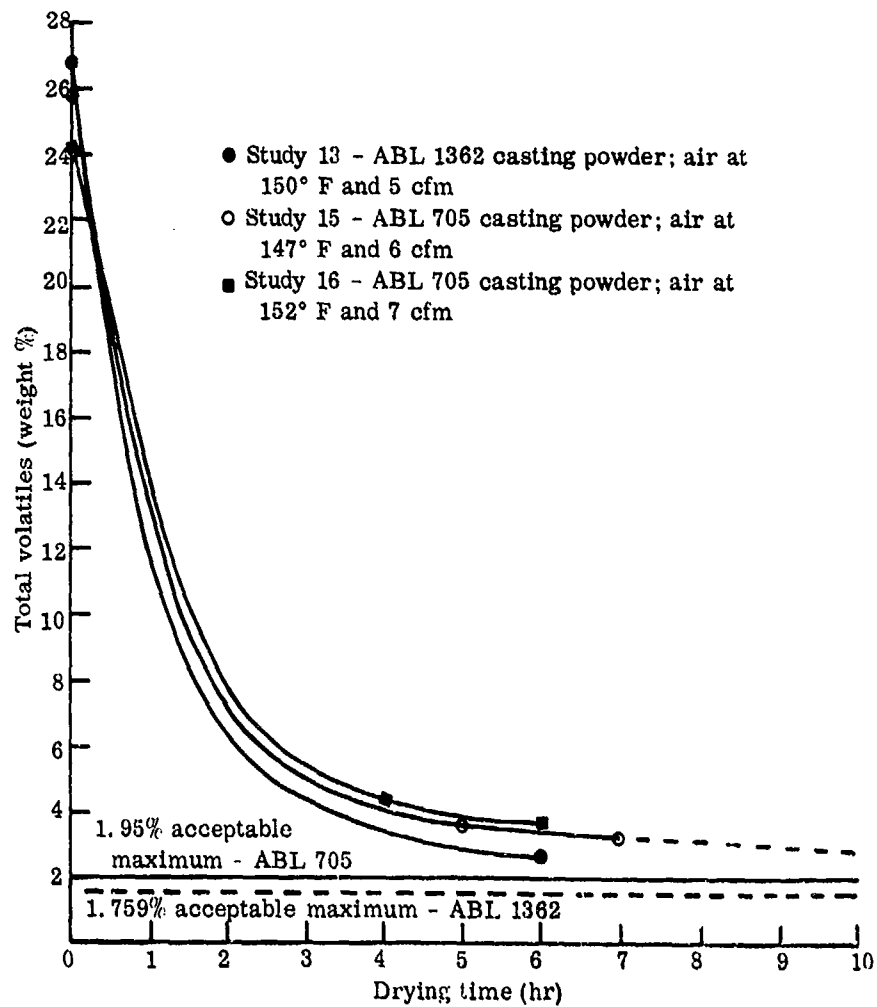


FIGURE 7. DRYING RATE CURVES FOR BED-DRYING STUDIES (STUDIES 13, 15, AND 16)

Encouraging results were obtained with ABL 2523 casting powder which requires approximately 40 hours in a dryhouse. In studies 14 and 17, the powder was dried below the acceptable maximum volatile content within 4 and 6 hours, respectively. Increasing the bed height from 4 to 13 inches accounted for the required longer drying time of study 17. Both studies were made with 150° F air circulated at the rate of 5 cfm. The results are shown in Figure 8.

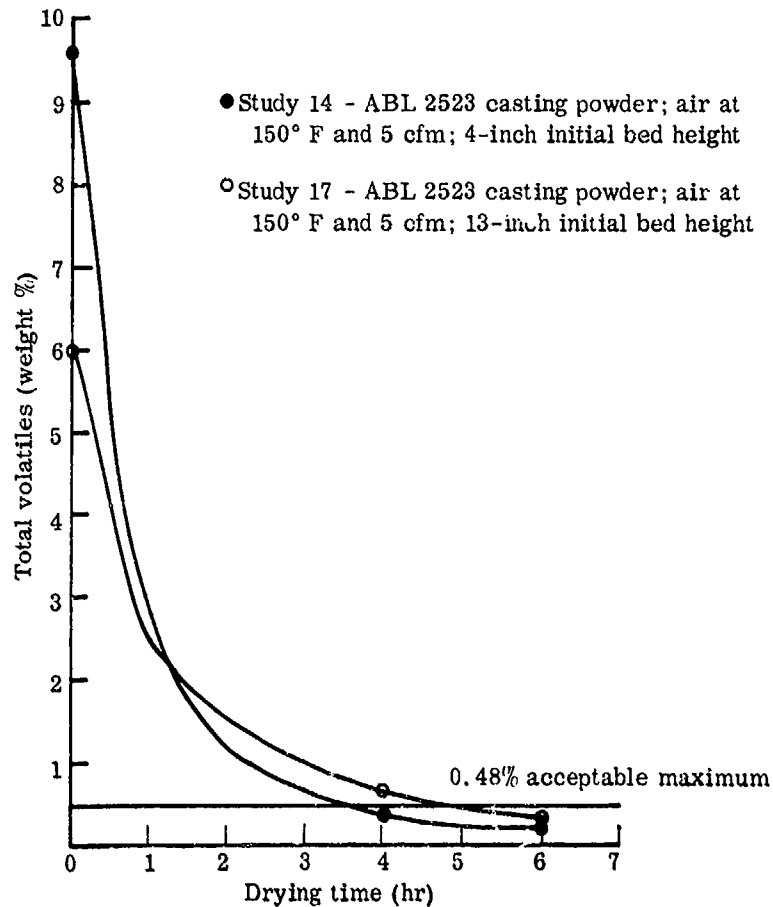


FIGURE 8. DRYING RATE CURVES FOR BED-DRYING STUDIES WITH ABL 2523 CASTING POWDER (STUDIES 14 AND 17)

The effect of the high air flow through the bed on the nitroglycerin content of the grains was not determined. Evaporation was suspected, since a yellow film was noted on the pipe wall above the bed upon completion of the studies. The evaporation of nitroglycerin, as a function of air flow, was investigated during the Roto-louvre dryer studies. These bed-drying studies were concluded upon receipt of a bench model Roto-louvre dryer in which air is circulated through the bed (as it was in these bed studies) while the bed is gently tumbled.

Roto-Louvre Drying Method:

Roto-louvre dryers are manufactured exclusively by the Link Belt Company. Commercial units may be batch or continuously operated. These dryers are through-circulation type where heated air is introduced beneath the material bed and passes through the bed while it is gently tumbled on rotating louvres. Exhaust gases are removed from the product-discharge end of the rotating cylinder. For purposes of these studies a bench model unit was rented from the Link Belt Company. The bench unit, which was modified by NPP for the safe handling of casting powder, was 16 inches in diameter by 6 inches in depth and held 4 quarts of material. The installation of the dryer with the various auxiliaries and instrumentation is shown in Figure 9.

The data from the studies made with the dryer are given in Table III. Studies made with double-base formulations, ABL 2434 and ABL 1362, were again not encouraging. The first two of this series of studies (18 and 19) were made with ABL 2434. By extrapolation, as shown in Figure 10, over 18 hours would be required to dry this powder with air at 145° F circulating at a rate of 30 cfm through an initial 4 quarts of powder tumbling at 5 rpm.

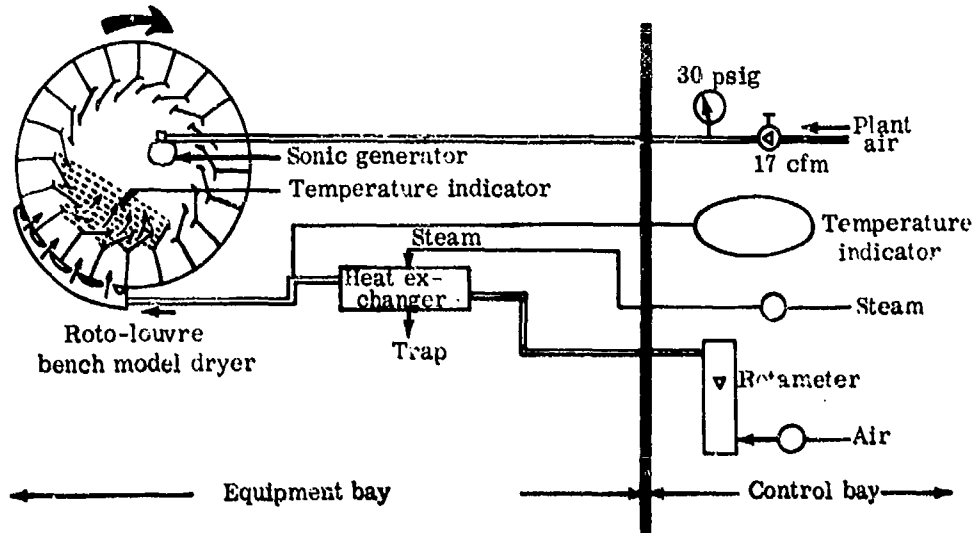


FIGURE 9. SCHEMATIC OF EQUIPMENT FOR ROTO-LOUVRE DRYER STUDIES

Table III  
 DATA FROM ROTO-LOUVRE DRYER STUDIES  
 [Dryer at 5 rpm]

Study no.	Casting powder	Air (cfm)	Air (°F)	Sonic generator	Total volatiles (%)							Final nitroglycerin content (%)	
					0 hr	1 hr	2 hr	3 hr	4 hr	5 hr	6 hr		
18	ABL 2434	30	145	Off	29.0	8.31	6.41	5.64	5.13	4.62	-	-	
19	ABL 2434	30	145	Off	29.0	-	6.42	-	5.04	-	4.50	-	
20	ABL 1362	30	145	Off	28.6	-	-	3.70	-	2.75	-	-	
21	ABL 1362	30	145	On	28.6	-	3.99	-	2.52	-	2.02	-	
22	ABL 2523	30	145	Off	6.84	-	-	1.63	-	0.42	-	-	
23	ABL 2523	30	145	On	7.40	-	-	0.46	-	0.39	-	-	
24	ABL 2523	10	145	On	7.35	2.74	1.65	1.30	0.92	0.81	0.67	8.62	
25	ABL 2523	18	145	On	6.55	1.66	1.02	-	0.50	0.39	-	9.67	
													9.38

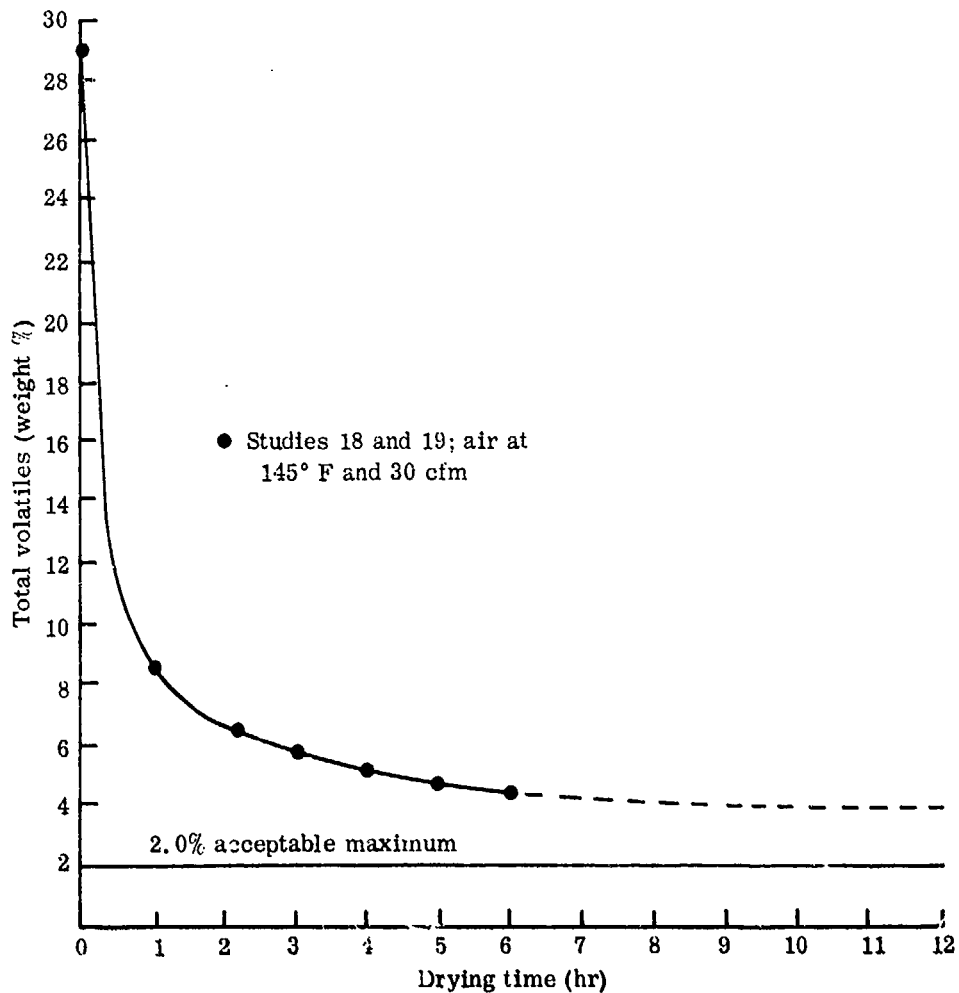


FIGURE 10. DRYING RATE CURVES FOR ROTO-LOUVRE DRYER STUDIES WITH ABL 2434 CASTING POWDER (STUDIES 18 AND 19)

Studies 20 and 21 were made with ABL 1362 casting powder. The operating conditions for these studies were identical (air at 145° F and 30 cfm) except for the use of the sonic generator in study 21. The sonic generator was the same one used in the sweetie barrel studies. By graphical extrapolation, as shown in Figure 11, 8 hours would be required to dry ABL 1362 casting powder with the sonic generator while more than 12 hours would be required without the sonic generator.

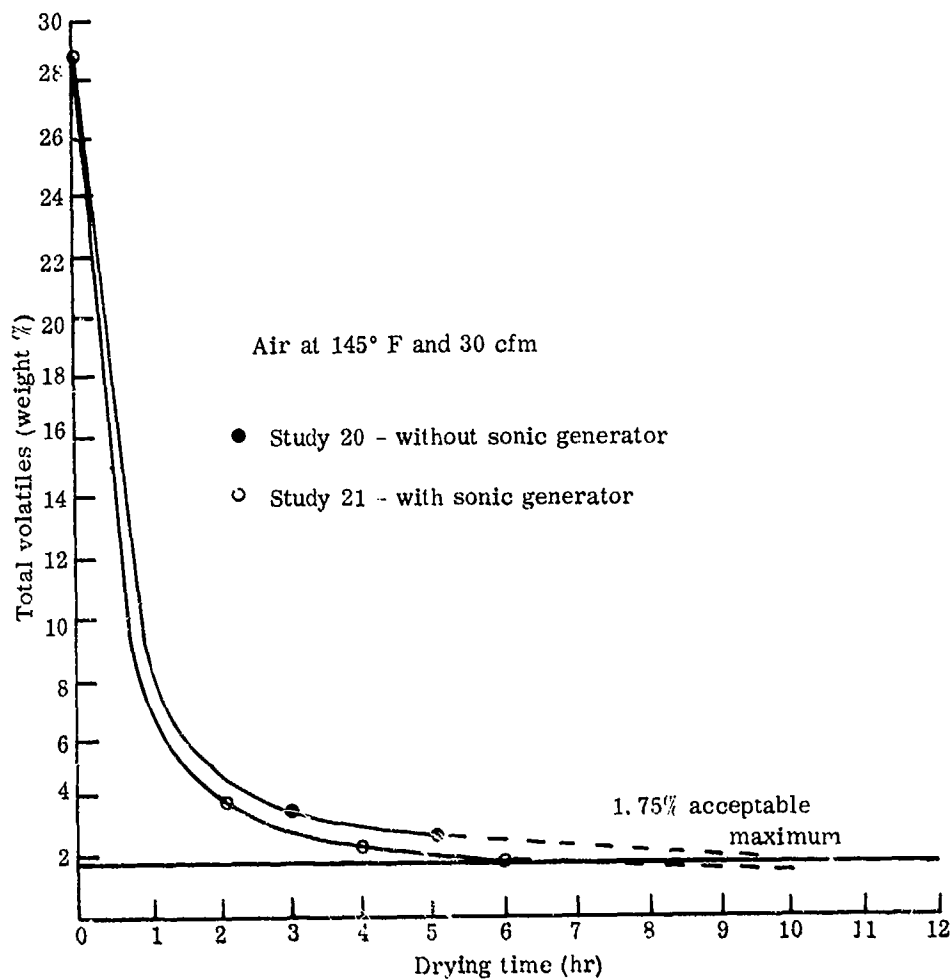


FIGURE 11. DRYING RATE CURVES FOR ROTO-LOUVRE DRYER STUDIES WITH ABL 1362 CASTING POWDER (STUDIES 20 AND 21)

Rapid drying was achieved with ABL 2523 casting powder in studies 22 and 23. Again the operating conditions for these studies were identical (air at 145° F and 30 cfm) except for the use of the sonic generator in study 23. As shown in Figure 12, 5 hours were required to dry the powder without the sonic generator while 3 hours were required with it. However, the nitroglycerin content of the powder was reduced below the specified minimum quantity in both of these studies.

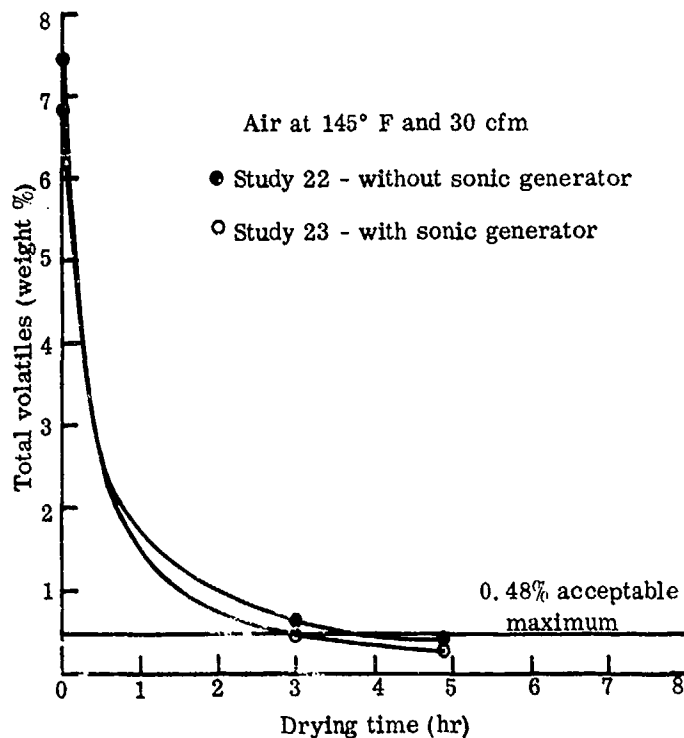


FIGURE 12. DRYING RATE CURVES FOR  
ROTO-LOUVRE DRYER STUDIES WITH  
ABL 2523 CASTING POWDER (STUDIES 22 AND 23)

Studies 24 and 25 were made on ABL 2523 casting powder at reduced air rates of 10 and 18 cfm, respectively. In each study the nitroglycerin content was not reduced below the specified minimum content, but a 0.29% lower nitroglycerin content was obtained at 18 cfm. As shown in Figure 13, satisfactory drying was estimated to require 8 hours during study 24 with air at 10 cfm and 5 hours during study 25 with air at 18 cfm.

The casting powder from study 25 was glazed with graphite and its final screen-loading density was determined to be 1.280; 1.290 is considered to be satisfactory. The low density indicates the advantage of wet-tumbling the powder prior to drying it.

The data from this series of studies were reviewed with the Link Belt Company. For drying ABL 2523 casting powder they recommended a batch-type dryer. A continuous unit was not recommended because of the difficulty in controlling the removal of internal moisture at a slow speed and the resulting long retention time. A specially

constructed 2400-pound-capacity unit with 4 to 8 hours retention time would cost an estimated \$55,000 to \$60,000.

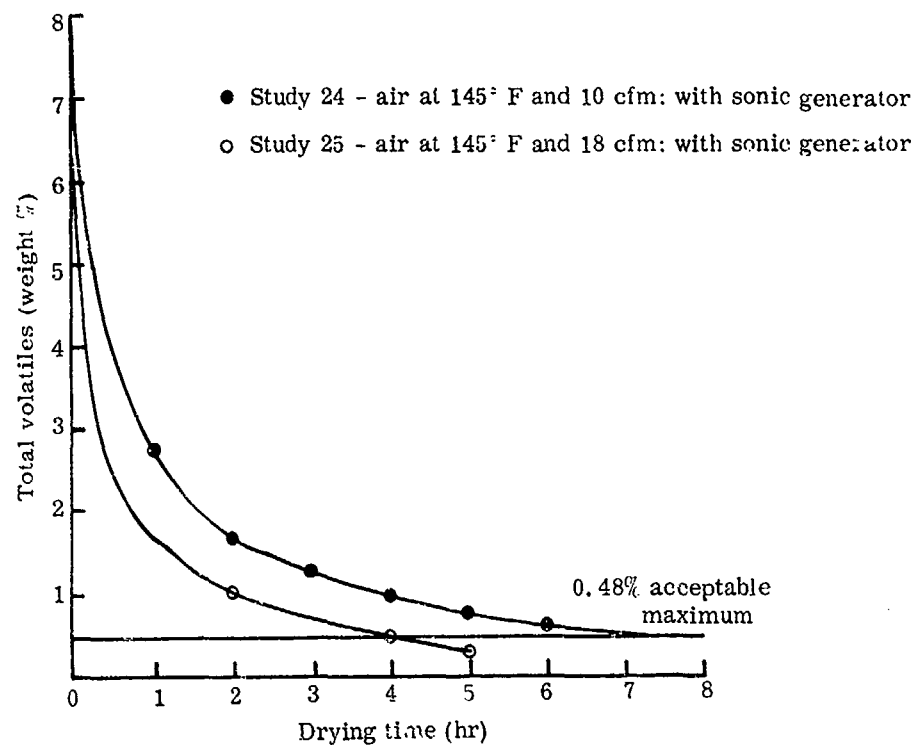


FIGURE 13. DRYING RATE CURVES FOR ROTO-LOUVRE DRYER STUDIES WITH ABL 2523 CASTING POWDER (STUDIES 24 AND 25)

Dielectric Drying Method:

The final report on dielectric-drying studies by Pratt and Whitney is included in the Appendix. An economic study based on the figures in the report is given in Table IV. This study shows that a total saving of \$178,260 for FY-1969 in handling and personnel costs would be obtained by using the dielectric-drying method in place of the present dryhouse method. The FY-1969 savings for drying ABL 2523 casting powder would be \$67,548. A schematic of the basic equipment is shown in Figure 14.

Table IV  
ECONOMIC STUDY FOR DIELECTRIC DRYING OF CASTING POWDER

Casting powder	FY-69 production (lb)	Present drying method			Proposed dielectric-drying method			Estimated savings/year by dielectric-drying method					
		Drying time <sup>1</sup> (hr)	Estimated steam cost	Estimated manpower <sup>2</sup> cost (8 men) <sup>3</sup>	Drying cost/lb	Total estimated drying cost	Drying time <sup>1</sup> (hr)	Estimated power cost	Estimated manpower <sup>2</sup> cost (2 men) <sup>3</sup>	Drying cost/lb	Total estimated drying cost	Power and steam	Manpower
ABL 705	329,371	216	\$2,134	\$60,505	\$0.190	\$62,739	7	\$148	\$26,316	\$0.08	\$26,464	\$1,986	\$34,289
ABL 917	215,959	120	778	33,623	0.187	40,401	-	-	17,136	-	-	-	22,487
ABL 559	95,359	120	340	17,305	0.185	17,645	-	-	7,140	-	-	-	10,165
ABL 1362	427,609	96	1,232	64,300	0.153	65,532	-	-	29,194	-	-	-	34,516
ABL 2434	88,900	168	448	17,211	0.198	17,659	-	-	7,956	-	-	-	9,255
ABL 2523	1,440,000	40	2,650	201,168	0.141	203,818	-	-	133,620	-	-	-	67,548
Total	2,597,238	-	\$7,582	\$400,212	-	\$407,794	-	-	\$221,952	-	-	Approx. \$7,000	\$178,260

<sup>1</sup> Drying time is independent of quantity.

<sup>2</sup> The labor cost used in this study include direct labor at \$3.60/hour (including fringe benefits) and overhead charges at \$9.15/hour.

<sup>3</sup> Includes cost of charging and discharging dryhouse (3 men); transportation cost \$0.18/mile; dryhouse watchmen cost (3 men); and preparing powder in cutting building (2 men).

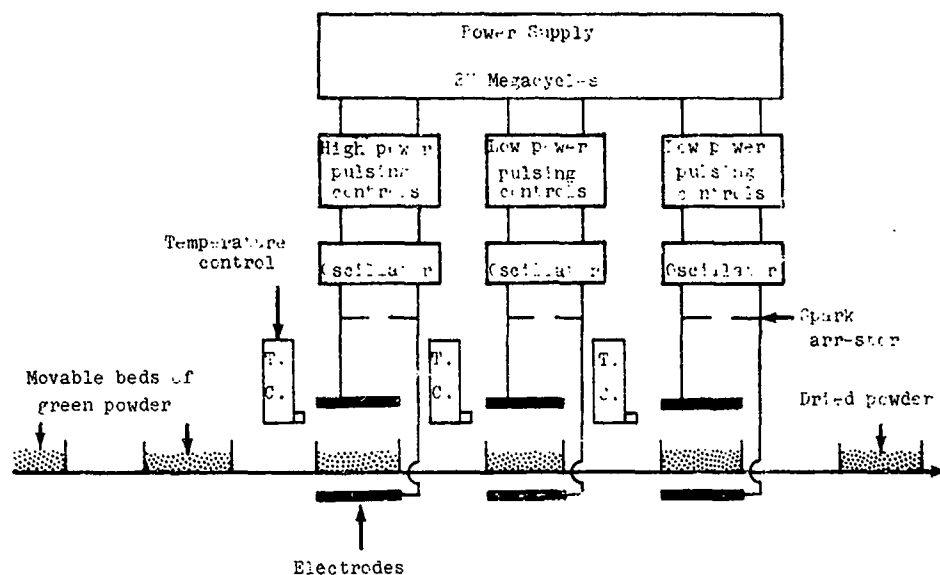


FIGURE 14. RECOMMENDED DIELECTRIC DRYER (PILOT PLANT UNIT)

The estimated cost of a dielectric-drying facility for processing 6,000 pounds per day of ABL 2523 casting powder is \$485,000. This cost includes engineering, utilities, equipment and installation costs for the dielectric dryer, a pneumatic conveyor to transport the casting powder to the dryer, and a covered roller conveyor for movement of the dry casting powder to an existing holding house. A similar facility for processing 6,000 pounds per day of multibase casting powder is estimated to cost \$426,000.

Appendix

This appendix is a reprint of a report prepared by the  
Fairbanks Whitney Corporation, 745 Fifth Avenue, New York, New York

DRYING STUDY OF  
NITROCELLULOSE - BASE PROPELLANT

Contract No. N174-14676 (X)

Project No. 161-50

Prepared For The  
U.S. Naval Propellant Plant  
Indian Head, Maryland

Registered Report No. 4 By J. A. Riveglia  
Issued To Naval Propellant Plant By J. C. Butler

Approved By W. G. Voorhes  
W. G. Voorhes

Approved By A. E. Snyder  
A. E. Snyder

## TABLE OF CONTENTS

1.0	Summary	1
2.0	Purpose	2
3.0	Introduction	3
3.1	Present Drying Process	3
3.2	Advantages of Dielectric Drying	5
3.3	Constant Rate vs. Falling Rate Periods	6
4.0	Technical Discussion	9
4.1	Equipment	9
4.2	Analytical Procedures	10
4.3	Experimental Work	13
4.3.1	Empirical Evaluation of Operating Parameters	13
4.3.2	Difficulty of Removing Ethyl Alcohol From Propellant	22
4.3.3	Electron Micrographs and Microphotographs	24
4.3.4	Differential Thermal Analysis	26
4.4	Mathematical Analysis of the Drying Process	26
5.0	Conclusions	30
6.0	Recommendations	31
	Illustrations	
	Tables	
	References	
	Appendix I	
	Appendix II	
	Appendix III	

## 1.0 Summary

Three dielectric heating techniques were used successfully to dry three to five gram samples of ADL-708 double base propellant to a total volatile content of about 1.8%:

1. Heating the propellant to 190°F for five hours
2. Heating the propellant to 180°F for seven hours
3. Heating the propellant to 170°F for twelve hours.

There was very little nitroglycerine loss with any of these techniques. However, after about three hours drying time, some darkening of the propellant grains was observed adjacent to the thermometer mounted in the propellant bed -- it is believed that this problem would be eliminated if no thermometer were used and if the propellant temperature were measured remotely, as with infrared techniques.

A theoretical mathematical analysis of the drying process was performed based upon the assumption that the drying mechanism is governed by thermal and vapor pressure gradients which establish the viscous flow of solvents through the propellant. The total volatile content versus drying time curve based upon this analysis was compared to a curve obtained from an actual run and the correlation was found to be excellent.

## 2.0 Purpose

The purpose of this program was to evaluate dielectric heating as a technique to obtain rapid drying of ABL-705 double base (nitro-cellulose plus nitroglycerine) propellant.

The double base propellant is made at the U.S. Naval Propellant Plant at Indian Head, Maryland, by the solvent-extrusion process. During the manufacturing process, the propellant is mixed with the volatile solvents ether and alcohol (some water being present in the alcohol) to promote plasticity and is extruded into spaghetti-like cylinders 0.04 inches in diameter which are then cut up into grains 0.04 inches long. The propellant subsequently must be dried from an initial total volatile content of about 33 - 35% to a final value of 1.8% before it can be incorporated in rocket motors.

The present drying process is very slow and requires fourteen days. The propellant is placed on trays in a dry house and is heated by blowing air at 140°F between the trays. Because the hot air contains explosive volatiles after one pass, it must be exhausted without recirculation; this results in excessive heating costs. Furthermore, numerous dry houses are required to match the production rate of propellant. This report will show that the application of dielectric heating can bring a significant reduction in propellant drying time.

### 3.0 Introduction

#### 3.1 Present Drying Process

Free alcohol, ether, and water have high vapor pressures\* at the propellant drying temperature and would evaporate readily. However, because these solvents are dissolved and diffused in a gel, their partial vapor pressures decrease with time as additional solvent is evaporated and thus their evaporation rates decrease. According to Raoult's law, the partial vapor pressure,  $p$ , of the solvent is equal to the vapor pressure,  $p^{\circ}$ , of the pure solvent multiplied by the mole fraction,  $N$ , of the solvent in solution:  $p = N p^{\circ}$ . During the drying operation, the temperature reached inside the grains probably exceeds the boiling points of the ether but does not exceed the boiling points of the alcohol and water. Thus, in its simplest analysis, the problem of drying the propellant to a low total volatile content would remain largely a problem of removal of alcohol and water.

---

<u>* Solvent</u>	<u>Vapor Pressure (<math>p^{\circ}</math>) @ 140°F</u>	<u>Boiling Point</u>
Ethyl alcohol	353 mm of Hg	173°F
Diethyl ether	1760 mm of Hg	94°F
Water	153 mm of Hg	212°F

From Reference 1

It is necessary also to consider the aspects of vapor transport across the body of the grain to the surface. Several mass transport mechanisms may be occurring here:

1. Vaporization and recondensation of liquid and, hence, motion of the vapor phase.
2. Viscous flow of liquid due to the gradient of vapor pressures.
3. Viscous flow of liquid due to the gradients of capillary pressure resulting from the temperature dependence of surface tension.

From theoretical considerations, the temperature profile across the propellant grain, during the present drying process, can be represented as shown in Figure 1. This positive temperature gradient can be expected to retard the transport of solvent vapors because the resulting partial pressure gradient would also be positive. Moreover, case hardening takes place on the propellant surface because of gel shrinkage during the drying process; this reduces the size of the passageways available to escaping solvent vapors and further restricts transport.

The net result of the interaction between the various processes is that the evaporation of solvent decreases with time, making it

difficult to remove enough solvent to meet acceptable total volatile content specifications.

### 3.2 Advantages of Dielectric Drying

Much of the difficulty in propellant drying might be avoided by establishing a constant temperature profile as shown in Figure 2. Such a profile would permit the surface temperature to be kept cooler for a given internal temperature than does the present drying technique; this would reduce the rate of case-hardening.

Dielectric heating appears to be the best technique available for effecting a constant temperature profile across the propellant.

In dielectric heating, the dielectric material to be heated (or dried) is positioned in a strong electrostatic field produced by a high frequency voltage. In a typical configuration, the material is placed between two flat plate electrodes to form a capacitor, the electrodes being connected to the terminals of a radio frequency electronic generator. During half of the electric cycle, one plate is charged positively and the other negatively to create a directional molecular stress in the dielectric material. A half cycle later, the plate polarity is reversed and the molecular stress in the dielectric material also reverses. These rapid stress reversals generate heat in the material (Reference 1).

Because the electric field creating the stress is uniform throughout the thickness of the dielectric material, the heating is uniform. A constant temperature profile can be maintained within the body of the material, although a negative temperature gradient is established near the surface of the material because of thermal convection, radiation and evaporation.

Preliminary calculations show that a semicontinuous dielectric drying unit with a 40 KW radio frequency generator and having a capacity to dry 250 pounds of green propellant in one hour could be built for less than \$50,000. Based upon a calculated thermal energy requirement of 108 BTU per pound of propellant dried and an operating efficiency of 25% (see Appendix I), the power cost would be 0.228 cents a pound. A schematic drawing of such a unit is shown in Figure 3. In this unit the conveyor would remain stationary in one position until a batch of propellant had dried to a desired level, then would index to the next position.

### 3.3 Constant Rate VS. Falling Rate Periods

The drying of solids can be distinctly divided into two time periods: the constant rate period and the falling rate period. The constant rate period is that portion of the drying cycle in which the surface of the solid is saturated with free liquid and the rate

of drying is totally dependent on the evaporation rate. The falling rate period is that part of the cycle in which the surface is unsaturated and the internal flow rate of the liquid is the controlling mechanism.

During the constant rate period, the type of atmosphere surrounding the propellant can be expected to affect drying kinetics and operating safety. For example, if the drying chamber were operated at reduced pressure, the drying rate might be increased because of more rapid evaporation from the surface. However, if this more rapid evaporation were to increase case-hardening, transport of solvent to the surface would be reduced. Thus, it might be necessary to maintain some level of humidity in the chamber atmosphere to prevent case-hardening; thus, optimum drying atmosphere could prove to be a compromise between reduced pressure and increased humidity.

The falling rate period is controlled by the diffusion rate. The flow rate of the internal liquid in a gel-like material during the falling rate period can be defined by the diffusion equation (Reference 2):

$$\frac{\partial C}{\partial \theta} = D \frac{\partial^2 C}{\partial x^2}$$

Where: C = concentration, #/in<sup>3</sup>

Q = time, hrs.

D = coefficient of diffusion, in<sup>2</sup>/hr

X = distance in direction of diffusion, inch

In order for the equation to be useful for determining the rate of flow (i.e., the rate of drying) it is necessary to know the value of the coefficient of diffusion D. For ideal gases, the relation describing the coefficient of diffusion was shown by Einstein to be (Reference 3):

$$D = \frac{RT}{NF}$$

Where: R = gas constant

T = absolute temperature

N = Avogadro's number

F = frictional coefficient

Through the use of this equation and the application of kinetic theory it is possible to predict quite accurately the coefficient for gases, but for liquids there is, as yet, no reliable analytical method for determining the diffusion coefficient. Einstein's equation is of value, however, for showing the effects that are of major importance; for example, to increase the magnitude of this coefficient one would increase the temperature.

As was pointed out, the equation describing the rate of diffusional flow ignores any effect of shrinkage. However, shrinkage during the drying of propellant is of major importance and renders the diffusion equation inadequate. Another complicating factor is the simultaneous existence of two or three different liquids in the solid. There is undoubtedly a compounding effect brought about by the mixture of several liquids (e.g., water and alcohol form an azeotropic mixture) which might not be accounted for in analyses of the individual components.

#### 4.0 Technical Discussion

##### 4.1 Equipment

A schematic drawing of the dielectric drying unit used during the program is shown in Figure 4. This unit was powered by a 750 watt output radio frequency generator operating at 27 megacycles. Three to five grams of propellant at a time were dried dielectrically in a cube-shaped glass screen basket suspended from an Ainsworth recording balance and positioned between two flat plate electrodes. Figure 5 is a photograph of the drying assembly in the test cell with the oscillator of the dielectric generator located beneath. Figure 6 is a photograph of the control panel in the control room. The drying assembly can be seen through the thick glass window. The temperature, as measured by a thermometer in the propellant basket,

was observed by means of a low powered telescope and controlled by means of the powerstat shown in the photograph. The rate of flow of gas through the drying assembly was monitored by the flow meter shown. Other temperature measurements were made by means of the Leeds & Northrup potentiometer using thermocouples and a Stoll-Hardy HL-4 Radiometer (infrared) having the sensing elements beneath the propellant sample basket. Figure 7 shows the power supply for the dielectric generator, the recorder for the balance and the analytical balance used in analyses.

The green propellant was received on June 16, 1964. Upon arrival, it was transferred to small 10 cc sample bottles to prevent the drying out which would have occurred if samples were repeatedly taken from the same container for experiments. The propellant was stored in a refrigerator at about 37°F (Figure 8).

Figure 9 shows the assembly constructed and used for total volatiles. This included a rocking assembly in the oven. Figures 10 and 11 show the "Fisher Titrimeter," "Unitron" microscope and "Deltatherm" differential thermal analysis apparatus used for the Karl Fisher water titrations, microphotograph and DTA work respectively.

#### 4.2 Analytical Procedures

The analyses listed below were performed both on green propellant

samples and on samples dried by the dielectric drying process. These analyses were performed also on similar samples of propellant dried by the present process and furnished by the U.S. Naval Propellant Plant.

1. Total Volatile Content

In this procedure\* the propellant was dissolved in dibutyl phthalate. The dibutyl phthalate propellant solution was placed in an oven and evacuated. Volatiles were evolved and determined quantitatively by changes in weight before and after the vacuum heat treatment. This determination gave total volatiles, water, alcohol, ether, etc.

Samples of propellant received from the Naval Propellant Plant were analysed by Pratt & Whitney. A comparison of Pratt & Whitney and Naval Propellant Plant values is shown in Table 1. The Pratt & Whitney results were slightly higher than those of the Naval Propellant Plant.

2. Moisture Content

The propellant was dissolved in pyridine and the moisture titrated with Karl Fisher reagent (a solution of iodine sulfur dioxide and pyridine in methyl

---

\* Military Standards 826A, August 18, 1961, Method 103.3.3, The Solution Evacuation Method

cellosolve). The end point was indicated electrometrically by a change in the conductivity. This analysis specifically provided the water content.

### 3. Differential Thermal Analysis (DTA)

DTA measures differences in temperature between a sample and an inert reference when both are heated at a uniform rate. These differences were plotted on a recorder vs. temperature (or time, since the temperature-time relationship was linear). Temperature changes that took place within the sample were due to a gain or loss of heat. Vaporization of solvents absorbed heat to produce endothermic peaks. Decomposition of the dry propellant evolved heat to produce exothermic peaks.

### 4. Dimensional Analysis

Case hardening occurs during the initial stages of the present drying process. This inhibits complete shrinkage of propellant during the final stages of drying. It was anticipated that dielectric drying would harden the propellant more uniformly and permit more uniform shrinkage. This should result in propellant grains having more uniform shapes; i.e.,

with less convexity, concavity, or other distortions than might be obtained in the present drying process. Thus, a dimensional analysis showing the average length, width, and size distribution of propellant grains produced by dielectric drying versus conventional drying was useful in helping to compare two processes. These dimensional measurements were made on a microscope and the external shape of representative propellant grains were recorded by microphotography.

#### 4.3 Experimental Work

##### 4.3.1 Empirical Evaluation of Operating Parameters

As pointed out in Section 3.3, the drying rate during the constant rate period would be affected by the drying environment. Consequently, it was decided to investigate the effects of humidity, pressure and gas flow rate upon the drying rates for given drying temperatures. Moreover, the use of pure nitrogen was evaluated with respect to air, since arcing between electrodes is less likely to occur in a pure nitrogen atmosphere than in air (Reference 4).

At the beginning of the program, immediately after equipment calibration, six preliminary experiments (Runs #1 through #6) were performed to furnish information about the operating characteristics

of the system. Based upon these runs, it was decided to evaluate the parameters at the following levels to establish their effects upon the total volatile content:

<u>Temperature</u>	<u>Pressure</u>	<u>Gas Flow Rate</u>	<u>Humidity</u>	<u>Type of Gas</u>
70°F	0.5 atmosphere	0 cc/minute	0 gm/meter <sup>3</sup>	Air
140°F	1.0 "	500 "	9½ "	Nitrogen
160°F	1.2 "	500 "	19 "	

If the stepping stone approach were used such that only one parameter was varied at a time while all other parameters were held constant, a total of 162 runs would be required to complete the evaluation ( $3 \times 3 \times 3 \times 3 \times 2 = 162$ ). This would mean that eight months would be required simply to perform the evaluation experiments, since it was decided during the first six trial runs that each evaluation run should last seven hours (or effectively one full day per run). Instead, however, the experiments were designed to utilize a response surface technique -- the experiments were programmed so as to furnish a reasonable coverage of the operating system with a much smaller number of experiments, then the data from these experiments were utilized to calculate a response surface equation from which all 162 possible combinations could be computed. After performing the computations for all possible combinations, it would be necessary only to establish the optimum operating point

(the point with the lowest total volatile content consistent with efficient and economic operating conditions), then perform a few additional confirming experiments.

A uniform operating procedure was followed for all of the experimental runs. A three to five gram propellant sample was placed in the electrode assembly and the charge weight was recorded. During the run, the sample weight loss during drying was continuously plotted against time. The sample temperature was obtained by means of a thermometer in the center of the propellant bed; the sample temperature was held to a desired level by varying the power output of the radio frequency generator. At the end of each drying experiment, the samples were analyzed, as described in Section 4.2, to obtain the total volatile content. From this total volatile analysis and from the weight loss vs. time recording, the total volatile content was computed and plotted as a function of drying time for each run.

Twelve experiments were run to obtain data for the response surface equation -- ten of these runs were primary runs and two were replications to establish reproducibility. These twelve runs covered Runs #7 through #19, of which all produced acceptable data except Run #12 which was discontinued because of an operating error. The figures within brackets in Table 2 are actual total volatile data

obtained from the experiments. Utilizing these data, the response surface equation was established from which the balance of the figures in Table 2 were computed. This response surface equation took the form:

$$T.V = 8.18 - .44H + 1.93P - .62T + .45F - 3.56A - .56PF - .12FT \\ + .12PTF + .02PFA$$

Where: T V = total volatiles (%)

H = humidity of atmosphere passing through drying chamber, with values of 0, 9.5 or 19 (see code at bottom of Table 2)

P = pressure inside drying chamber, with values of 0.5, 1.0, or 1.2

T = drying temperature of propellant, with values of -3, 4, or 6

F = rate of gas flow through drying chamber, with values of 0, 5, or 9

A = type of gas in drying chamber, e.g., air or nitrogen, with values of 0.8 or 1.0

It is interesting to note that the response equation, as generated, gave excellent correlation with the raw data from which it was computed. The total volatile values, as predicted from the response surface equation, are compared below with the actual raw data results:

<u>Run #</u>	<u>Predicted</u>	<u>Actual</u>
7	3.81%	3.87%
8	4.31%	4.58%
9	8.65%	8.59%
10	3.62%	3.58%
11	3.54%	3.73%
12	Discontinued	
13	3.62%	3.43%
14	2.69%	2.48%
15	2.57%	2.49%
16	3.93%	3.80%
17	3.47%	3.46%
18	2.57%	2.49%
19	3.50%	3.67%

Table 3 contains the complete summary of the results of all experiments performed during the program. The significance of the various runs is explained below:

1. Runs #1-6 were performed to obtain information about the operating characteristics of the system.
2. Runs #7-19 were used to establish the response surface equation.

3. Run #20 was performed as a check on Run #15 and showed that the total volatile reproducibility was good (2.63% vs. 2.49%).
4. Run #21 was performed as the first check on the usefulness of the response equation and showed an encouraging correlation -- an actual total volatile content of 1.79% vs. a predicted value of 1.76%.
5. Runs #22-25 were performed to obtain samples which were sent to NPP for nitroglycerine analysis. The NPP results showed no undue loss of nitroglycerine at temperatures as high as 170°F.
6. Runs #26-30 were performed in an attempt to utilize the response surface to minimize the total volatile content of the dried propellant. However, there was very poor correlation between actual figures and the predicted values, the actual values being much higher. This is discussed subsequently.
7. As a result of the failure of runs #26-30 to yield sufficiently low total volatile values, Runs #31-46 were performed at higher temperatures (170, 180, or 190°F) in a successful effort to develop a technique for achieving lower total volatile values. This also is discussed subsequently.

8. Runs #47-50 were performed to obtain samples which were sent to N.P.P. for inspection and nitroglycerine analysis. The N.P.P. results showed no undue loss of nitroglycerine at temperatures as high as 190°F.

In referring to the response surface (Table 2), it appears that very low total volatile results would be obtained for operating conditions such as are defined by the lower right corner of the chart. However, the results of Runs #26-30 showed poor correlation with the response surface. The predicted vs. actual results are shown below:

<u>Run #</u>	<u>Predicted</u>	<u>Actual</u>
26	0.25%	2.33%
27	-0.59%	1.37% (Total Volatile Analysis Probably Incorrect)
28	-0.59%	2.29%
29	0.10	2.52%
30	0.10	2.64%

At first glance it seems puzzling that the response surface equation should fall down for these total volatile values of less than 2.5%, since it fits so very well for values above this. However, as was pointed out in Section 3.3, the drying of solids falls into two time periods: the constant rate period and the falling rate

period. During the constant rate period, evaporation is the controlling mechanism; the drying rate is a function both of the environmental conditions and the temperature. During the falling rate period, diffusion is the controlling mechanism; the drying is a function of temperature only. The failure of the response surface equation to operate satisfactorily at low total volatile contents may have occurred because the transition to the falling rate period had been completed. The response equation falls down suddenly in this range because it contains several environmental terms (pressure, gas flow rate, humidity, and type of atmosphere) which no longer apply.

Having established that, at total volatile contents below about 2.5%, temperature was the only operating parameter which had a significant effect upon the drying rate, the next step was to perform a series of experiments at higher drying temperatures. As shown in Table 3, sixteen experiments (Runs #31-46) were performed at higher temperatures (170, 180, or 190°F) for periods of time up to twelve hours. As a result of these experiments, three techniques were established for reducing the total volatile content to acceptable levels:

1. The propellant was heated to 190°F for five hours to obtain a total volatile content of 1.87%. Figure

12 shows the total volatile content vs. drying time curve for this technique.

2. The propellant was heated to 180°F for seven hours to obtain an average total volatile content of 1.82%. Figure 13 shows the total volatile content vs. drying time curves for this technique.
3. The propellant was heated to 170°F for twelve hours to obtain a total volatile content of 1.75%. Figure 14 shows the total volatile content vs. drying time curve for this technique.

In all three of these techniques there was some darkening of a few pellets adjacent to the thermometer after three or more hours of drying time. The presence of the thermometer apparently caused some uneven heating of the bed which should not occur if larger samples were dried or a remote means of temperature measurement (e.g., an infrared device) were employed. It is believed that as long as a solvent is evolved from the propellant in large quantities, the vaporization of these solvents causes a cooling effect which protects the propellant.

Figure 15 shows the average total volatile content vs. drying time for various drying temperatures. Temperatures of at least 170°F are necessary to achieve acceptable total volatile contents in

reasonably short drying times. These curves probably best summarize the important findings of this drying study.

#### 4.3.2 Difficulty of Removing Ethyl Alcohol From Propellant

The boiling points of pure diethyl ether, ethyl alcohol and H<sub>2</sub>O are 94.3, 173.0 and 212.0°F respectively. The percent of these components in the dry and wet propellant are:

COMPONENT	WET	DRY
H <sub>2</sub> O	.83%	.63%
Ethyl alcohol	15.67	.82
Diethyl ether	16.5	0
Propellant (NC, NG, etc)	67.0	98.55
Total	100.00%	100.00%

Experiments #39 and #40 (Figure 16) show inflection points in the temperature vs. time curves at about 143°F. This is believed to be due to the evolution of the ether in a very short period of time. This shows that the problem in drying the propellant to an acceptably low total volatile content is largely the removal of ethyl alcohol. This appears to be confirmed by Figure 17 showing the total volatile content drying temperature after different periods of time. Extrapolation of these curves to 190°F shows the probable boiling point of the ethyl alcohol from the NG-NC solution.

Deviation from 190°F occurs because diffusion of the solvent from the propellant is very slow when the last of the volatiles are being removed.

The apparent boiling point of ethyl alcohol (190°F) minus the boiling point of pure ethyl alcohol (173°F) gives a boiling point elevation of 17°F (10°C). According to the Clausius-Clapeyron equation,  $\Delta T = K_b m$ , where  $\Delta T$  is the boiling point elevation,  $K_b$  is the molal boiling point constant and  $m$  is the molality of the solution...  $m = \frac{\Delta T}{K_b} = \frac{10}{1.22} = 8.2$  moles of solute/1000 g solvent which is equivalent to 0.82 moles of solute/100 g solvent. If nitroglycerine (molecular weight = 227) is the solute, then  $0.82 \times 227 = 186$  g nitroglycerine/100 g ethyl alcohol. The solubility of nitroglycerine in ethyl alcohol at 25°C is 25 g NG/100 g EtOH. It is conceivable that the solubility could increase this much at 190°F.

If nitrocellulose (molecular weight = 594) were the solute, then  $0.82 \times 594 = 486$  g nitrocellulose/100 g ethyl alcohol. This is a very high figure. The problem of drying the propellant to an acceptably low total volatile content is probably the removal of ethyl alcohol from a nitroglycerine-ethyl alcohol solution and the diffusion of the ethyl alcohol through the nitrocellulose-nitroglycerine gel.

### 4.3.3 Electron Micrographs and Microphotographs

Figures 18 through 21 show the electron micrographs obtained on the following samples:

Figure 18 - End of propellant cylinder; dried by N.P.P. 10 days

Figure 19 - Center cut cross section of propellant cylinder; dried by N.P.P. 10 days

Figure 20 - End of propellant cylinder; dielectrically dried, run #45

Figure 21 - Center cut cross section of propellant cylinder; dielectrically dried, Run #45

These micrographs are replicas preshadowed with 10 angstroms of platinum and 100 angstroms of carbon under  $10^{-4}$  mm Hg vacuum. The propellant was then dissolved away with acetone leaving the impression of the surface. The magnification factor was 52,000.

The conclusions to be drawn from these pictures are:

- A. Very solid surfaces with absence of passageways are shown indicating the difficulty in removing solvent.
- B. Few, if any, distinct fibers are seen indicating the probable complete gelation of all components in the propellant.
- C. Center cut cross sections of propellant dried by N.P.P. show many micro-cracks. Dielectrically dried

propellant does not exhibit this phenomenon.

Microphotographs (magnification 17.75) were taken of almost all drying experiments. Figures 22 through 27 show the following propellant samples:

Figure 22 - Propellant dried 10 days in present N.P.P. process

Figure 23 - Green propellant as received on June 16, 1964

Figure 24 - Green propellant after 2 months storage at 37°F

Figure 25 - Dielectrically dried propellant, Run #37  
(Dried at 170°F for 12 hours)

Figure 26 - Dielectrically dried propellant, Run #49  
(Dried at 180°F for 7 hours)

Figure 27 - Dielectrically dried propellant, Run #50  
(Dried at 190°F for 5 hours)

White fluffy material developed on the green propellant while in storage and was not a result of dielectric heating. It is believed to be some nitrocellulose expressed from the propellant.

Table 4 contains the average dimensional analysis of the propellant cylinders from the above pictures. It was very difficult to make these measurements because of the irregularity of the pellets. Most of the shrinkage during the drying of propellant occurs in the diameter. Much less shrinkage occurs in the length. Quite possibly, some shrinkage occurred in the green propellant in storage.

Few, if any, differences in diameter and length existed between propellant dried by the N.P.P. present and by the dielectric process.

#### 4.3.4 Differential Thermal Analysis

Figure 28 shows the differential thermal analysis of propellant dried by N.P.P. for various periods of time in their present process. Distinct peaks were not observed for ether, alcohol, and water as might be expected, but one long endothermic peak was observed over the temperature range of 25°C to 100°C. It is believed that the shrinkage of the propellant caused a change in density and thus a change in thermal conductivity which also contributed to the extent of the endothermic peak. The very sharp exothermic peak at 165°C was due to the sudden decomposition of the propellant.

#### 4.4 Mathematical Analysis of the Drying Process

A mathematical analysis of the drying process was performed simultaneously with the experimental effort. The purpose of this analysis was to investigate, on a theoretical basis, the removal of solvents from a double base propellant containing nitrocellulose and nitroglycerine in order to better understand the drying mechanism and to determine ways of shortening the drying time. The volatile content versus drying time curve based on this analysis was compared with the results of Run #35 and the correlation was

found to be excellent (Figure 24).

The analytical investigation was based on the assumption that the drying process is a diffusion process and that the drying mechanism is due to thermal and vapor pressure gradients which establish the viscous flow of solvents. Ether, alcohol and water are the constituents which must be removed. Ether and alcohol each make up about 17% by weight of the green propellant, whereas water makes up such a small portion of the propellant that it can be considered to be removed with the alcohol. Of the two main solvents present, ether has a higher vapor pressure than alcohol and consequently will be removed more rapidly; depending upon the power applied to the propellant, ether will be completely removed within 15-60 minutes.

The mathematical analysis developed in Appendix II examined the simplest case, one in which the propellant is considered already to have reached the drying temperature and to be at steady state conditions as soon as the power is turned on. A differential equation was generated expressing the fraction of total volatiles remaining as a function of drying time. When the theoretical total volatile content versus drying time curve from this differential equation was compared with the actual curve from Run #35, good correlation was obtained in the range of operating times of one

hour to seven hours but poor correlation was obtained during the operating time range of zero to one hour. Since Run #35 had been programmed to reach the drying temperature of 180°F in 45 minutes from the time power was turned on, the first hour of drying time can be considered to be a temperature transient range. Thus, the assumption that the drying temperature is uniform throughout the entire time period is unsatisfactory.

Appendix III was an obvious refinement in which it was considered that the propellant is initially at room temperature when the power is turned on and requires some finite time to reach the final drying temperature. By assuming that the temperature increased from room to final drying temperature as a parabolic function of time (i.e., the temperature increased at an ever decreasing rate until the drying temperature of 180°F was reached at the end of 45 minutes), a differential equation was generated to cover this transient temperature condition. By applying the differential equation from Appendix III to the transient temperature period and the differential equation from Appendix II to the steady state temperature period, the theoretical curve presented in Figure 29 was generated. This curve shows that there is a very rapid removal of solvent as soon as the pellet is exposed to the environment of the test cell. However, as drying time increases, solvent removal occurs at an ever-decreasing rate and theoretically the solvent is never

completely removed because the diffusion gradient approaches zero.

This excellent correlation between theory and test results suggests that the original assumption of the flow mechanism being a diffusion process is essentially correct. Two interesting facts emerge from this analysis to indicate that, for any given drying temperature, improvement in the drying process is possible in the initial part of the cycle but impossible after thermal equilibrium has been reached:

1. The first phenomenon noted is that rapid application of power at the beginning of the cycle results in a shorter time cycle. In Appendix III a comparison is made between a linear increase in temperature with time and a more rapid parabolic increase in temperature with time; time is saved in the latter case.
2. The second phenomenon noted is that, once the steady state temperature is reached, the rate of diffusion is established and can be increased only by increasing the drying temperature.

Thus, it is evident that the drying process can be optimized by raising the power to the highest possible level consistent with obtaining a satisfactory (e.g., non-degraded) product.

It is interesting to note that, when the test data for Run #35 is plotted in log-log form as in Figure 30, the total volatile vs. time plot can be represented by two linear functions over most of the time cycle. Upon further analysis, it can be shown in Figure 31 that both the ether and the alcohol-water removal can be represented by linear functions. This result cannot be explained at this time; perhaps it is a purely empirical result. However, the existence of this linear log-log relationship could be a great convenience; for example, one could predict total volatile contents for longer drying times simply by extrapolation.

#### 5.0 Conclusions

The results of this program show that dielectric heating is a very feasible technique to use for drying propellant and that it can give drying times as short as five hours. Furthermore, because the operating temperature has considerably more significance upon the drying rate than do environmental parameters such as pressure, humidity, gas flow rate and type of gas (and this is especially true at the lower total volatile contents), a relatively inexpensive yet effective production drying apparatus could be designed which could operate at ambient atmospheres; this would eliminate the expense of providing a controlled atmosphere chamber around the electrodes and also would allow the drying process to be continuous.

Thus, one could envision a drying unit similar to that shown in Figure 3 but with no atmospheric chamber necessary. The device could be further modified to have a series of independent electrodes positioned overhead along the belt, the power to the electrodes being programmed such that the greenest propellant would receive the highest power inputs; this would bring the propellant to the desired drying temperature in the shortest possible time. Down stream electrodes would be programmed at lower power levels sufficient to maintain the partially dried propellant at the desired drying temperature.

#### 6.0 Recommendations

The work to date has been devoted to establishing the feasibility of utilizing dielectric heating as a technique for drying ABL-705 propellant. Having established the basic feasibility of the technique, the next step should be to gather information about the operating characteristics of a production drying system, especially a system which operates at ambient atmospheric conditions. To that end, it is recommended that the existing equipment be modified somewhat to handle one pound propellant samples and that the existing thermometer arrangement be replaced with a remote infrared temperature sensing device. A program should then be run to gather information about the power and energy requirements, economics, and

other operating characteristics as functions of the drying temperature, electrode configuration, power programming cycle, etc. This information should be utilized during the design and construction of a pilot plant drying system.

## LIST OF ILLUSTRATIONS

<u>FIGURE</u>	<u>TITLE</u>
1	Temperature Profile of Propellant-Dielectric Process
2	Temperature Profile of Propellant-Dielectric Process
3	Semicontinuous Dielectric Propellant Dryer
4	Schematic of Drying Apparatus
5	Photograph of Drying Apparatus in Test Cell
6	Photograph of Control Panel in Control Room
7	Photograph of Power Supply for Dielectric Generator, Recorder Balance and Analytical Balance Used in Analysis
8	Photograph of Refrigerator Used For Propellant Storage
9	Photograph of Total Volatile Analysis Apparatus
10	Photograph of Water Determination and Microphotography Apparatus
11	Photograph of Differential Thermal Analysis Apparatus
12	Volatile Content VS. Drying Time, 190°F
13	Volatile Content VS. Drying Time, 180°F
14	Volatile Content VS. Drying Time, 170°F
15	Volatile Content VS. Drying Time at Various Temperatures
16	Temperature VS. Drying Time for Experiments #39 & #40
17	Volatile Content VS. Drying Temperature
18	Electron Micrograph, End of Propellant Cylinder Dried by N.P.P. 10 Days

- 19 Electron Micrograph, Center Cut Cross Section of Propellant Cylinder Dried by N.P.P. 10 Days
- 20 Electron Micrograph, End of Propellant Cylinder Dielectrically Dried, Experiment 45
- 21 Electron Micrograph, Center Cut Cross Section of Propellant Cylinder Dielectrically Dried, Experiment 45
- 22 Propellant Dried by N.P.P. 10 Days
- 23 Green Propellant
- 24 Green Propellant After 2 Months Storage at 37°F
- 25 Propellant Dielectrically Dried at 170°F for 12 Hours, Experiment 37
- 26 Propellant Dielectrically Dried at 180°F for 7 Hours, Experiment 49
- 27 Propellant Dielectrically Dried at 190°F for 5 Hours, Experiment 50
- 28 Differential Thermal Analysis of ABL-705
- 29 Total Volatiles VS. Drying Time - Comparison Between Analytical Data and Test Run #35
- 30 Total Volatiles VS. Drying Time as Plotted on Log-Log Scale - Run #35
- 31 Total Volatiles VS. Drying Time for Ether and Alcohol - Log-Log Scale - Run #35
- 32 Central Point Concentration History for a Finite Cylinder of Propellant
- 33 Fractional Amount of Solvent Remaining as a Function of Time for a Finite Cylinder of Propellant - Temperature Invariant
- 34 Fractional Amount of Solvent Remaining as a Function of Time for a Finite Cylinder of Propellant Diffusion Constant Proportional to the Square of the Temperature

Fractional Amount of Solvent Remaining as a Function  
of Time for a Finite Cylinder of Propellant - Diffusion  
Constant Proportional to the Temperature

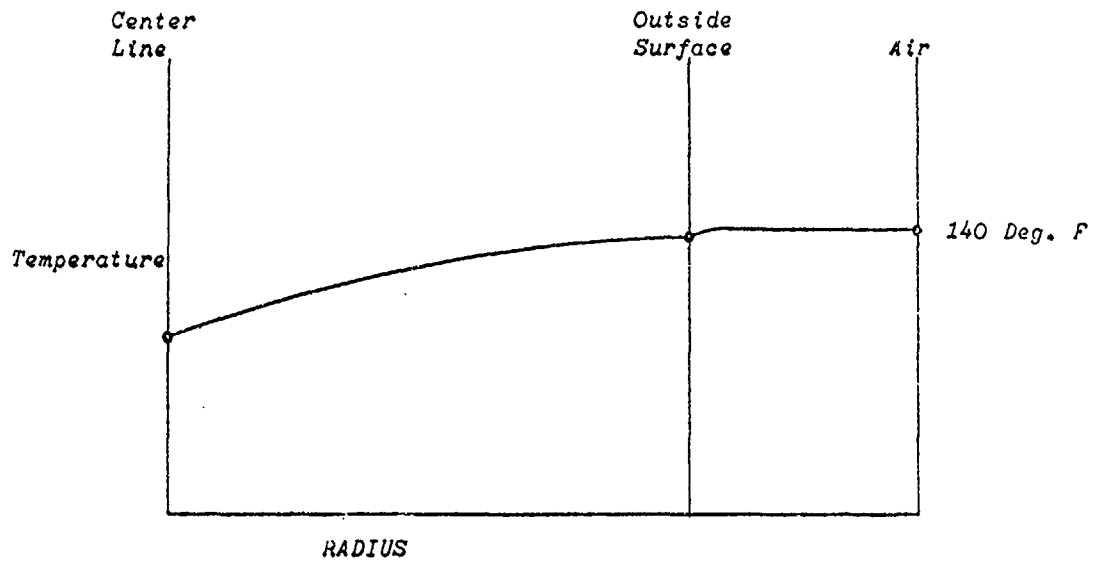


Figure 1 TEMPERATURE PROFILE OF PROPELLANT - PRESENT PROCESS

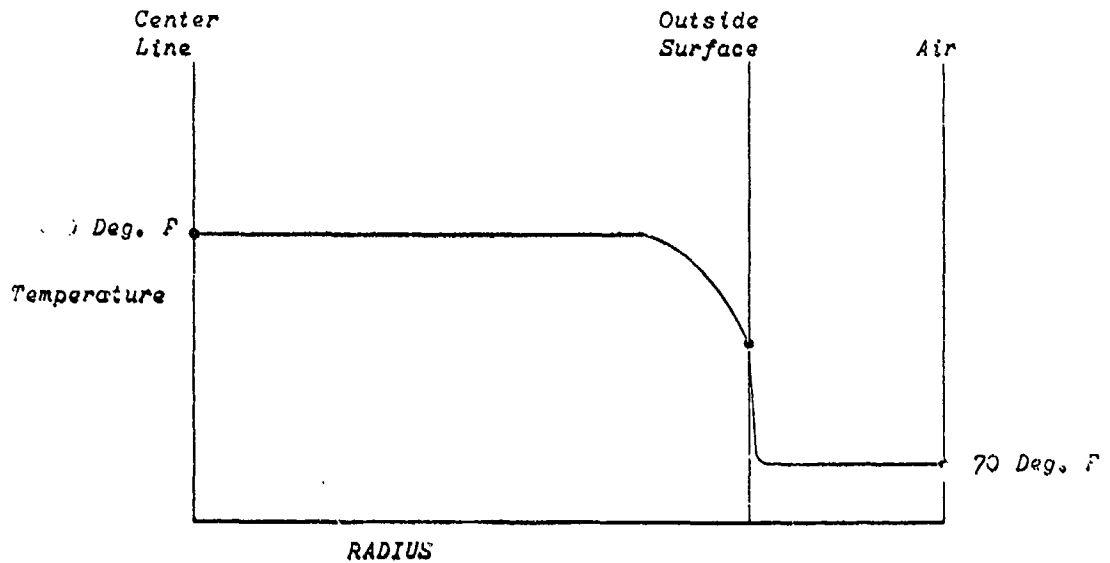


Figure 2 TEMPERATURE PROFILE OF PROPELLANT - DIELECTRIC PROCESS

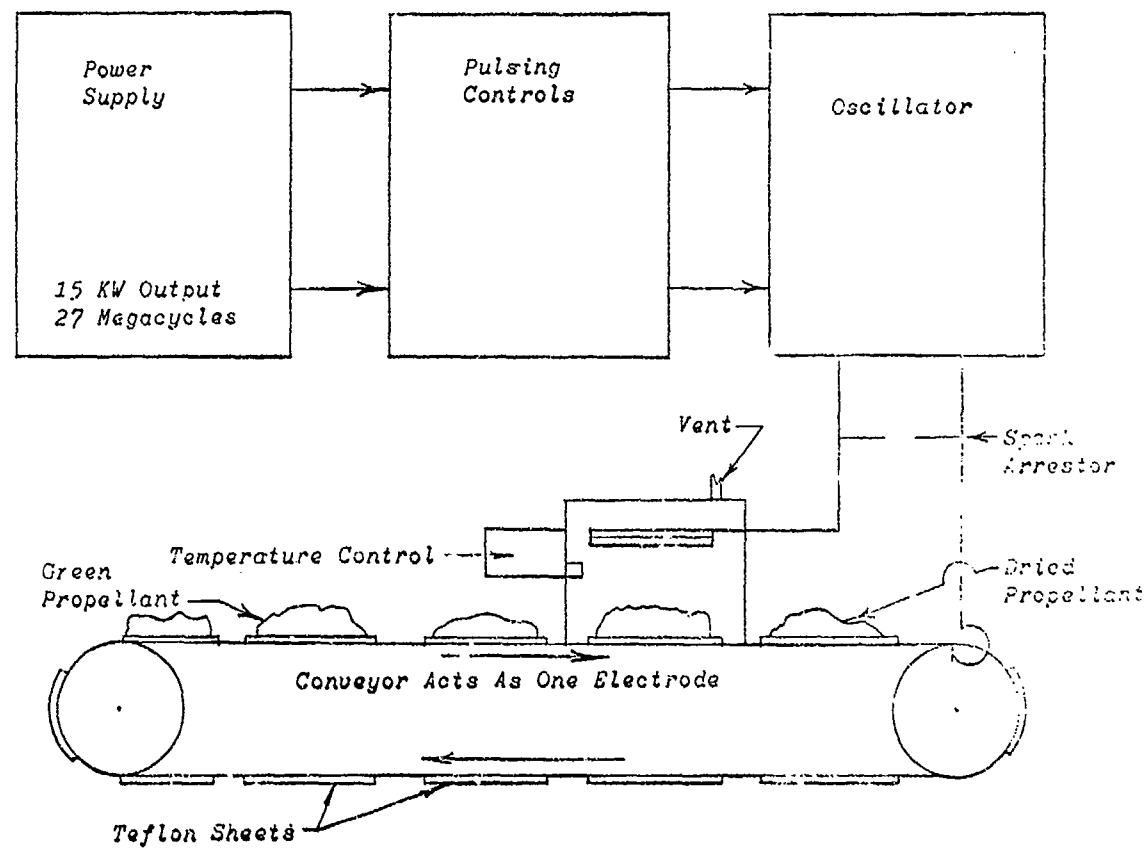


Figure 3 SEMI-CONTINUOUS DIELECTRIC PROPELLANT DRYER

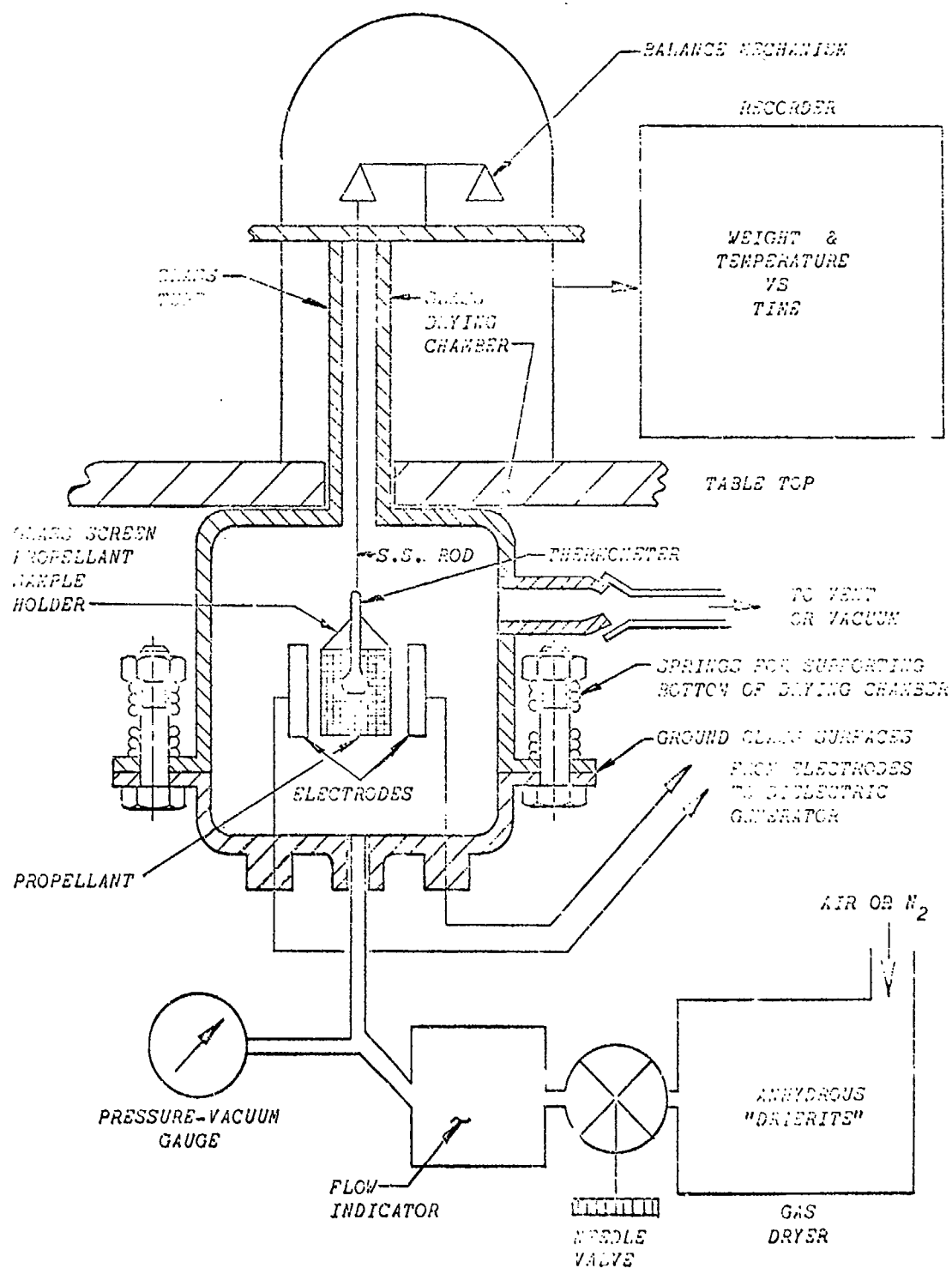


FIG. 4  
 SCHEMATIC OF DRYING APPARATUS

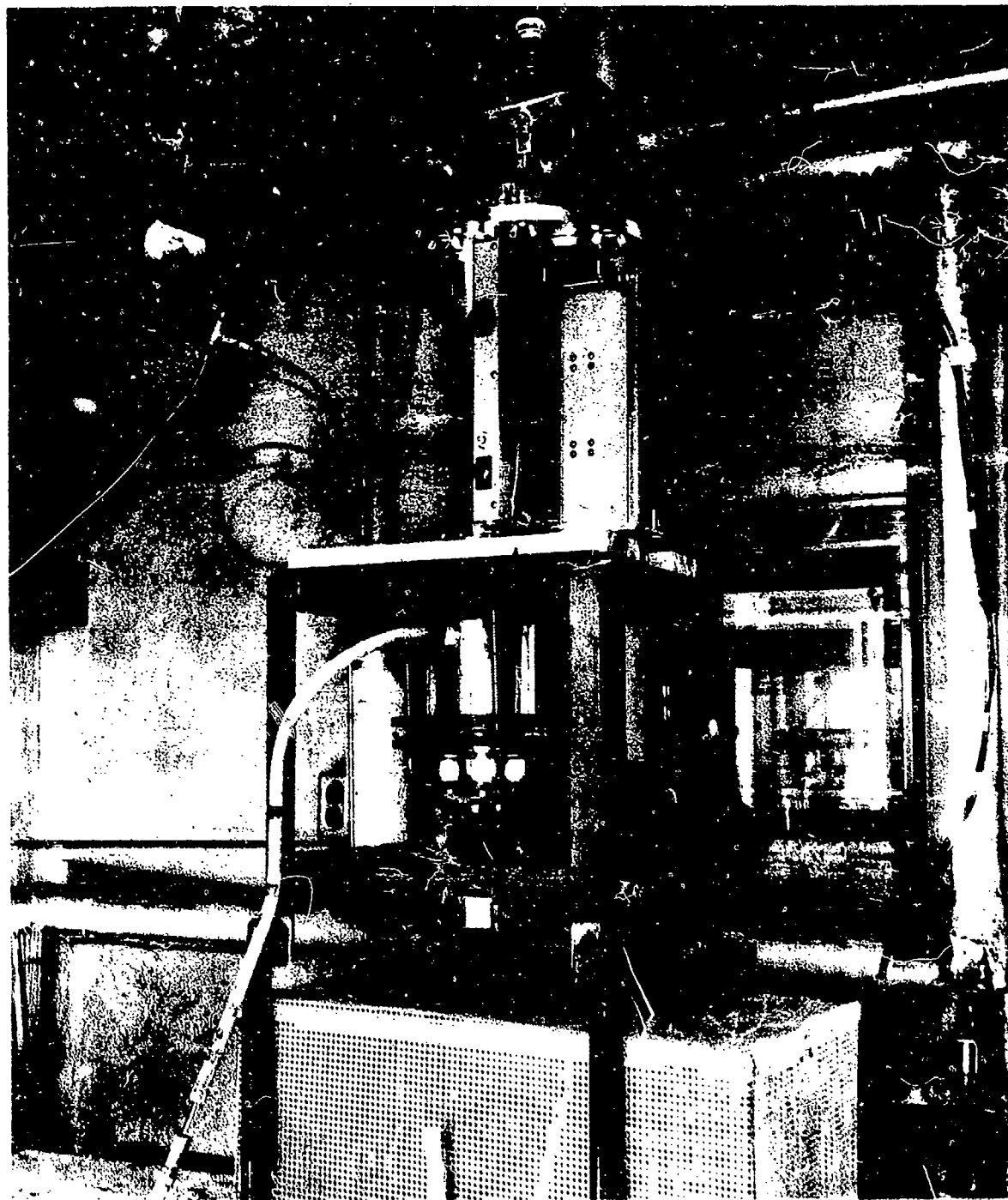


FIGURE 5  
Photograph of drying apparatus in test  
cell

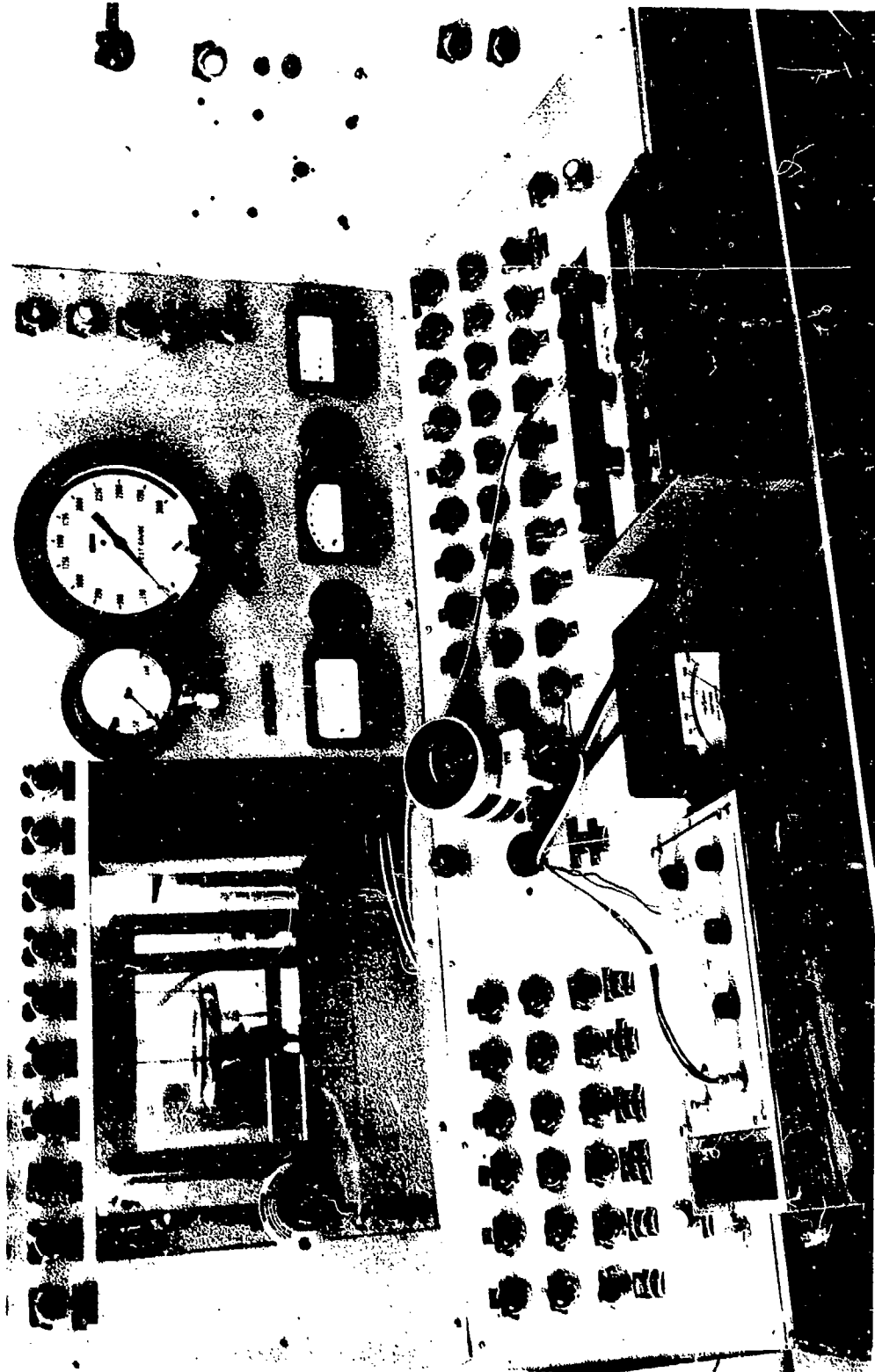


FIGURE 6  
Photograph of control panel in control  
room

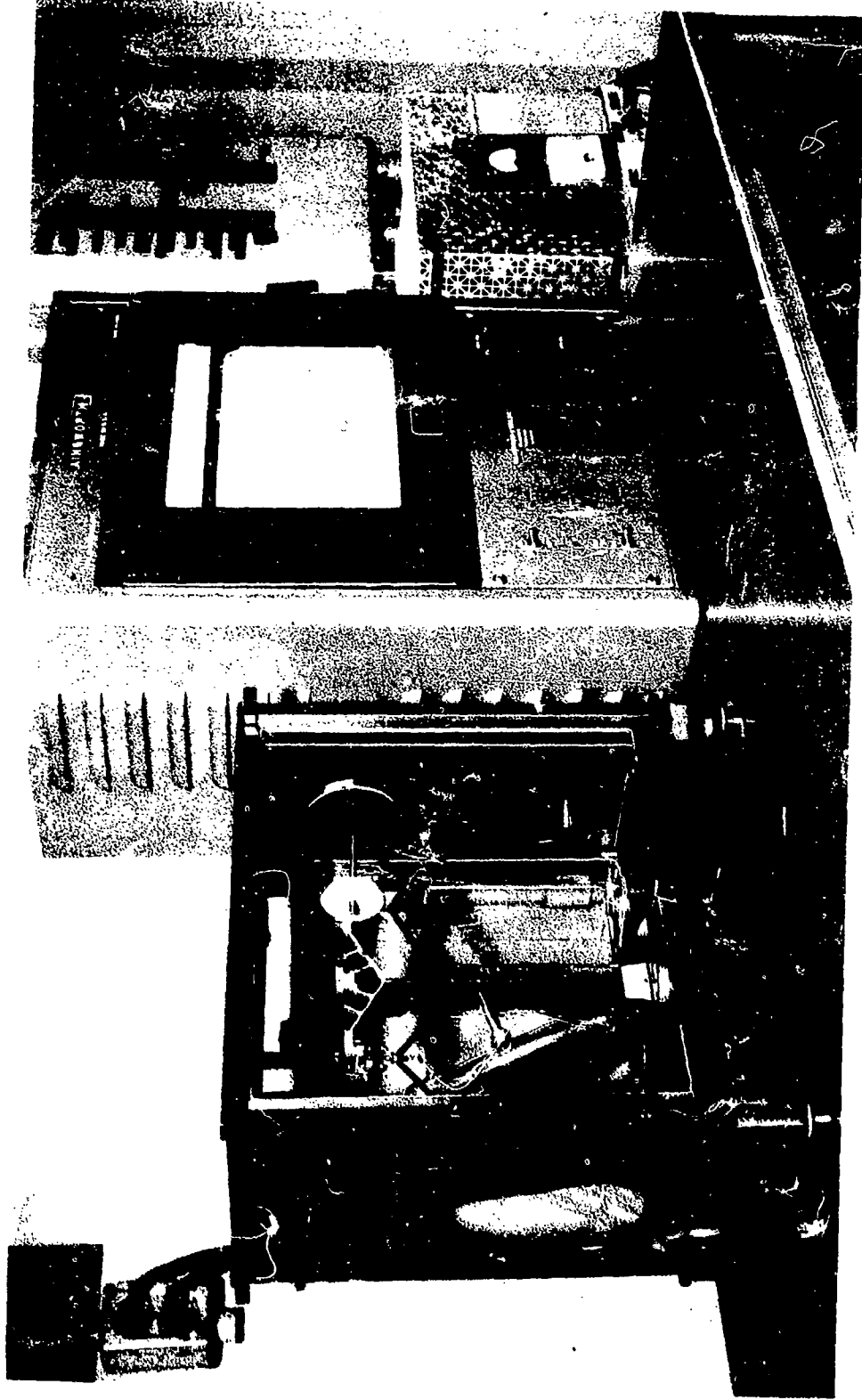


FIGURE 7  
Photograph of power supply for dielectric generator, recorder balance, and analytical balance used in analysis

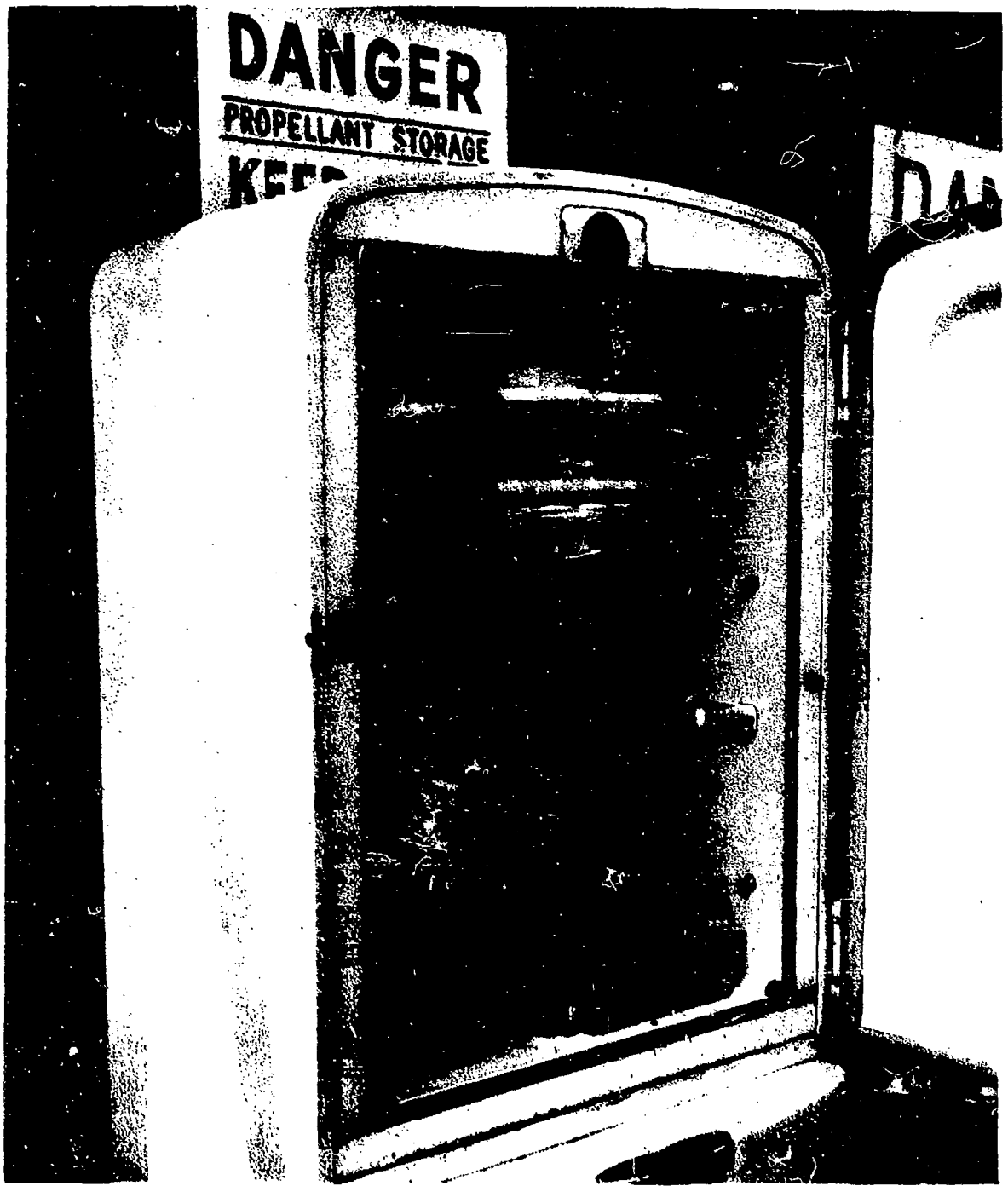
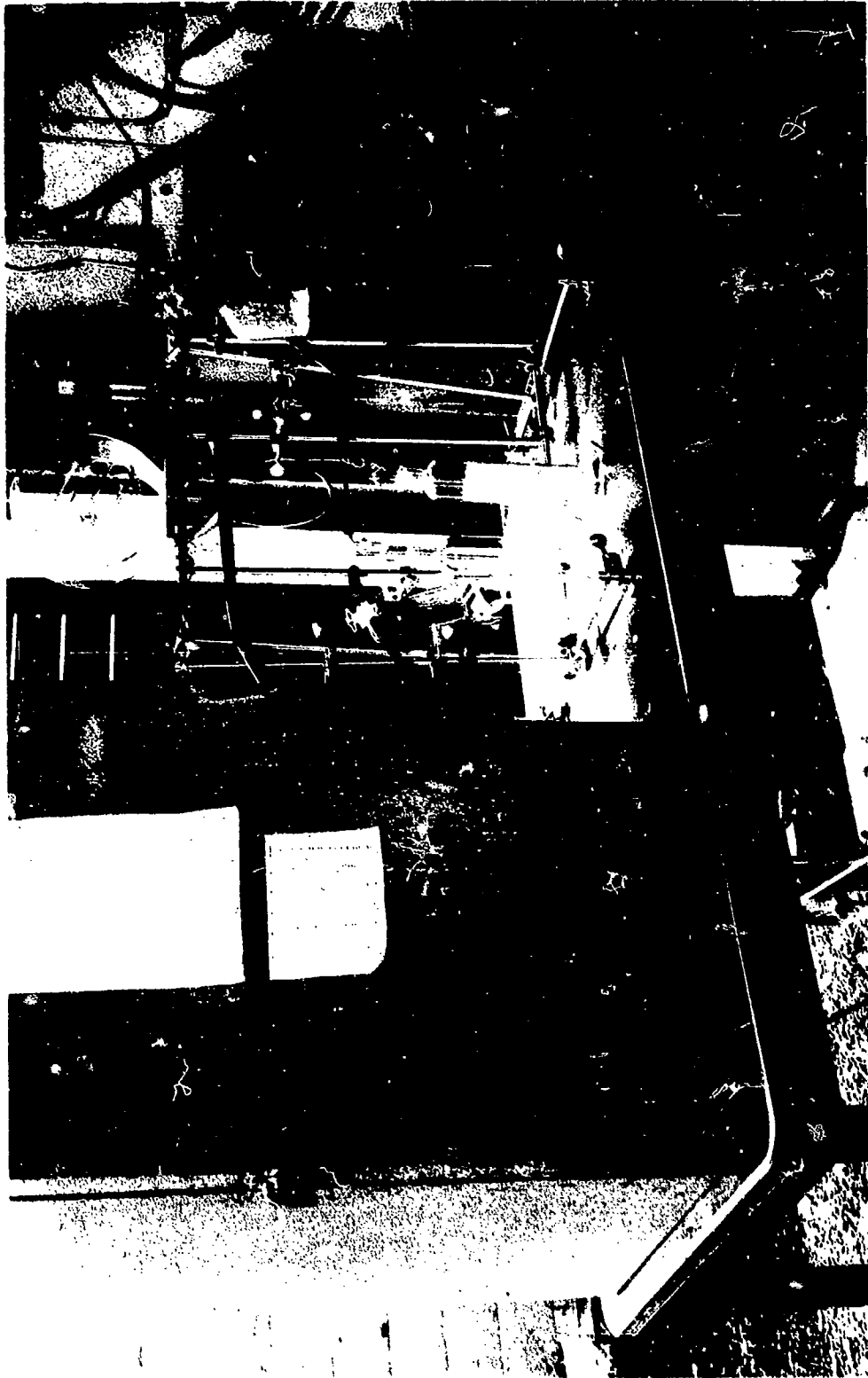


FIGURE 8  
Photograph of refrigerator used for  
propellant storage



**FIGURE 2**  
Photographs of total volatile analysis  
apparatus

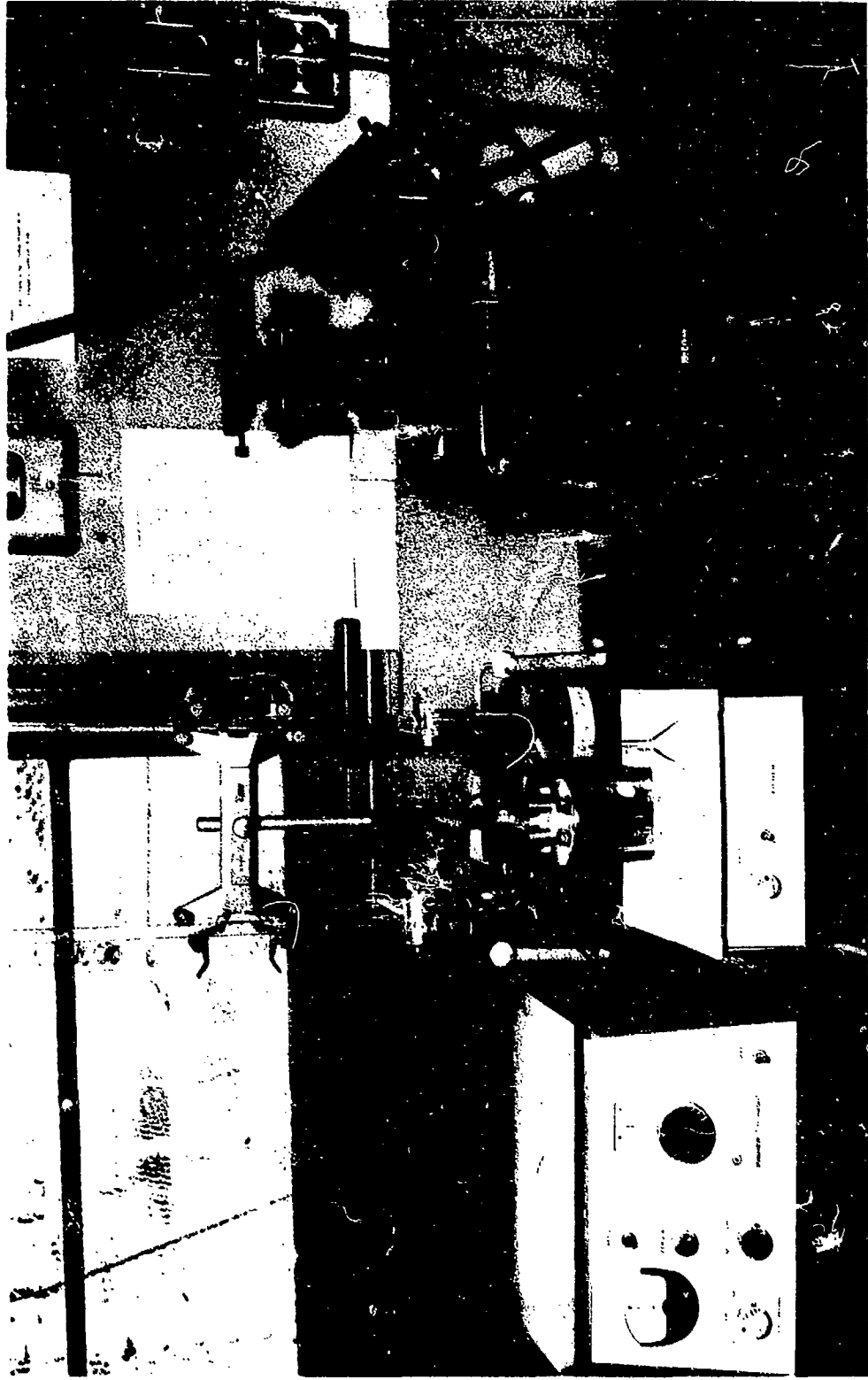


FIGURE 10  
Water determination and microphotography  
apparatus



FIGURE 11  
Differential thermal analysis apparatus

VLATILE CONTENT VS. DRYING TIME-  
190°F. 0 HUMIDITY, ATMOSPHERIC PRESSURE  
900 cc/min. FLOW OF N<sub>2</sub>  
RUN 43

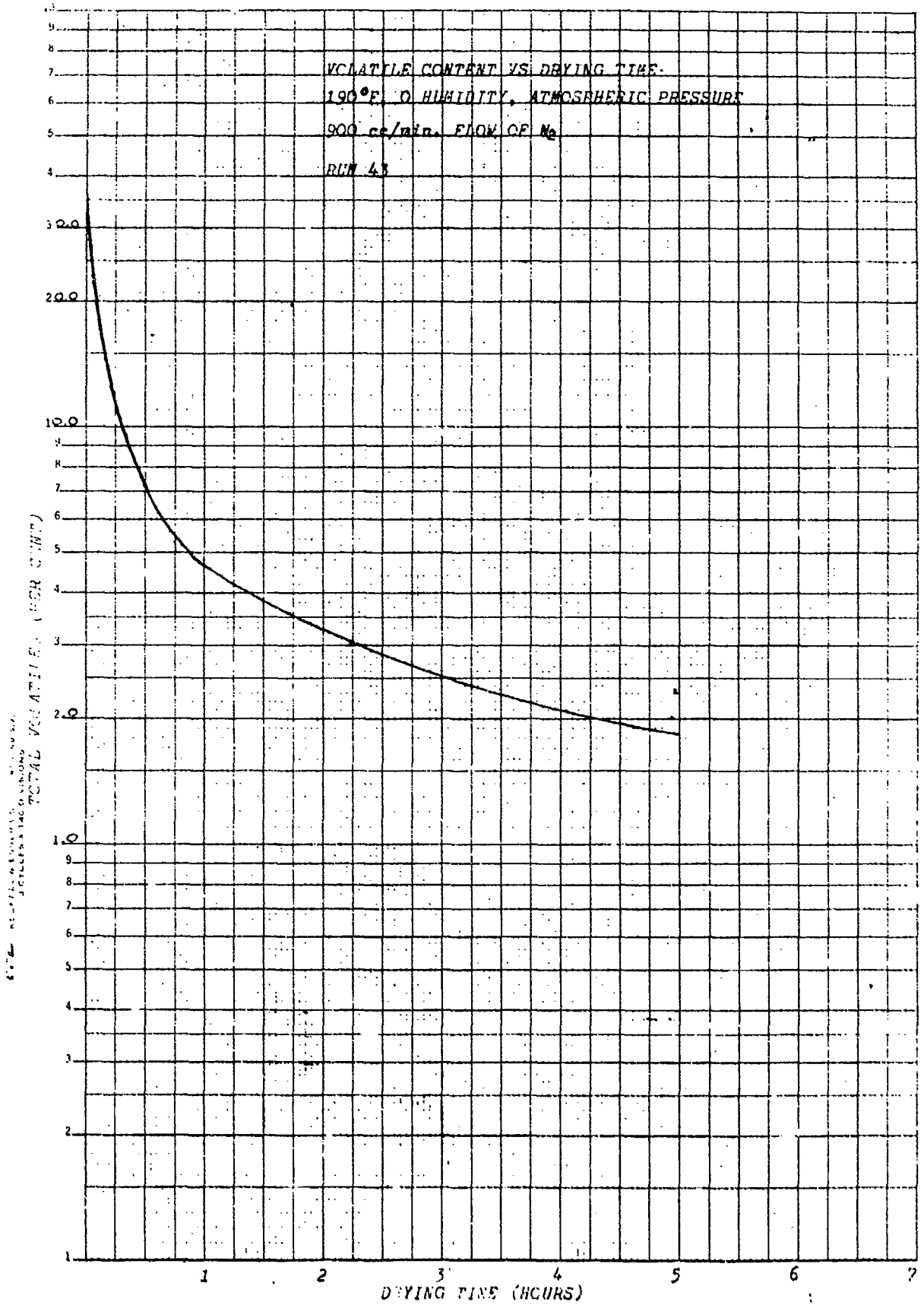


FIG 15

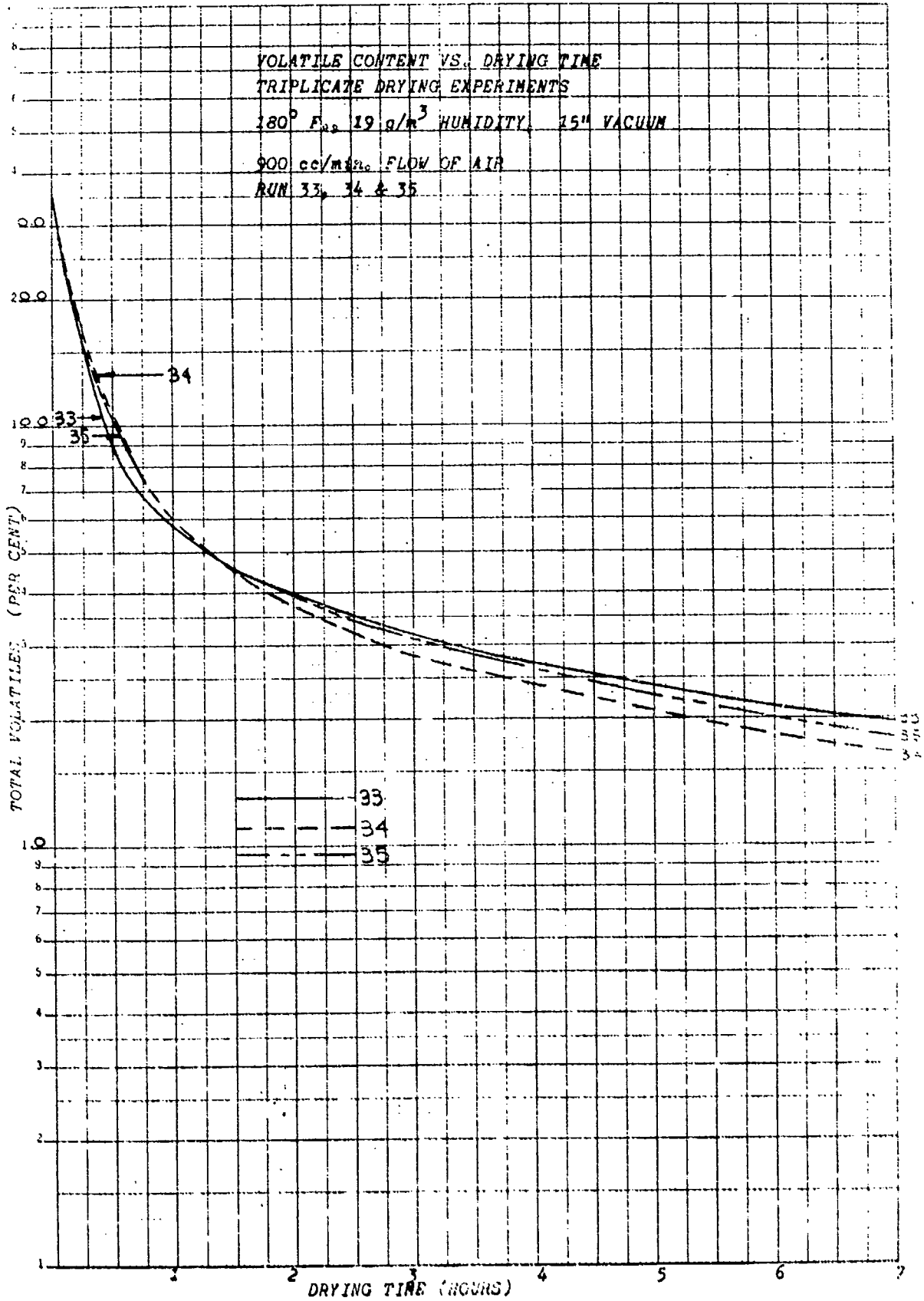


FIG. 14

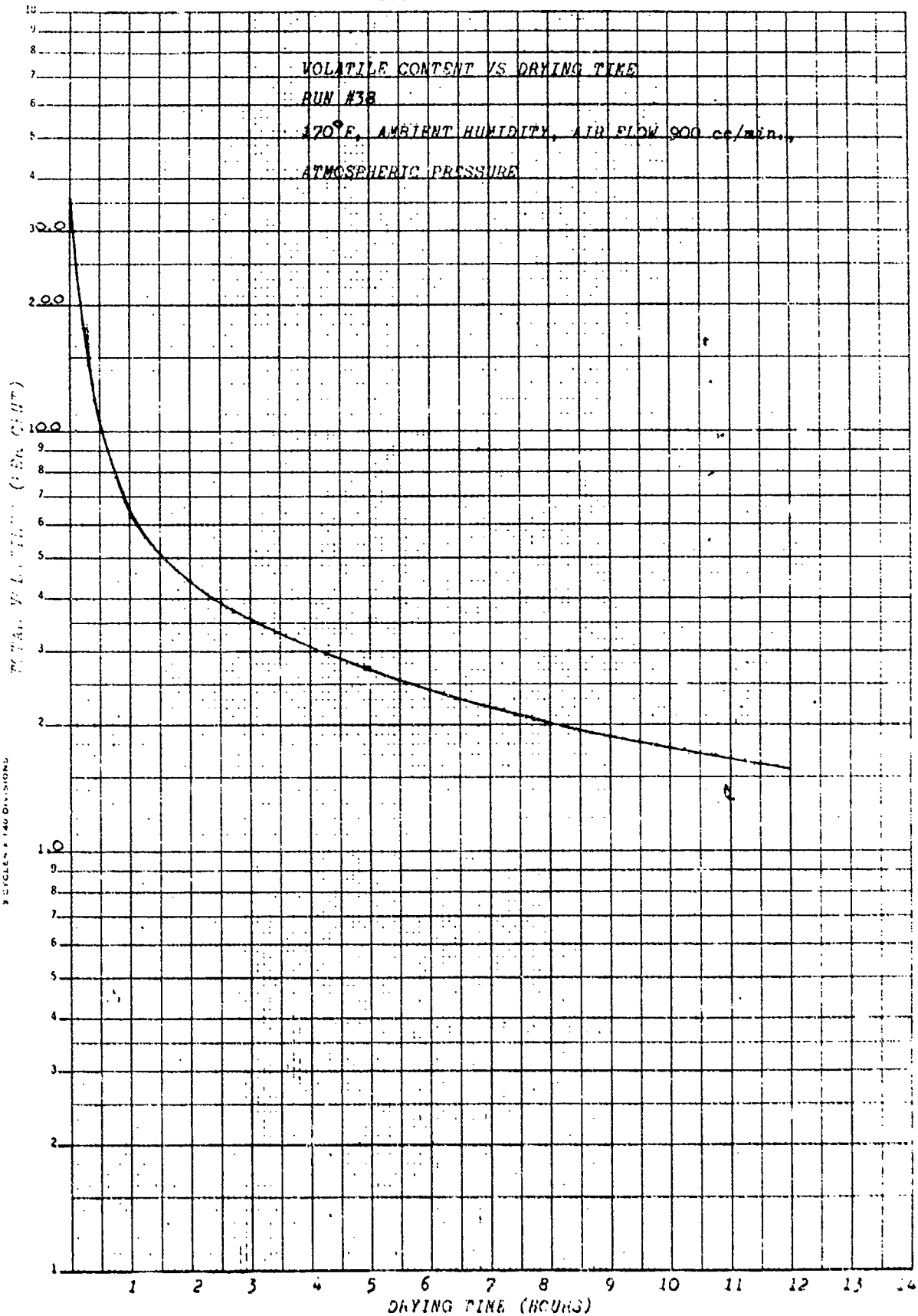


FIG. 14 VOLATILE CONTENT VS DRYING TIME  
 RUN #38 170°F, AMBIENT HUMIDITY, AIR FLOW 900 cc/min.,  
 ATMOSPHERIC PRESSURE

FIG. 15

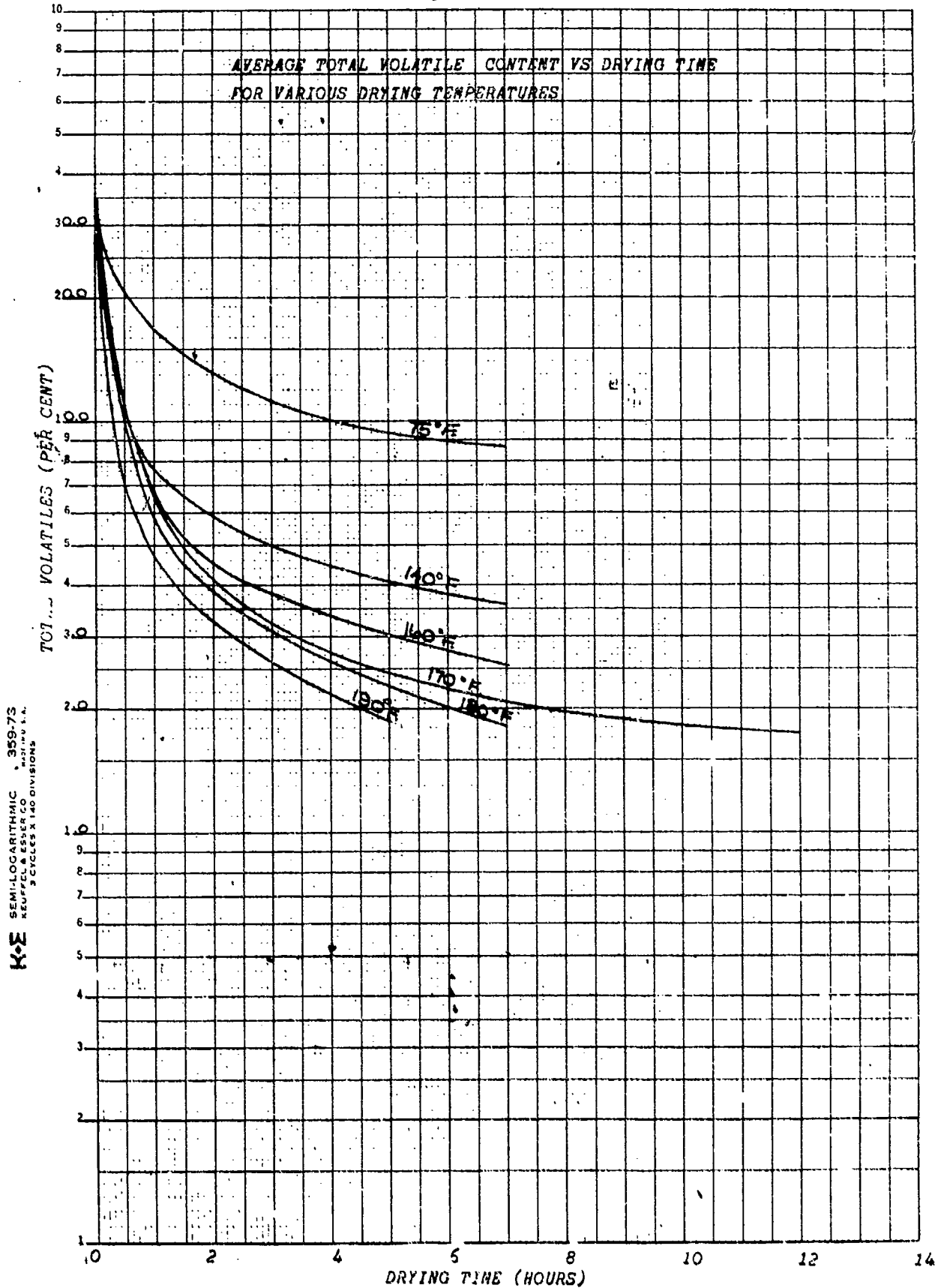


FIG. 16

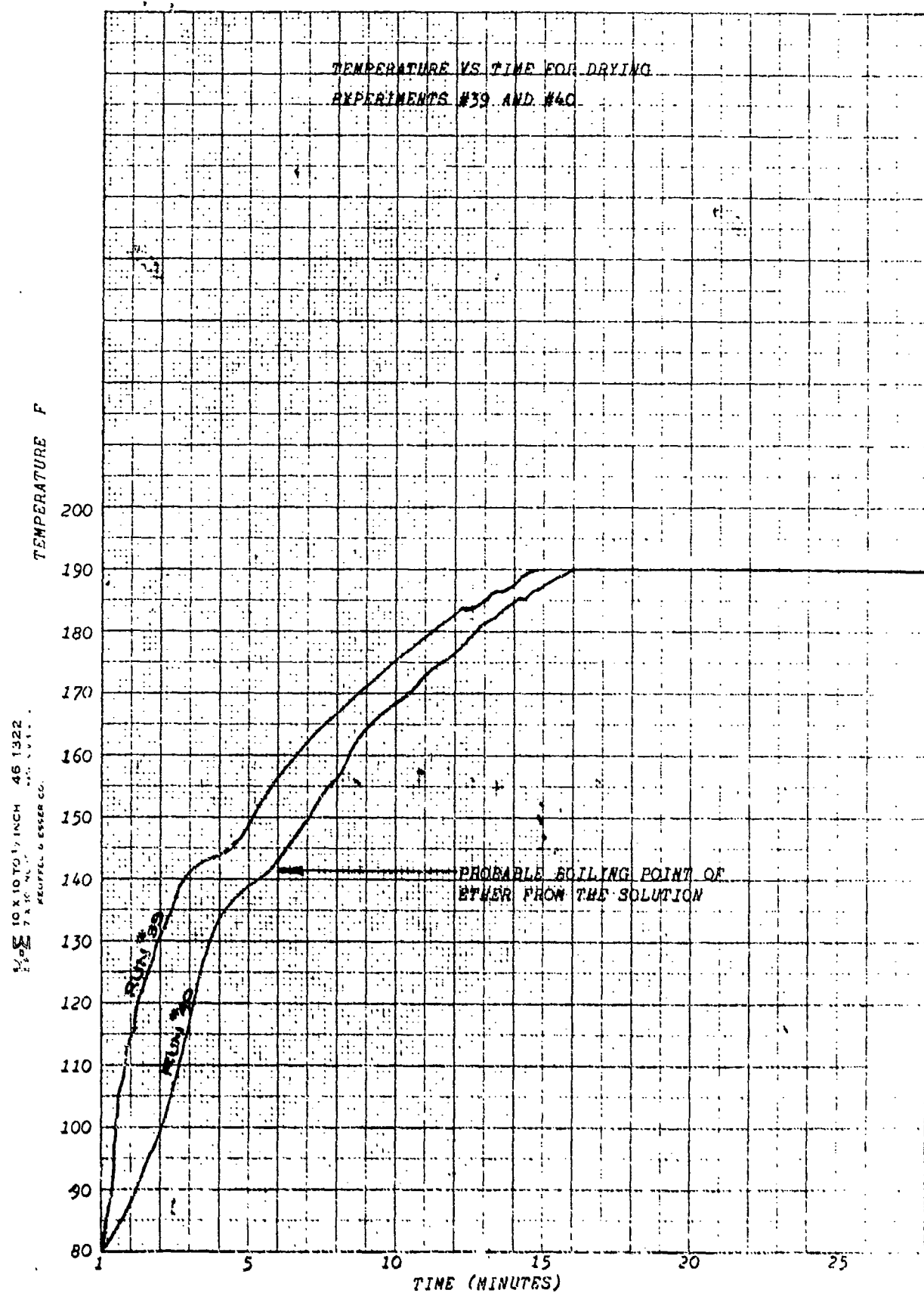


FIG. 17

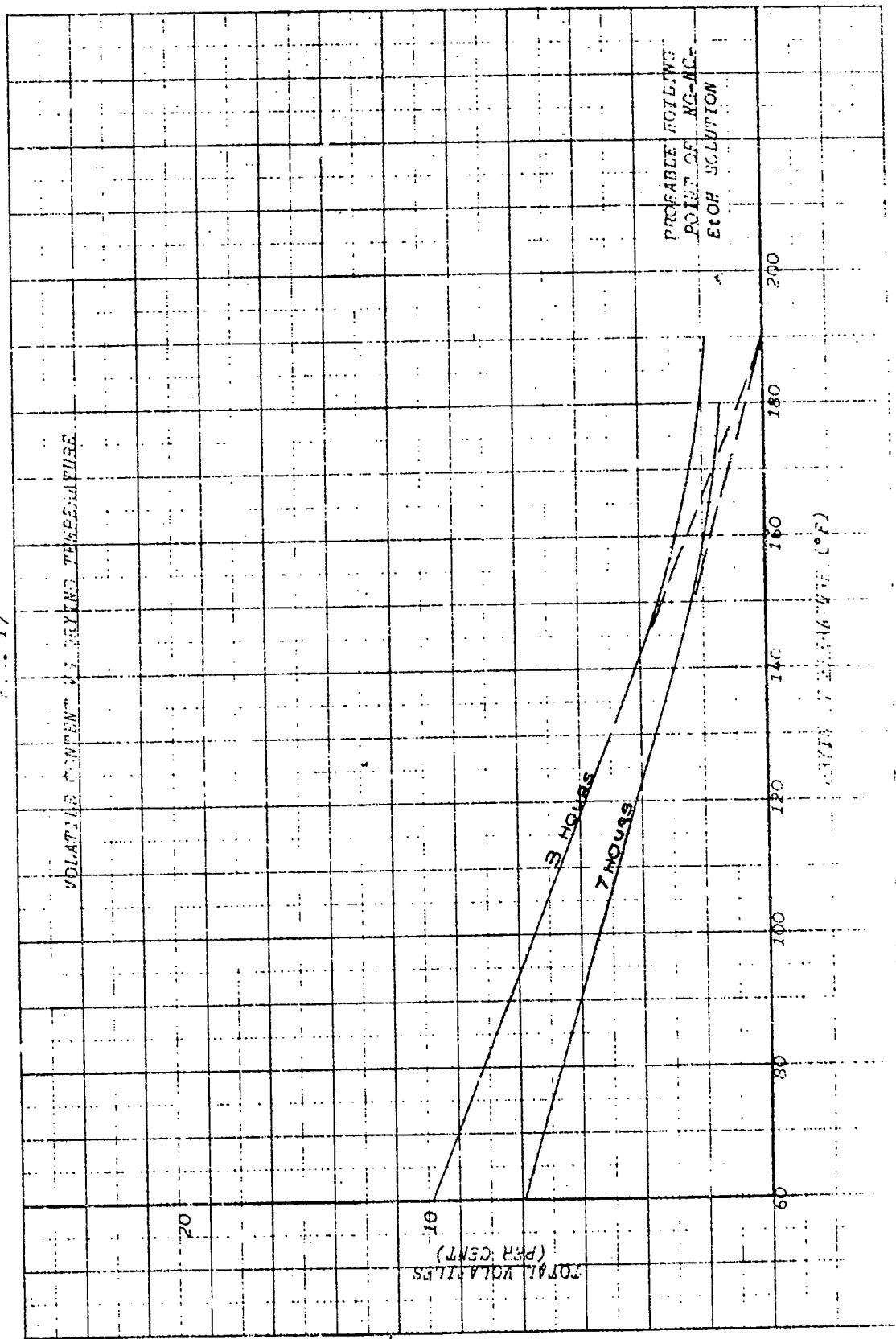




FIGURE 18  
End of propellant cylinder - Dried by  
NPP 10 days ,

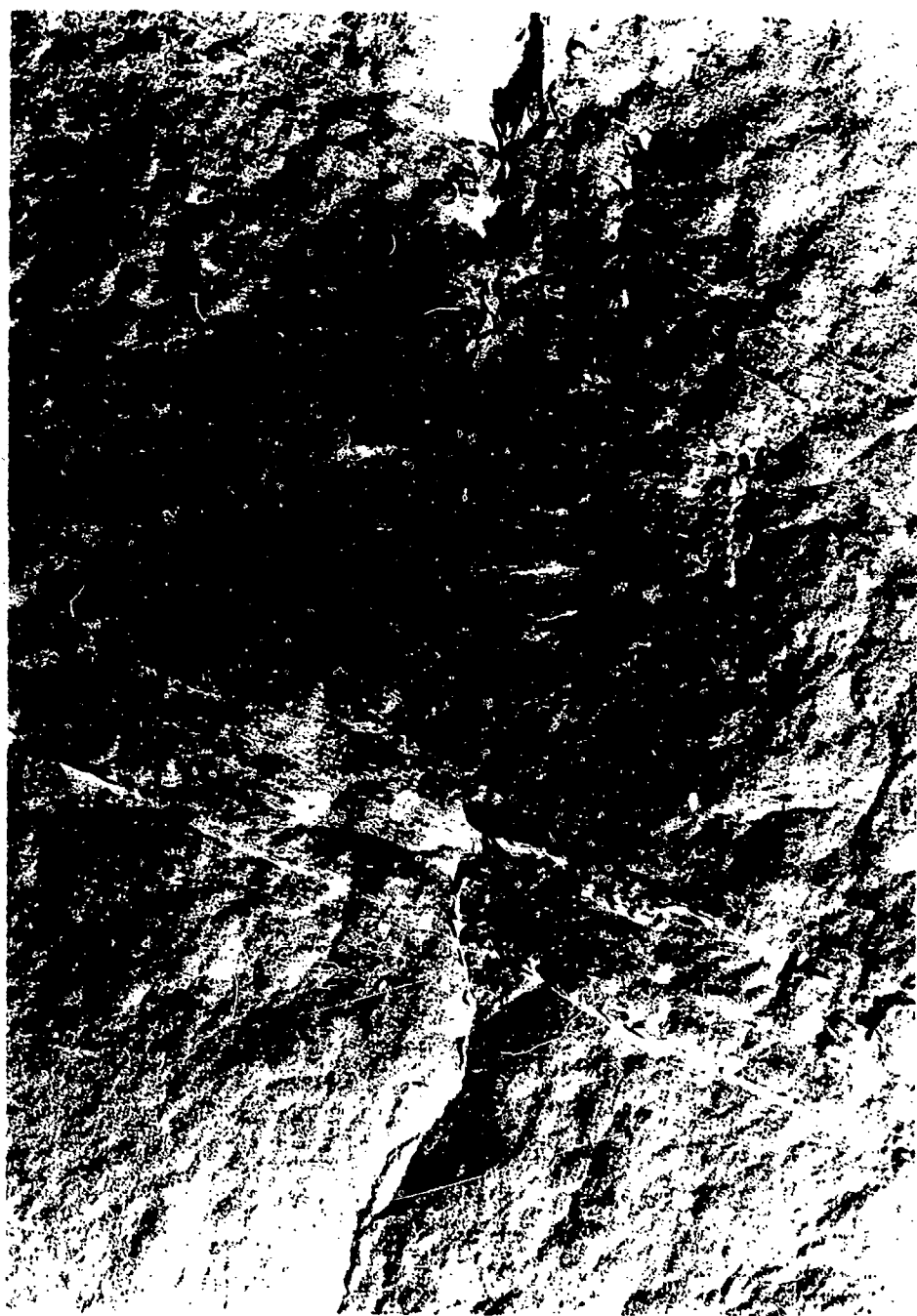


FIGURE 19  
Center cut cross section of propellant  
cylinder - Dried by NPP 10 days

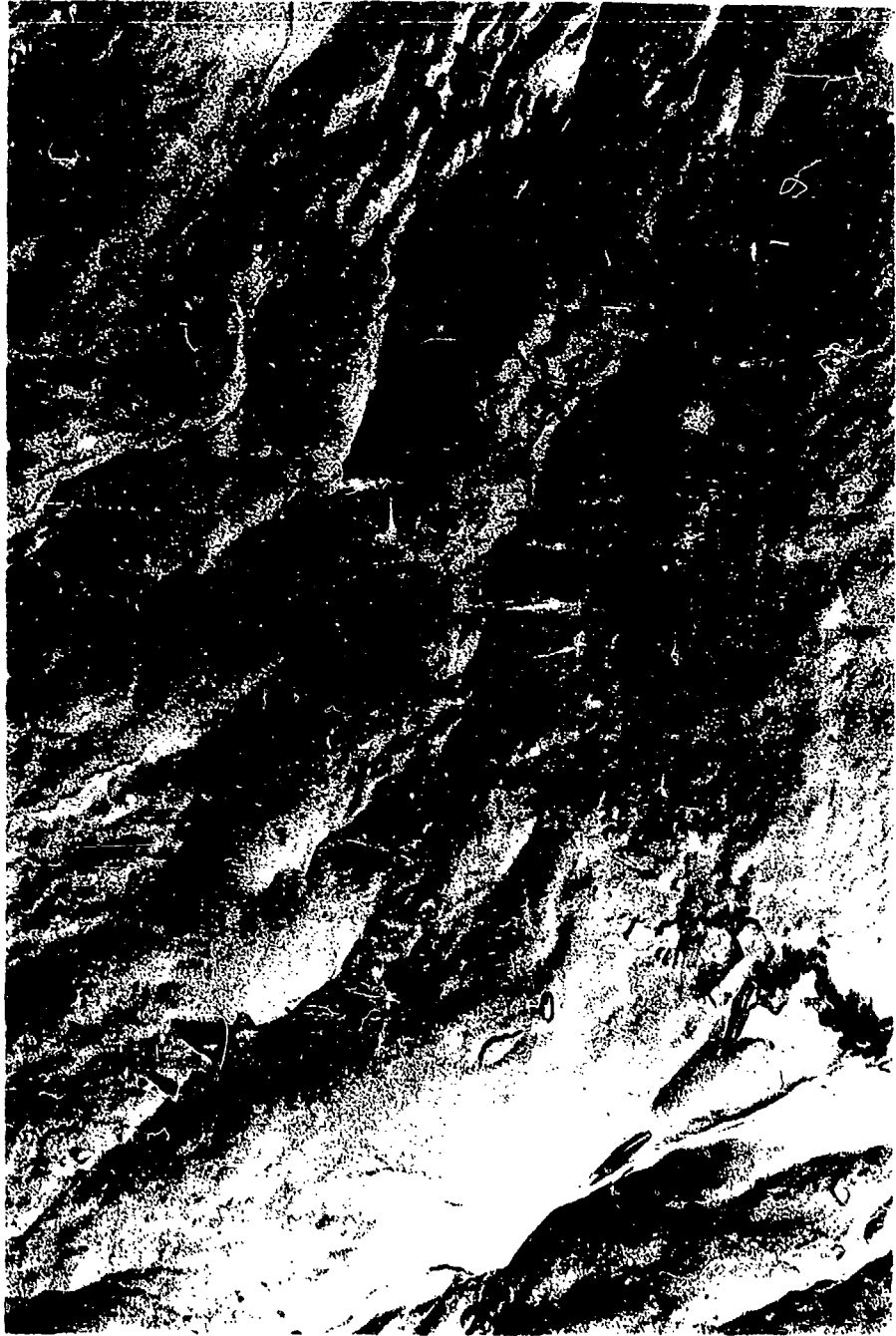


FIGURE 20  
End of propellant cylinder dielectrically  
dried (Experiment 45)



FIGURE 21  
Center cut cross section of propellant  
cylinder - Dielectrically dried  
(Experiment 45)

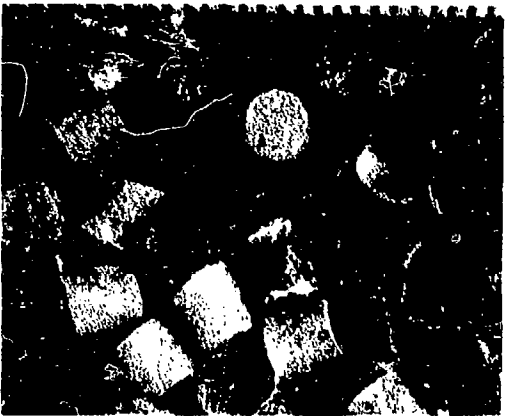
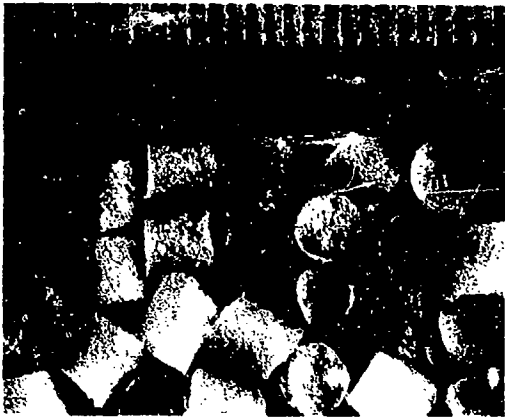


FIGURE 22  
Propellant dried 10 days by NPP

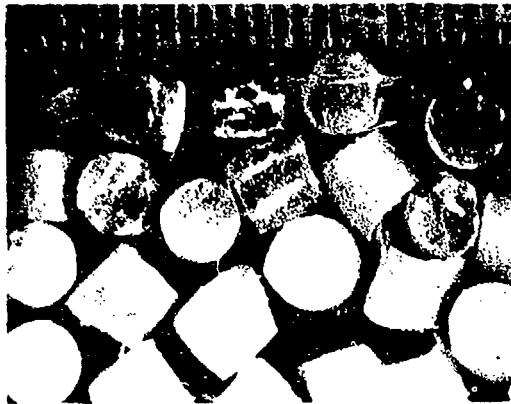
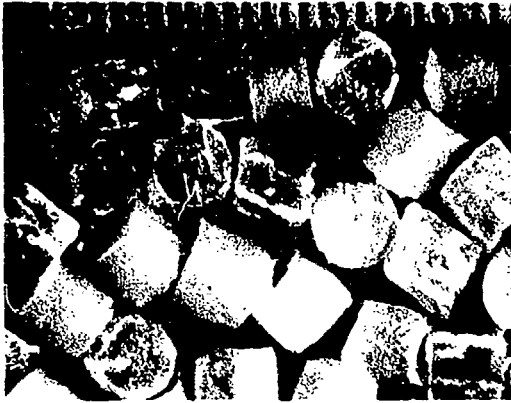


FIGURE 23  
Green propellant

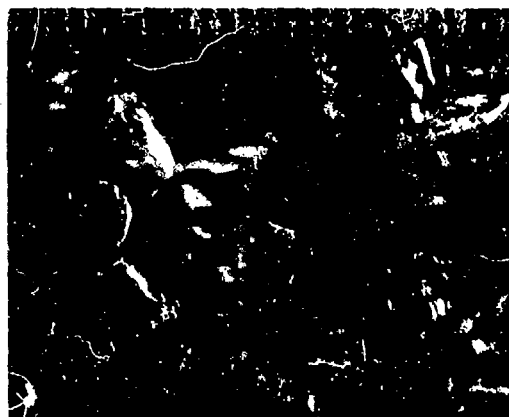


FIGURE 24  
Green propellant after 2 months storage  
at 37°F.

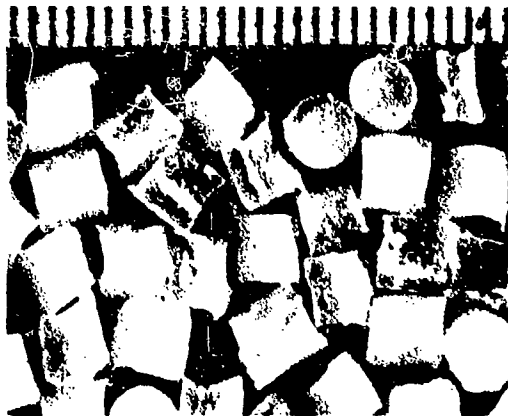
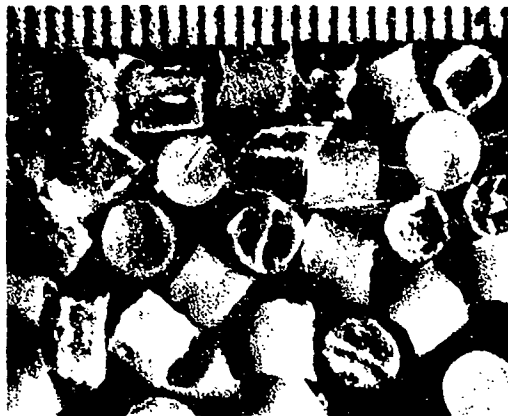


FIGURE 25  
Propellant dielectrically dried at 170°F  
for 12 hours (Experiment 37)



FIGURE 26  
Propellant dielectrically dried at 180°F  
for 7 hours (Experiment 49)

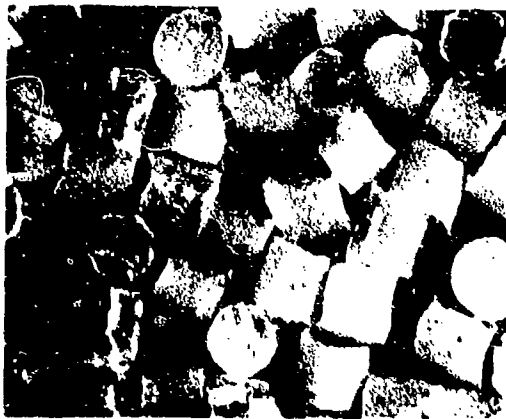
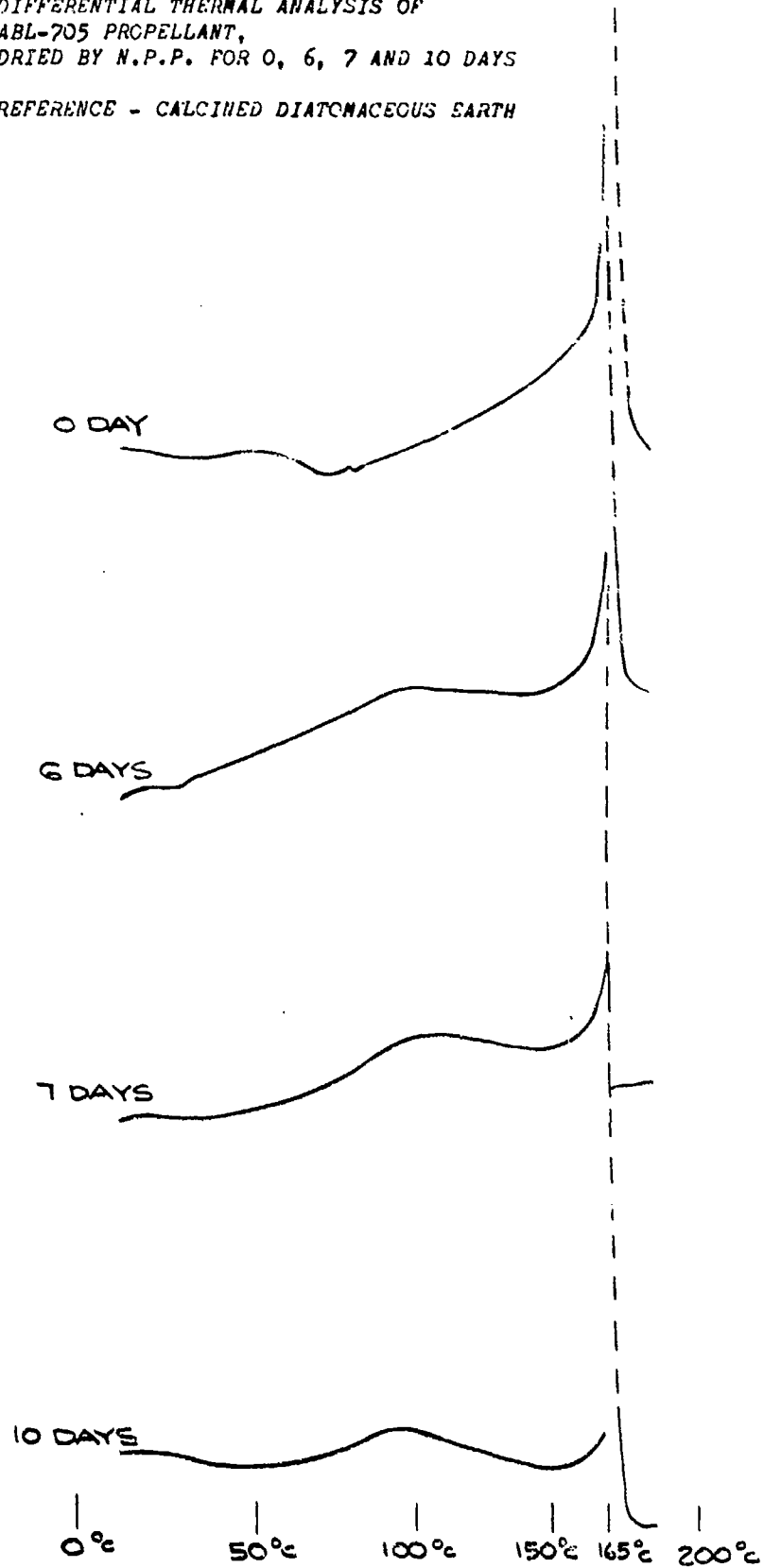


FIGURE 27  
Propellant dielectrically dried at 190°F  
for 5 hours (Experiment 50)

FIG. 28

DIFFERENTIAL THERMAL ANALYSIS OF  
ABL-705 PROPELLANT,  
DRIED BY N.P.P. FOR 0, 6, 7 AND 10 DAYS

REFERENCE - CALCINED DIATOMACEOUS EARTH



358-60  
SEMILOGGRAPHIC  
PAPER

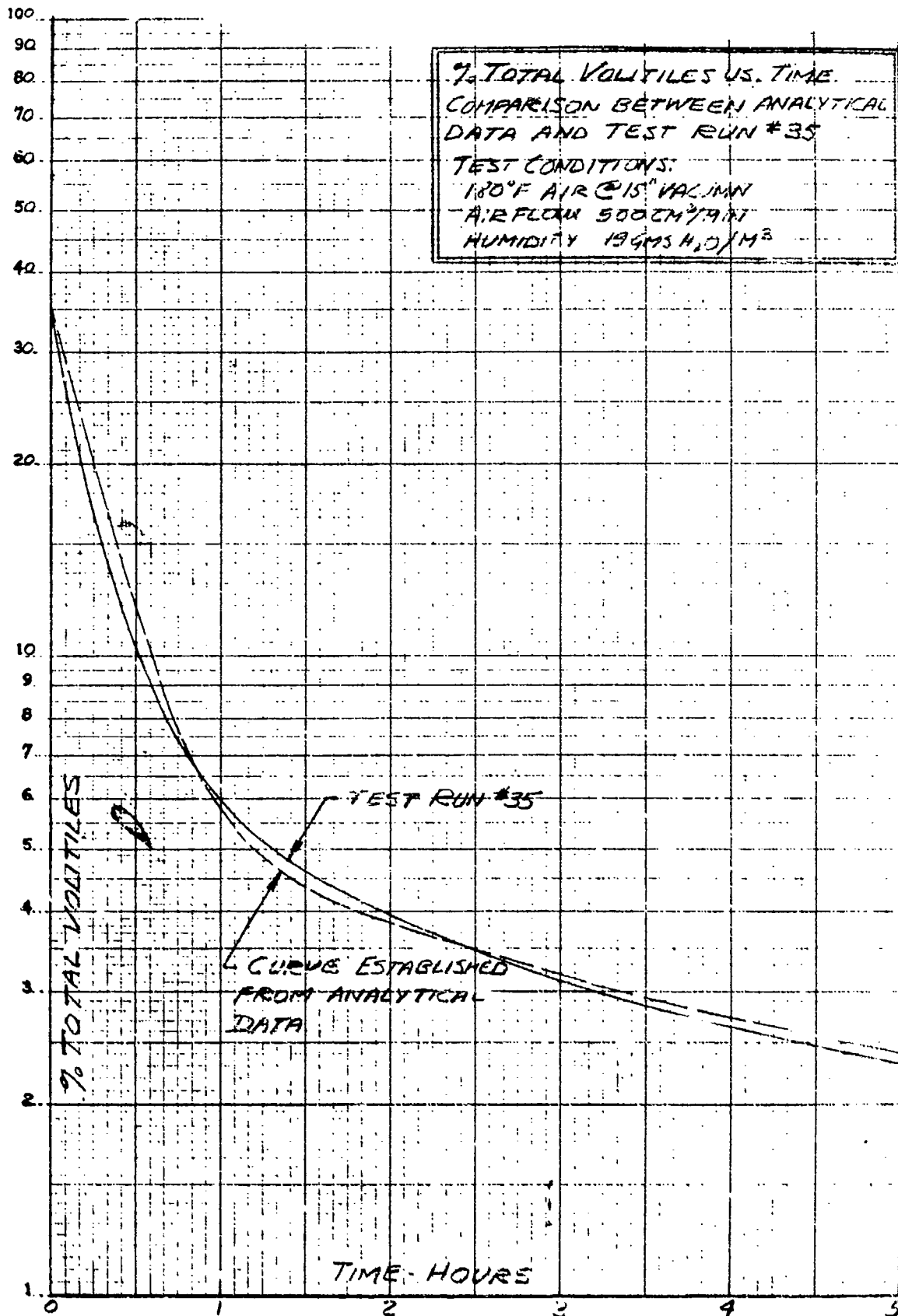


FIGURE #29

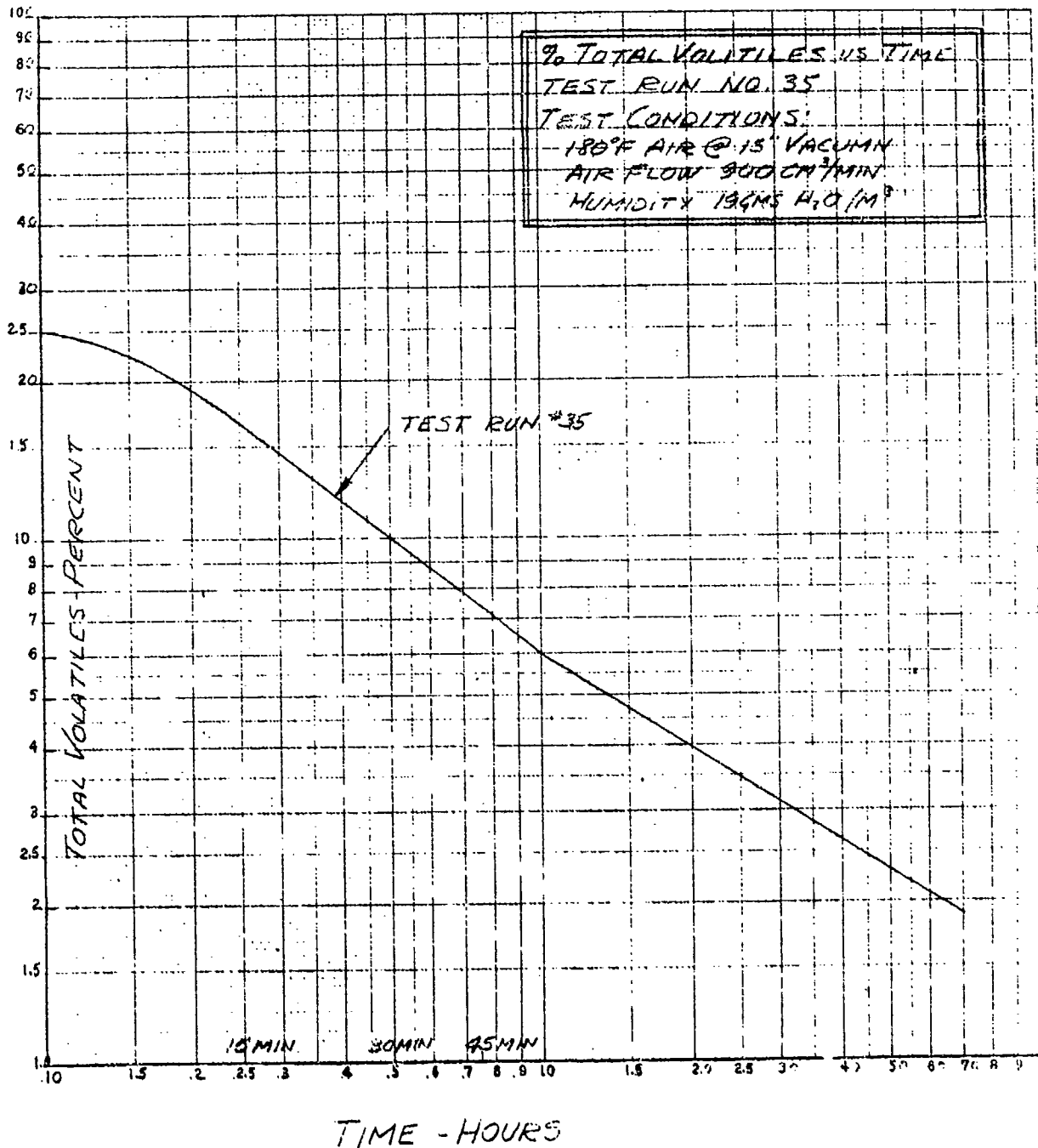


FIGURE 30

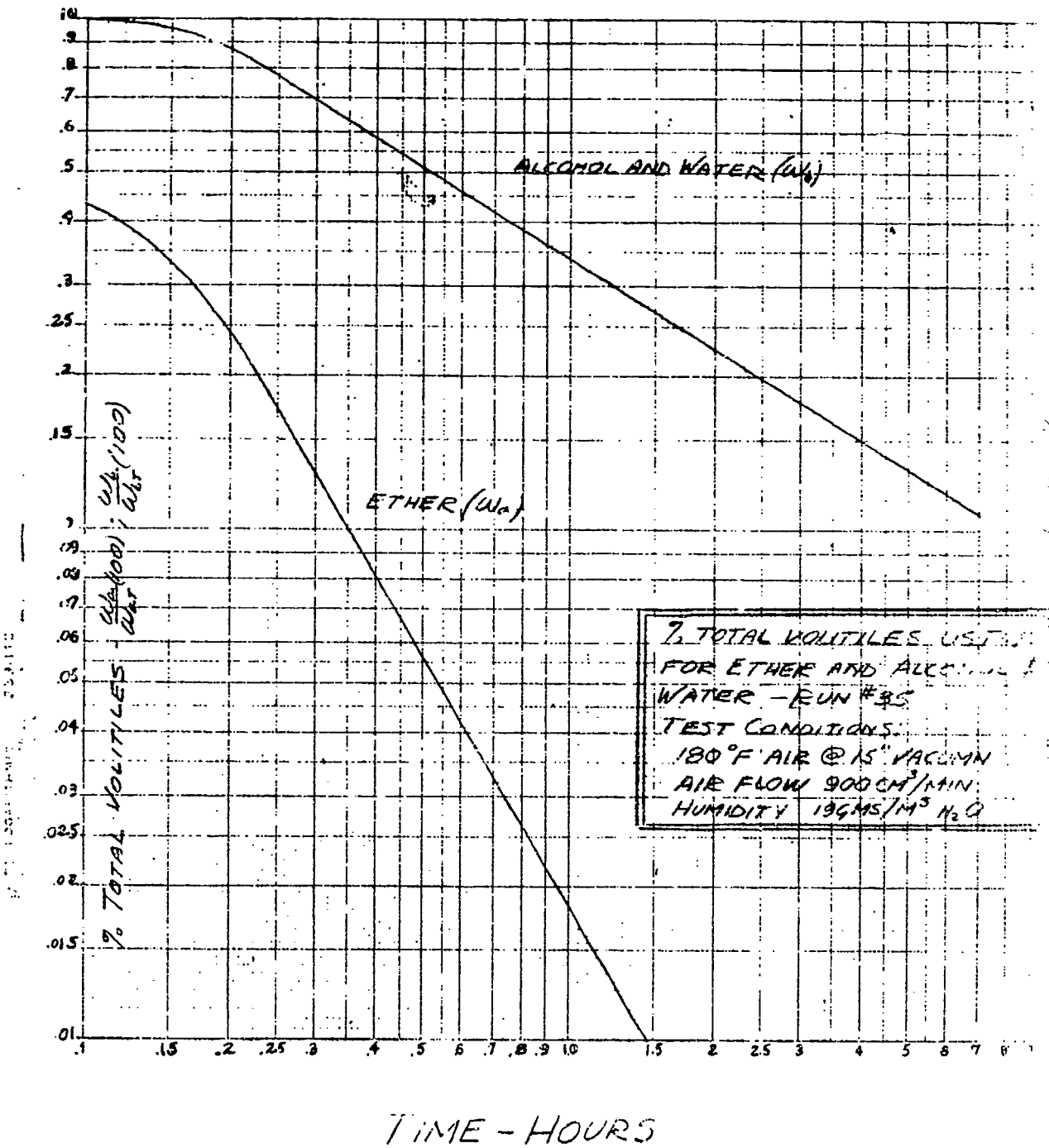
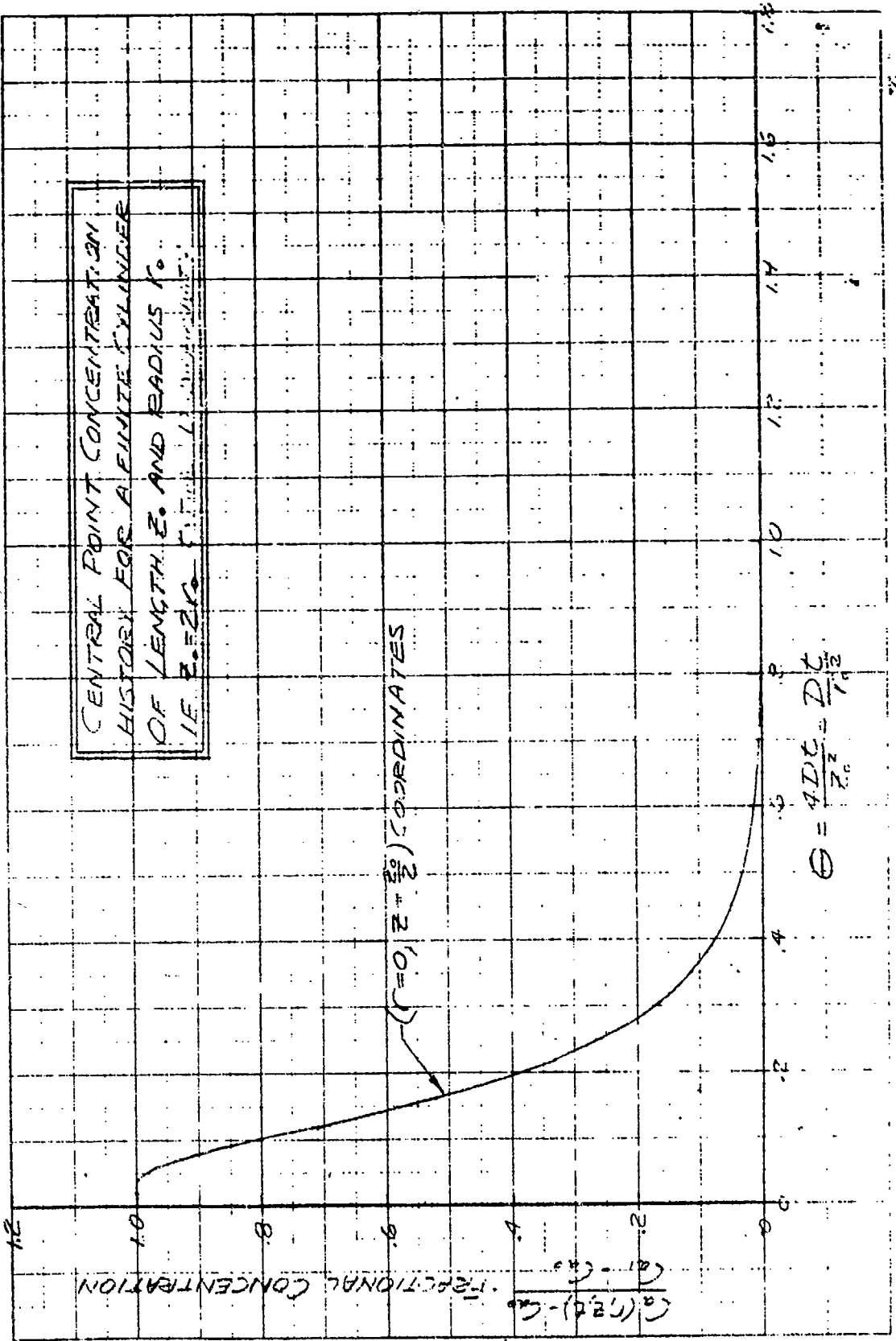
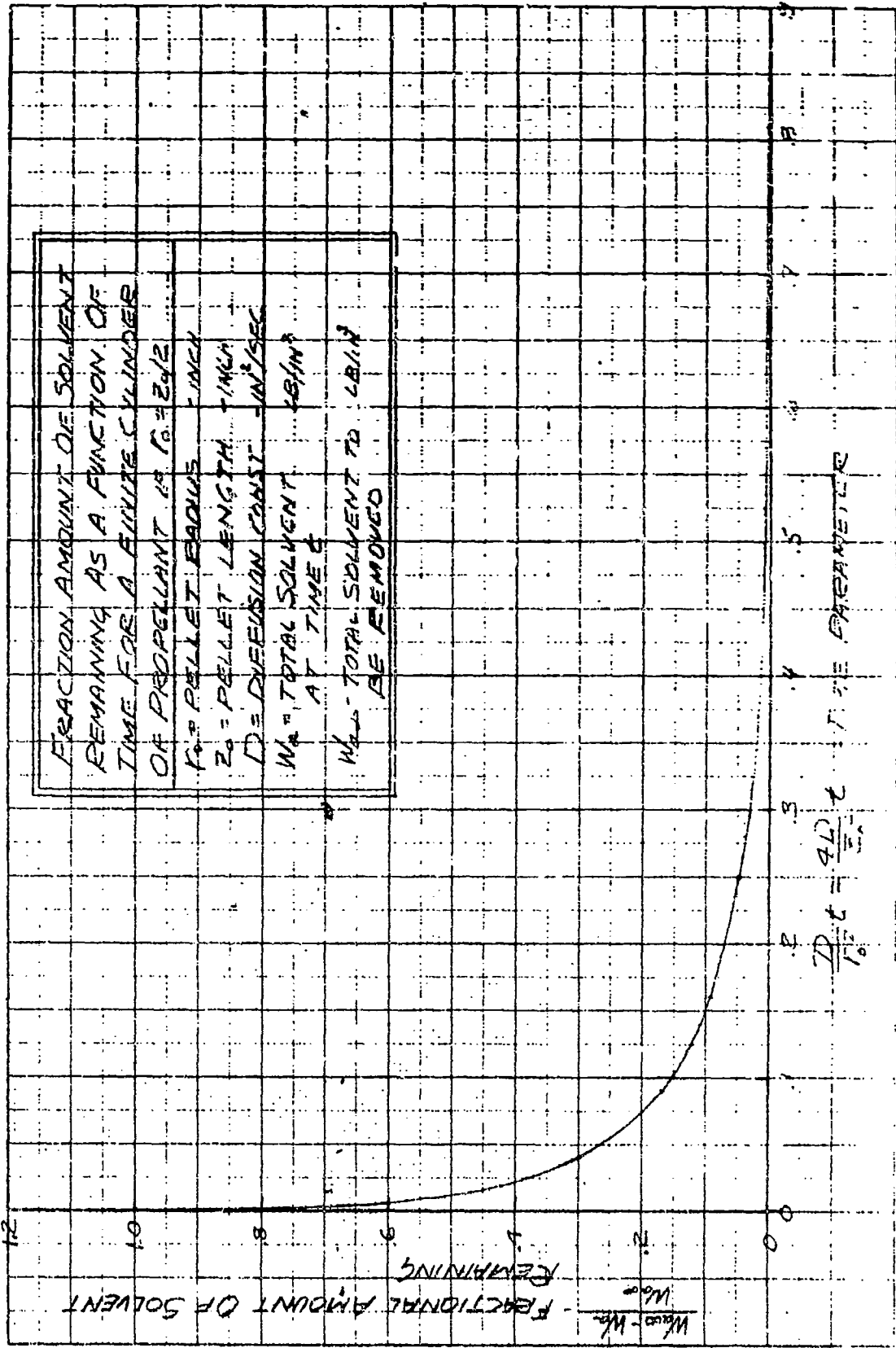
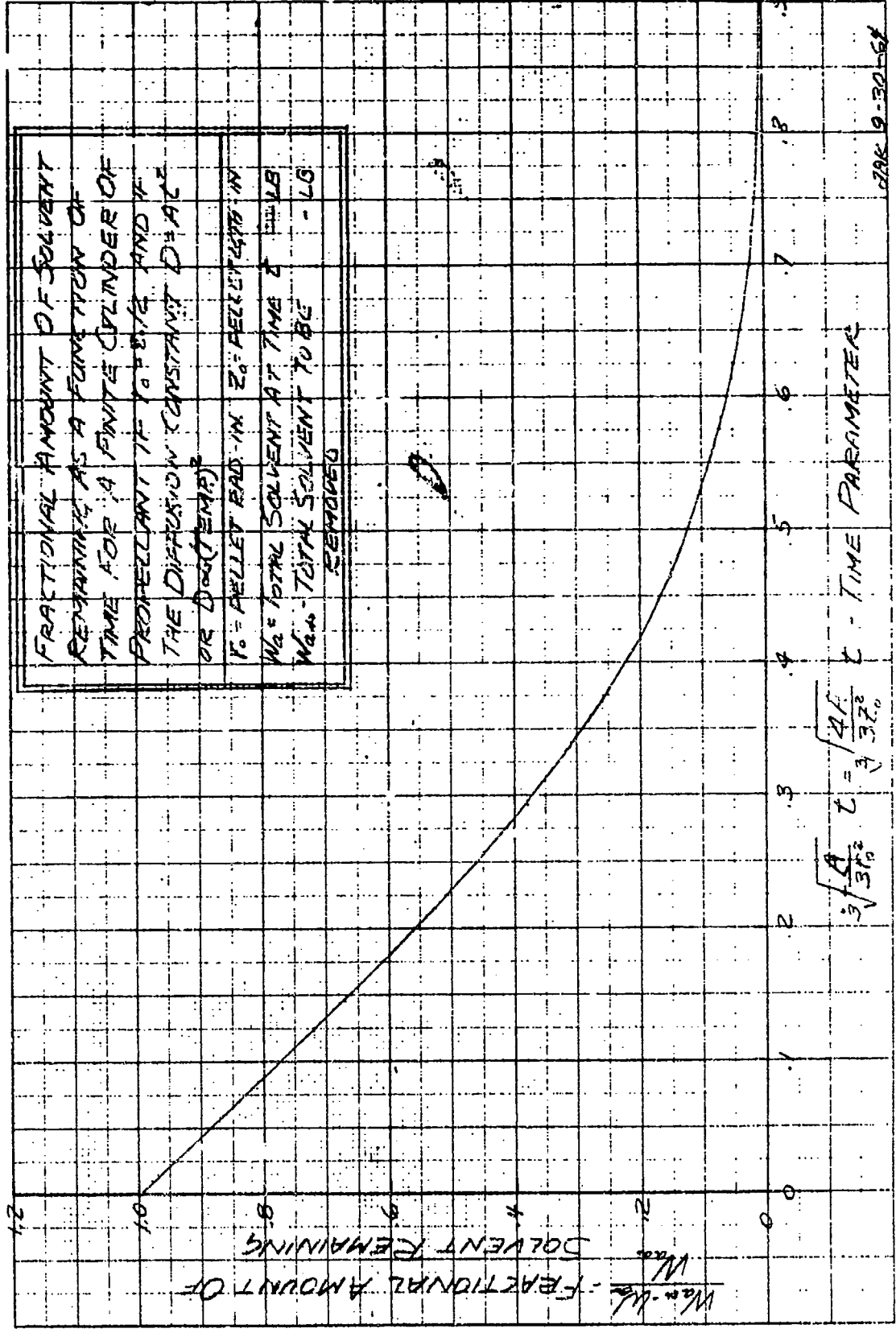


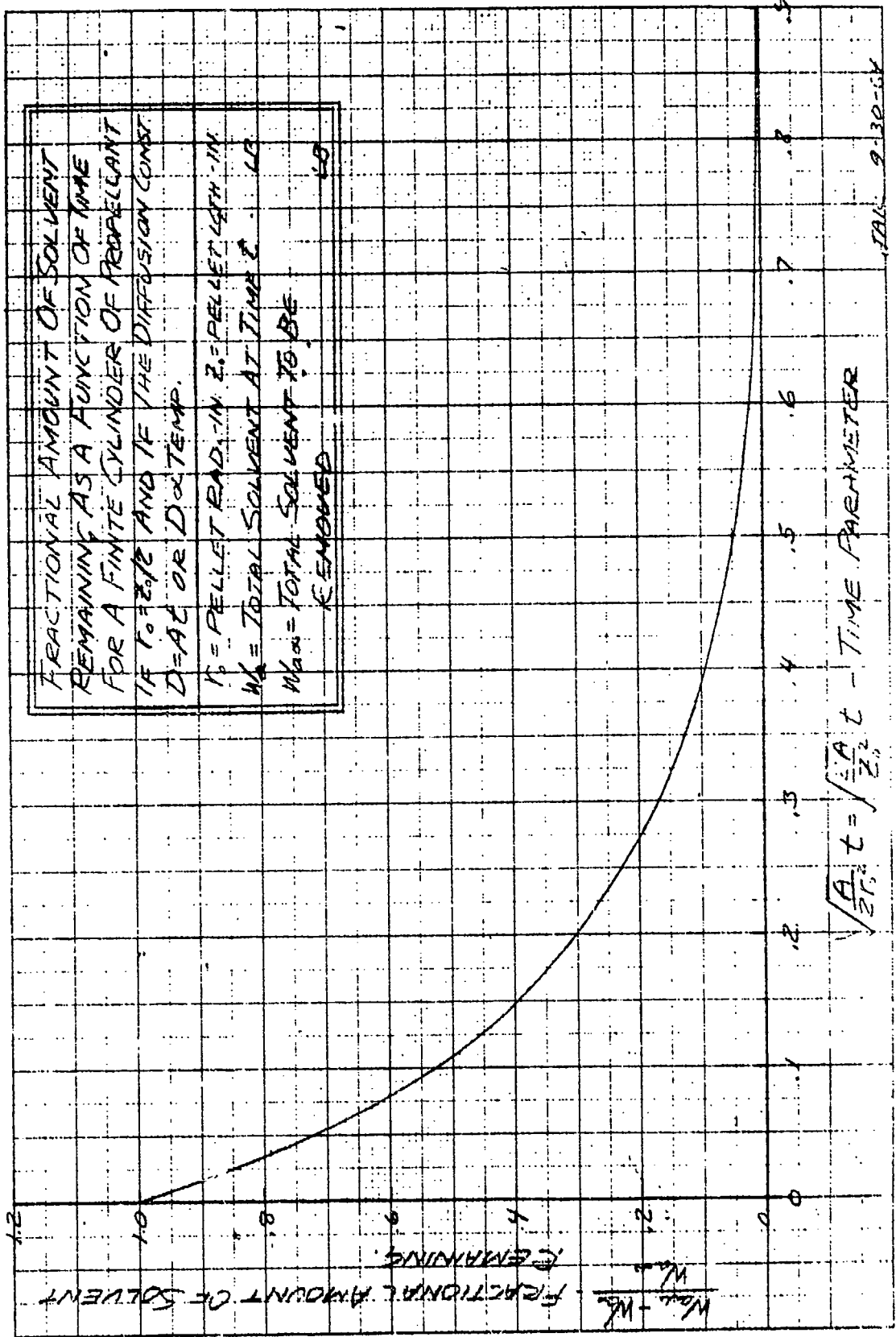
FIGURE #31

CENTRAL POINT CONCENTRATION HISTORY FOR A FINITE CYLINDER OF LENGTH  $z_0$  AND RADIUS  $r_0$  IF  $z = z_0/2$









TAK 9-30-54

LIST OF TABLES

Table 1 - Comparison of N.P.P. & P&W Total Volatile Analysis Results

Table 2 - Response Surface

Table 3 - Complete Summary of Results of Drying Experiments

Table 4 - Dimensional Analysis



TABLE #2

## RESPONSE SURFACE

(Experimental Results Are In Brackets)

	P1.2			P1.0			P.5			
	H0	H9.5	H19	F0	H9.5	H19	H0	H9.5	H19	
T70	A air	9.51	9.09	8.67	9.12	8.70	8.29	8.16	7.74	7.32
	A N2	8.80	8.38	7.96	8.41	7.99	7.57	7.45	7.03	6.61
	F500	8.14	7.72	7.30	(8.65)	8.23	7.81	9.95	9.53	9.11
	A air	7.45	6.99	6.57	7.92	7.50	7.08	9.25	8.83	8.41
	A air	7.03	6.61	6.19	8.27	7.85	7.43	11.38	10.96	10.54
	A N2	6.37	5.95	5.53	7.60	7.18	6.76	10.69	10.27	9.85
T140	A air	5.17	4.75	4.33	4.78	4.36	3.95	(3.82)	3.40	2.98
	A N2	4.46	4.04	3.62	4.07	3.65	3.23	3.11	2.69	2.27
	F500	4.64	4.22	3.80	(4.31)	3.89	(3.47)	(3.51)	3.09	2.67
	A air	3.95	3.53	3.11	(3.62)	3.20	2.78	2.81	2.39	1.97
	A air	4.20	3.78	3.36	(3.93)	3.51	3.09	3.26	2.84	2.42
	A N2	(3.54)	3.12	2.70	3.26	2.84	2.42	2.57	2.15	1.73
T160	A air	3.93	3.51	3.09	3.54	3.12	2.71	(2.58)	2.16	1.74
	A N2	3.22	2.80	2.38	2.83	2.41	1.99	1.87	1.45	1.03
	F500	3.64	3.22	2.80	3.07	2.65	2.23	1.67	1.25	0.83
	A air	2.95	2.53	2.11	2.38	1.96	1.54	0.97	0.55	0.13
	A air	3.40	2.98	2.56	(2.69)	2.27	1.85	0.94	0.52	0.10
	A N2	2.74	2.32	1.90	2.02	1.60	1.18	0.25	-0.17	-0.59

## CODE

Temperature	Pressure	Gas Flow Rate	Humidity	Type of Gas
T70 = T-3 = 70°F	P1.2 = 1.2 atmosphere	F0 = 0 cc/min, H0 = 0 gm/meter <sup>3</sup>	= 0 gm/meter <sup>3</sup>	A air = A .8 = air
T140 = T 4 = 140°F	P1.0 = 1.0 atmosphere	F500 = 500 cc/min, H 9.5 = 9.5 gm/meter <sup>3</sup>	= 9.5 gm/meter <sup>3</sup>	A N2 = A1.0 = nitro gen
T160 = T 6 = 160°F	P .5 = .5 atmosphere	F900 = 900 cc/min, H19 = 19.0 gm/meter <sup>3</sup>	= 19.0 gm/meter <sup>3</sup>	

TABLE #3

Complete Summary of Results of Drying Experiments

Run	H	P	F	A	T	Time	T.V.	N.G.	Remarks
	g/m <sup>3</sup>	atm.	cc/min.	—	°F	hrs	%	%	
1									
2	"	"	"	"	"	"			
3	"	"	"	"	"	"			
4	"	"	"	"	"	"			
5	"	"	"	"	"	"			
6	"	"	"	"	"	"			
7	0	.5	0	a	140	7	3.87		
8	0	1	500	a	140	7	4.58		
9	0	1	500	a	75	7	8.50		
10	0	1	500	N	140	7	3.58		
11	0	1.2	900	N	140	7	3.73		
12	D I S C O N T I N U E D								
13	0	1	500	N	140	7	3.43		Operating error
14	0	1	900	a	160	7	2.48		
15	0	.5	0	a	160	7	2.49		
16	0	1	900	a	140	7	3.80		
17	19	1	500	a	140	7	3.46		
18	0	.5	0	a	160	7	2.49		
19	0	.5	500	a	140	7	3.67		
20	0	.5	0	a	160	7	2.63		
21	0	1	500	N	170	7	1.79		
22	0	.5	0	a	160	7		11.80	
23	0	1	500	N	170	7		11.79	
24	0	1	500	N	140	7		12.11	
25	0	1	500	N	160	7		12.19	
26	0	.5	900	N	160	7		2.33	
27	19	.5	900	N	160	7		1.37	T.V. believed to be in error
28	19	.5	900	N	160	7		2.29	
29	19	.5	900	a	160	7		2.52	
30	19	.5	900	a	160	7		2.64	
31	19	.5	900	a	170	7		2.00	
32	19	.5	900	a	170	7		2.14	
33	19	.5	900	a	180	7		1.99	

TABLE #3 (Cont'd)

Run	H	P	F	A	T	Time	T.V.	N.G.	Remarks
	g/m <sup>3</sup>	atm.	cc/min.		°F	hrs.	%	%	
34	19	.5	900	a	180	7	1.67		Some propellant darkened around thermometer
35	19	.5	900	a	180	7	1.81		" "
36	19	.5	900	a	180	7			H <sub>2</sub> O by Karl Fisher - 0.25%
37	amb.	1	900	a	170	12	1.91		
38	amb.	1	900	a	170	12	1.58		Reached 190°F in 15 minutes
39	0	1	900	N	190	1/4	8.0		
40	0	1	900	N	190	1/2	5.76		
41	0	1	900	N	190	3/4	4.56		
42	0	1	900	N	190	1 1/2	3.27		Very little darkening of propellant around thermomete
43	0	1	900	N	190	5	1.87		Propellant darkened around thermometer
44	{ 0	{ 1	{ 900	{ N	{ 190	{ 1	{ 2.61		Ran one hour at 190°F and six hours at 160°F
	{ 0	{ 1	{ 900	{ N	{ 160	{ 6			
45	{ 0	{ 1	{ 900	{ N	{ 190	{ 1	{ 2.37		Ran one hour at 190°F and six hours at 160°F
	{ 0	{ 1	{ 900	{ N	{ 160	{ 6			Electron micrographs obtained on this sample
46	{ 0	{ 1	{ 900	{ N	{ 190	{ 1	{ 2.29		Ran one hour at 190°F and six hours at 160°F
	{ 0	{ 1	{ 900	{ N	{ 160	{ 6			
47	{ 0	{ 1	{ 900	{ N	{ 190	{ 1			Discontinued experiment - operating error
	{ 0	{ 1	{ 900	{ N	{ 160	{ 6			
48	{ 0	{ 1	{ 900	{ N	{ 190	{ 1			Ran one hour at 190°F and six hours at 160°F
	{ 0	{ 1	{ 900	{ N	{ 160	{ 6			
49	0	1	900	N	180	7	11.93		Samples sent to N.P.P. for inspection and nitro-
50	0	1	900	N	190	5	12.08		glycerine analysis

CODE

H = humidity in drying chamber  
P = pressure in drying chamber  
F = flow of gas through drying chamber  
A = type of gas in drying chamber,  
i.e. a = air, N = nitrogen  
T = drying temperature of propellant

Time = drying time  
T.V. = total volatile analysis results at end  
of drying time  
N.G. = nitroglycerine analysis results at end  
of drying time

TABLE #4

Dimensional Analysis

	<u>Average Diameter (inch)</u>	<u>Average Length (inch)</u>
Run 50 (190° F - 5 hours)	.0391	.0381
Run 49 (180° F - 7 hours)	.0394	.0375
Run 37 (170° F -12 hours)	.0391	.0378
N.P.P. dried 10 days by preserve process	.0388	.0387
Green propellant	.0451	.0410
Green propellant (after 2 months storage at 37° F)	.0429	.0403

#### REFERENCES

1. Perry, J. "Chemical Engineers Handbook" McGraw-Hill Book Company, Third Edition, 1950.
2. Rohsenow, W. and Choi, H. "Heat, Mass, and Momentum Transfer" Prentice-Hall, Inc., 1961.
3. Daniels, E. and Alberty, R. "Physical Chemistry" John Wiley & Sons, Inc., 1955.
4. McGraw-Hill Encyclopedia of Science and Technology, Vol. 7, 1960, p. 158.
5. Ball, A.M. "Nitrocellulose Base Propellants" Chemical Engineering Progress, Part I, Vol. 57, No. 9, September, 1961, pp. 80-82.
6. "U.S. In Space" Chemical and Engineering News, September 30, 1963, p. 75.
7. Lange, N. "Handbook of Chemistry" Handbook Publishers, Inc. Third Edition, 1950.

APPENDIX I

POWER REQUIREMENTS

Double base propellant = 30% total volatiles  
(15% alcohol and 15% ether)

Specific heat of propellant = .35 BTU/lb/°F

Heat of vaporization of alcohol = 367 BTU/lb

Heat of vaporization of ether = 162 BTU/lb

Heat to raise propellant to temperature

$$= (.35 \text{ BTU/lb/}^\circ\text{F}) (140^\circ\text{F} - 57^\circ\text{F}) (1 \text{ lb})$$
$$= 29.05 \text{ BTU}$$

Heat to vaporize solvents -

Alcohol - (367 BTU/lb) (1 lb) (.15) = 55.0 BTU

Ether - (162 BTU/lb) (1 lb) (.15) = 24.3 BTU

Total heat required to dry one pound of propellant

$$= 29.05 + 55.0 + 24.3 = 108.05 \text{ BTU}$$

Assume 25 per cent efficiency of heating process (50 per cent electrical efficiency of dielectric dryer) x (50 per cent thermal efficiency because of convection and radiation losses); .50 x .50 = .25

Total heat = 432.2 BTU

but 3413 BTU = 1 KW-hr

Total heat =  $432.2 \div 3413 = .1268$  KW-hr per pound of propellant

Dielectric heater output size needed

$$= (0.1268 \text{ KW-hr/lb}) (250 \text{ lbs/hr}) = 31.8 \text{ KW}$$

Cost of electricity to dry one pound of propellant

$$= 0.1268 \text{ KW-hr/lb} (\$0.018/\text{KW-hr}) = \$0.00228/\text{lb}$$

## APPENDIX II

### DIFFUSION OF A SINGLE COMPONENT FROM A DOUBLE BASE PROPELLANT WHICH IS ASSUMED TO BE A NON-REACTIVE STATIONARY MEDIUM

Dielectric heating of a cylindrically shaped double base propellant will be used to remove undesirable residual solvents of ether and alcohol and a small quantity of water.

An analytical investigation of the drying of solvents from a double base propellant containing nitrocellulose and nitroglycerine will be conducted.

Of the two solvents present, ether has a higher vapor pressure than alcohol; consequently, this constituent is more easily removed than alcohol. During the drying of the propellant the temperature reached inside the pellet probably exceeds the vapor pressure of ether but not the vapor pressures of alcohol and water; thus, in its simplest analysis, the drying of the propellant is largely a problem of the removal of alcohol and water. The ether will diffuse faster than the alcohol and water. The analytical investigation which follows will assume that alcohol and water mixture is to be removed.

Mass transport mechanisms can be one of three types. They are:

- 1) Vaporization and recondensation of liquid within the media or motion of the vapor phase.
- 2) Viscous flow of liquid due to thermal and vapor pressure gradients.
- 3) Viscous flow of liquid due to the gradient of capillary pressure which is caused by the dependence of surface tension on temperature gradients.

For the case considered, the phenomenon of mass transport is type 2 or the viscous flow of constituents due to thermal and vapor pressure gradients. If a uniform concentration of solvents is assumed to exist initially and dielectric heating of the propellant is investigated, the temperature of the propellant will be uniform initially. However, due to the temperature increase, some of the solvent will diffuse across the boundary of the solid and a concentration gradient will be immediately established. Since a concentration gradient exists at this point, in time the dielectric heating of the propellant will no longer be uniform but will concentrate at points of higher resistivity. This is so because the propellant is more resistive and less capacitive at points of high solvent concentration and less resistive and more capacitive at points of low solvent concentration.

The drying process can be considered as occurring in two separate

regimes. Initially, drying will occur at a constant rate since the surface of the solid will have free liquids and the evaporation rate will be governed by environmental conditions. Pressure, humidity, flow rate, and environmental temperature will, during this period of time, have a significant effect on the drying of the solid propellant because the highest impedance to the mass diffusion of the solvents is at the surface of the cylindrical pellet. However, this constant evaporation rate period described above may be of very short duration; consequently, although control of the environment is most significant during this drying regime, the overall effect of environment will be minimized due to the longer drying cycle time of the second regime.

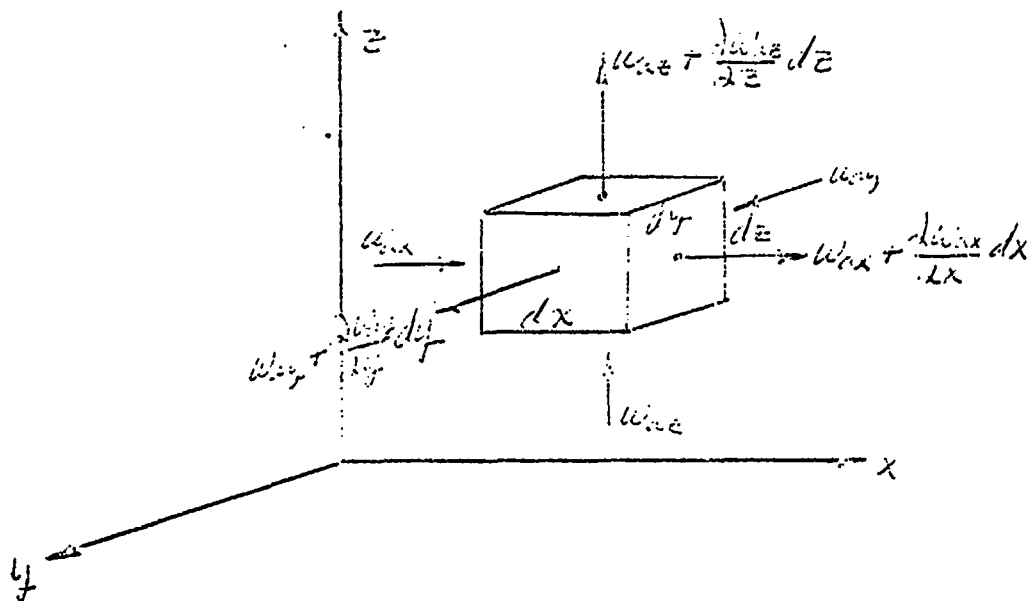
The second regime is the falling drying rate period which is the portion of the total drying cycle in which the surface of the solid is unsaturated and the internal diffusion characteristics of the propellant is the controlling drying mechanism. This appendix proposes to solve this problem which most significantly effects the total time cycle.

In retrospect, the general problem definition will be to determine how long it will take to remove the alcohol during the falling rate period with no environmental control. The propellant is assumed to have the form of a finite cylinder.

Definition of Parameters:

- $X$  - Coordinate in Cartesian frame of reference - inch  
 $Y$  - Coordinate in Cartesian frame of reference - inch  
 $Z$  - Coordinate in Cartesian frame of reference - inch  
 $r$  - Radial coordinate in cylindrical frame of reference - inch  
 $\theta$  - Angular coordinate in cylindrical frame of reference - inch  
 $C_A$  - Concentration of solvent "A" - lb/in<sup>3</sup>  
 $D$  - Diffusivity or coefficient of diffusion - in<sup>2</sup>/sec  
 $A$  - Diffusion area - in<sup>2</sup>  
 $W_A$  - Diffusion rate of solvent "A" - lb/sec  
 $\mu_A$  - Fluid viscosity of solvent "A" - lb/sec/in<sup>2</sup>  
 $\rho_A$  - Fluid density of solvent "A" - lb/in<sup>3</sup>  
 $C_{pA}$  - Specific heat of solvent "A" - BTU/lb<sup>o</sup>F  
 $K_A$  - Thermal conductivity of solvent "A" - BTU/in/sec<sup>o</sup>F  
 $\nu_A$  - Kinematic viscosity of solvent "A" - in<sup>2</sup>/sec  
 $Sc$  - Schmidt number  
 $Le$  - Lewis number  
 $Q_A$  - Storage of solvent "A" in control volume - lbs/sec  
 $Q_{pA}$  - Mass production rate - lbs/sec

Mass balance depicting the diffusion of a single component solvent  
"A" in a non-reactive stationary medium:



Assume that the mass production in the above control volume is  $Q_{pa}$ ; then the storage of the component "A" in the control volume is

$$dQ_{pa} = Q_{pa} dx dy dz \quad (1)$$

Furthermore, the rate of change of storage within the control volume is the product of the rate of change of concentration of  $C_a$  and the incremental volume  $dx dy dz$ .

$$dQ = \frac{dC_a}{dt} dx dy dz \quad (2)$$

From mass balance considerations, the storage  $dQ$  will equal the sum of the mass flow rates in the  $x, y, z$  directions and the rate of production of solvent "A"  $dQ_{pa}$ .

$$\frac{dC_a}{dt} dx dy dz = (w_{ax} - w_{ax} - \frac{dw_{ax}}{dx} dx) + \quad (3)$$

$$(w_{ay} - w_{ay} - \frac{dw_{ay}}{dy} dy) + (w_{az} - w_{az} - \frac{dw_{az}}{dz} dz) + Q_{pa} dx dy dz$$

From equation (3)

$$\frac{\partial C_a}{\partial t} = -\frac{\partial}{\partial x} \left( \frac{u_{ax}}{A} \right) - \frac{\partial}{\partial y} \left( \frac{u_{ay}}{A} \right) - \frac{\partial}{\partial z} \left( \frac{u_{az}}{A} \right) + C_a \quad (4)$$

However,  $Q_a = 0$  since no solvent "A" is assumed to be produced or immobilized during the diffusion and drying process

$$\frac{\partial C_a}{\partial t} = -\frac{\partial}{\partial x} \left( \frac{u_{ax}}{A} \right) - \frac{\partial}{\partial y} \left( \frac{u_{ay}}{A} \right) - \frac{\partial}{\partial z} \left( \frac{u_{az}}{A} \right) \quad (5)$$

From Fick's law of diffusion the concentration flux in the "n" direction is proportional to the change in concentration of fluid in the "n" direction, where  $D$  is the diffusivity or constant of proportionality.

$$\left( \frac{u_{an}}{A} \right) = -D \frac{\partial C_a}{\partial n} \quad (6)$$

Fick's law of diffusion for the  $x, y, z$  directions gives:

$$\left( \frac{u_{ax}}{A} \right) = -D \frac{\partial C_a}{\partial x} \quad (7)$$

$$\left( \frac{u_{ay}}{A} \right) = -D \frac{\partial C_a}{\partial y} \quad (8)$$

$$\left( \frac{u_{az}}{A} \right) = -D \frac{\partial C_a}{\partial z} \quad (9)$$

The diffusion flow continuity equation can now be obtained from equations 5, 7, 8 and 9.

$$\frac{\partial C_a}{\partial t} = D \left[ \frac{\partial^2 C_a}{\partial x^2} + \frac{\partial^2 C_a}{\partial y^2} + \frac{\partial^2 C_a}{\partial z^2} \right] = D \nabla^2 C_a \quad (10)$$

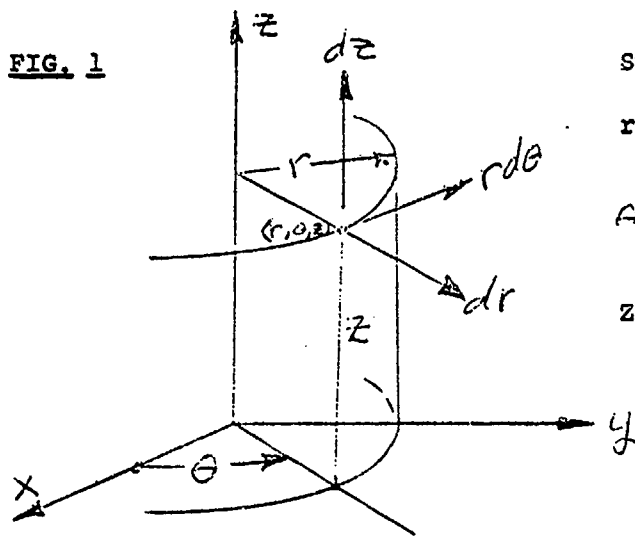
or

$$\frac{\partial C_a}{\partial t} = D \nabla^2 C_a \quad (11)$$

In order to solve the problem proposed, equations 10 and 11 should be transferred into cylindrical coordinates to conform to the geometry of the pellet.

At point  $(r, \theta, z)$  the three surfaces (cylindrical, vertical plane, and horizontal plane) are at right angles to each other and constitute an orthogonal set.

FIG. 1



Surfaces:

$r = \text{const.}$  - cylindrical surface

$\theta = \text{const.}$  - vertical plane surface

$z = \text{const.}$  - horizontal plane surface

In generalized curvilinear coordinates the following two equations hold

$$\nabla^2 C_a = \frac{1}{h_1 h_2 h_3} \left[ \frac{d}{d\lambda} \left( \frac{h_2 h_3}{h_1} \frac{dC_a}{d\lambda} \right) + \frac{d}{d\mu} \left( \frac{h_1 h_3}{h_2} \frac{dC_a}{d\mu} \right) + \frac{d}{d\nu} \left( \frac{h_1 h_2}{h_3} \frac{dC_a}{d\nu} \right) \right] \quad (12)$$

where  $\lambda, \mu,$  and  $\nu$  are the generalized curvilinear coordinates and in an orthogonal system are related to the arc length by

$$ds^2 = h_1^2 d\lambda^2 + h_2^2 d\mu^2 + h_3^2 d\nu^2 \quad (13)$$

If  $\lambda=r$ ,  $\mu=\theta$  and  $\nu=z$  when cylindrical coordinates as shown in Figure 1 are used, the arc length is:

$$ds^2 = dr^2 + (r d\theta)^2 + dz^2 \quad (14)$$

and a comparison between equations (13) and (14) indicate that in this system  $h_1=1$ ,  $h_2=r$  and  $h_3=1$ .

The diffusion flow continuity equation in cylindrical coordinates can now be obtained from equation (12).

$$\nabla^2 C_a = \frac{1}{r} \left[ \frac{d}{dr} \left( r \frac{dC_a}{dr} \right) + \frac{d}{d\theta} \left( \frac{1}{r} \frac{dC_a}{d\theta} \right) + \frac{d}{dz} \left( r \frac{dC_a}{dz} \right) \right] \quad (15)$$

From equations (11) and (15)

$$\frac{dC_a}{dt} = \frac{D}{r} \left[ \frac{d}{dr} \left( r \frac{dC_a}{dr} \right) + \frac{d}{d\theta} \left( \frac{1}{r} \frac{dC_a}{d\theta} \right) + \frac{d}{dz} \left( r \frac{dC_a}{dz} \right) \right] \quad (16)$$

In the problem to be considered, the concentration will be assumed to be a function of  $r$  and  $z$  only since diffusion rates will be symmetrical with the  $z$  axis and  $\frac{dC_a}{d\theta} = 0$ .

The diffusion flow equation which must be solved follows

$$\frac{dC_a}{dt} = D \left[ \frac{1}{r} \frac{d}{dr} \left( r \frac{dC_a}{dr} \right) + \frac{d^2 C_a}{dz^2} \right] \quad (17)$$

An attempt will be made to solve equation (17) by assuming that  $C_a$  is a function of three separability equations which are uniquely functions of  $r$ ,  $z$ , and  $t$  respectively.

$$C_a(r, z, t) = R(r) Z(z) T(t) \quad (18)$$

The following three differential equations are obtained when equation (18) is differentiated and substituted into equation (17).

The separability condition assumed is therefore satisfied

$$\frac{dT}{dt} + \alpha^2 T = 0 \quad (19)$$

$$\frac{d^2 Z}{dz^2} + \left(\frac{\alpha^2}{D} - \beta^2\right) Z = 0 \quad (20)$$

$$\frac{d^2 R}{dr^2} + \frac{1}{r} \frac{dR}{dr} + \beta^2 R = 0 \quad (21)$$

The solution to equation (19) is:

$$T = C_1 e^{-\alpha^2 t} \quad (22)$$

The solution to equation (20) is:

$$Z = C_2 \sin\left(\sqrt{\frac{\alpha^2}{D} - \beta^2} z\right) + C_3 \cos\left(\sqrt{\frac{\alpha^2}{D} - \beta^2} z\right) \quad (23)$$

Equation (21) is recognized as a zero order Bessel equation and has the following general solution:

$$R = C_4 J_0(\beta r) + C_5 Y_0(\beta r) \quad (24)$$

However, in equation (24)  $C_5 = 0$  since  $Y_0(\beta \cdot 0) = -\infty$  and this solution doesn't apply. The solution for  $R(r)$  is then:

$$R = C_4 J_0(\beta r) \quad (25)$$

At the boundary  $r=r_0$ ,  $C_4 = 0$  (since  $C_a = C_{a0}$ ) and therefore the following condition must hold:

$$C_4 J_0(\beta r_0) = 0 \quad (26)$$

where the following eigenvalues make equation (26) equal to zero.

$$\beta r_0 = M_n \quad (27)$$

The solution for  $R$  is:

$$R = C_4 J_0 \left( M_n \frac{r}{r_0} \right) \quad n = 1, 2, 3, 4, \text{ etc.} \quad (28)$$

In equation (23), the solution for  $Z$ ,  $C_3 = 0$  if  $C_a = C_1$ , and when  $\bar{C}_a = 0$ . Then, the solution in terms of  $Z$  will be a sine series.

Furthermore, if  $\bar{C}_a = 0$  at  $Z = Z_0$  then  $C_2 \sin \left( \sqrt{\frac{\alpha^2}{D} \cdot \beta^2} Z_0 \right) = 0$

and, since  $C_2 \neq 0$ , then

$$\frac{\alpha^2}{D} - \beta^2 = \frac{m^2 \pi^2}{Z_0^2} \quad m = 1, 2, 3, 4, \text{ etc.} \quad (29)$$

$$\alpha^2 = D \left( \frac{M_n^2}{r_0^2} + \frac{m^2 \pi^2}{Z_0^2} \right) \quad (30)$$

The total solution for  $Z(z)$  is:

$$Z = C_2 \sin \frac{m \pi}{Z_0} z \quad (31)$$

The total solution for  $\bar{C}_a$  can now be obtained from equations (18), (22), (28), and (31) and will be a series solution consisting of Fourier and Bessel Series components.

$$\bar{C}_a = \sum_{n=1}^{\infty} C_n e^{-\left(\frac{M_n}{r_0}\right)^2 D t} \int_0^{r_0} \left( \frac{M_n r}{r_0} \right) C_m e^{-\left(\frac{m \pi}{Z_0}\right)^2 D t} \sin \frac{m \pi}{Z_0} z \quad (32)$$

The coefficient  $C_m$  for a Fourier sine series is:

$$C_m = \frac{2}{Z_0} \int_0^{Z_0} C_{am} \sin \frac{m \pi}{Z_0} z dz \quad (33)$$

Similarly, the coefficient  $C_n$  for a Bessel series is

$$C_n = \frac{2}{r_0^2 [J_0(M_n) + J_2(M_n)]} \int_0^{r_0} r C_{an} J_n(M_n \frac{r}{r_0}) dr \quad (34)$$

However,  $J_0(M_n) = 0$  and  $C_n$  becomes:

$$C_n = \frac{2}{r_0^2 J_2(M_n)} \int_0^{r_0} r C_{an} J_n(M_n \frac{r}{r_0}) dr \quad (35)$$

If the initial concentrations are uniform, then  $C_{am}$  and  $C_{an}$  are both constants and the following integrals are evaluated to be:

$$\int_0^{r_0} r J_n(M_n \frac{r}{r_0}) dr = \frac{r_0^2}{M_n} J_1(M_n) \quad n = 1, 2, 3, \text{etc.} \quad (36)$$

$$\int_0^{z_0} \frac{\sin \frac{m\pi z}{z_0}}{z} dz = \frac{2z_0}{m\pi} \quad m = 1, 3, 5, 7, \text{etc.} \quad (37)$$

The coefficient  $C_m$  for a Fourier sine series becomes:

$$C_m = \frac{4}{m\pi} \quad m = 1, 3, 5, 7, \text{etc.} \quad (38)$$

The coefficient  $C_n$  for a Bessel series becomes

$$C_n = \frac{2}{M_n J_1(M_n)} C_{an} \quad n = 1, 2, 3, \text{etc.} \quad (39)$$

The total solution for  $\bar{C}_a$  is obtained from equations (32), (38) and (39).

$$\bar{C}_a = C_{an} C_{am} \sum_{n=1}^{\infty} e^{-\left(\frac{M_n}{r_0}\right)^2 Dt} \frac{2 J_1(M_n \frac{r}{r_0})}{M_n J_1(M_n)} \sum_{m=1}^{\infty} e^{-\left(\frac{m\pi}{z_0}\right)^2 Dt} \frac{4}{m\pi} \frac{\sin \frac{m\pi z}{z_0}}{z} \quad (40)$$

Define the following constants:

$$\Theta_r = \frac{Dr}{r_0^2} \quad (41)$$

$$\Theta_z = \frac{4Dt}{z_0^2} \quad (42)$$

$$C_{ai} - C_{ao} = C_{ai} - C_{ao} \quad (43)$$

where  $C_{ai}$  is the initial concentration in the solid and  $C_{ao}$  is the concentration at the boundary after  $t = 0$ .

$$\frac{C_a}{C_{ai} - C_{ao}} = \sum_{n=1}^{\infty} \frac{e^{-M_n^2 \Theta_r} J_0(M_n \frac{r}{r_0})}{M_n J_1(M_n)} \sum_{m=1}^{\infty} \frac{e^{-(\frac{m\pi}{z_0})^2 \Theta_z} \frac{4}{m\pi} \sin \frac{m\pi}{z_0} z}{m\pi} \quad (44)$$

where  $m = 1, 3, 5, 7, \dots$  and  $n = 1, 2, 3, \dots$

$$\bar{C}_a(r, z, t) = C_a(r, z, t) - C_{ao} \quad (45)$$

The % concentration is obtained from equations (44) and (45)

$$\frac{C_a(r, z, t) - C_{ao}}{C_{ai} - C_{ao}} = \frac{8}{\pi} \sum_{n=1}^{\infty} \frac{e^{-M_n^2 \Theta_r} J_0(M_n \frac{r}{r_0})}{M_n J_1(M_n)} \sum_{m=1}^{\infty} \frac{e^{-(\frac{m\pi}{z_0})^2 \Theta_z} \frac{1}{m} \sin \frac{m\pi}{z_0} z}{m} \quad (46)$$

At  $r=0$  and  $z=z_0/2$  the central concentration history of a finite cylinder can be obtained from equation (46)

$$\frac{C_a(0, z_0/2, t) - C_{ao}}{C_{ai} - C_{ao}} = \sum_{n=1}^{\infty} \frac{2 e^{-M_n^2 \Theta_r}}{M_n J_1(M_n)} \sum_{m=1}^{\infty} \frac{4}{m\pi} e^{-(\frac{m\pi}{z_0})^2 \Theta_z} \sin \frac{m\pi}{2} \quad (47)$$

Define the following parameters:

$$P(\theta_z) = \sum_{m=1}^{\infty} \frac{4}{m\pi} e^{-\left(\frac{m\pi}{2}\right)^2} \sin \frac{m\pi}{2} \quad m = 1, 3, 5, 7 \text{ ETC.} \quad (48)$$

$$C(\theta_r) = \sum_{n=1}^{\infty} \frac{2e^{-M_n^2 \theta_r}}{M_n J_0(M_n)} \quad n = 1, 2, 3, \text{ ETC.} \quad (49)$$

$$\frac{C_a(t) - C_{a0}}{C_{a1} - C_{a0}} = P(\theta_z) C(\theta_r) \quad (50)$$

We have, by equation (50), established the equation for the fractional removal of alcohol and water at the central point ( $z = z_0/2$ ,  $r = 0$ ) of a cylindrical pellet. Figure 32 shows the central concentration history for a finite cylinder and illustrates that initially there is a very rapid removal of solvent but that the removal rate decreases with time so that the solvent theoretically is never 100% removed.

In the analysis which follows the concentration for all points ( $r, \theta, z$ ) at time  $\tau$  will be considered in order to obtain an equation for the instantaneous diffusion rate of the cylinder. This analysis extends the previous analysis which solves the continuity equation for the central point in the cylinder.

The instantaneous concentration diffusion rate from the cylinder consists of two components, one of which emanates from the radius  $r = r_0$  and the other which diffuses from the two surfaces  $z = 0$  and  $z = z_0$ .

At radius  $r = r_0$  the concentration diffusion rate is:

$$W_{ar} = -2\pi r_0 D \int_0^{z_0} \left. \frac{\partial C}{\partial r} \right|_{r=r_0} dz \quad (51)$$

At surfaces  $z = 0$  and  $z = z_0$  the concentration diffusion rate is:

$$W_{az} = -4\pi D \int_0^{r_0} r \left. \frac{\partial C}{\partial z} \right|_{z=z_0} dr \quad (52)$$

The radial concentration diffusion rate can now be obtained from equations (46) and (51)

$$W_{ar} = \frac{32}{\pi} z_0 D (C_{ai} - C_{ao}) \sum_{n=1}^{\infty} e^{-M_n^2 \theta} \sum_{m=1}^{\infty} \frac{1}{m^2} e^{-\left(\frac{m\pi}{z_0}\right)^2 \theta} \quad (53)$$

Similarly, the axial concentration diffusion rate can be obtained from equations (46) and (52)

$$W_{az} = \frac{32\pi r_0^2}{z_0} D (C_{ai} - C_{ao}) \sum_{n=1}^{\infty} \frac{1}{M_n^2} e^{-M_n^2 \theta} \sum_{m=1}^{\infty} e^{-\left(\frac{m\pi}{z_0}\right)^2 \theta} \quad (54)$$

The cumulative solvent loss in the radial direction is:

$$W_{ar} = \frac{32 z_0}{\pi} (C_{ai} - C_{ao}) \sum_{n=1}^{\infty} \sum_{m=1}^{\infty} \frac{1/m^2}{\left(\frac{M_n^2}{r_0^2} + \frac{m^2 \pi^2}{z_0^2}\right)} \left[ 1 - e^{-\left(\frac{M_n^2}{r_0^2} + \frac{m^2 \pi^2}{z_0^2}\right) \theta} \right] \quad (55)$$

Similarly, the cumulative solvent loss in the axial direction is:

$$W_{az} = \frac{32\pi r_0^2}{z_0} (C_{ai} - C_{ao}) \int_0^{\infty} \sum_{n=1}^{\infty} \sum_{m=1}^{\infty} \frac{1/M_n^2}{\left(\frac{M_n^2}{r_0^2} + \frac{m^2 h^2}{z_0^2}\right)} \left[ 1 - e^{-\left(\frac{M_n^2}{r_0^2} + \frac{m^2 h^2}{z_0^2}\right) Dt} \right] Dt \quad (56)$$

It is now possible to obtain the total loss of solvent by summing the cumulative loss in the radial direction  $W_{ar}$  and the cumulative loss in the axial direction  $W_{az}$ .

The total loss is

$$W_a = \frac{32z_0 r_0^2}{\pi} (C_{ai} - C_{ao}) \left[ \sum_{n=1}^{\infty} \frac{1}{M_n^2} \sum_{m=1}^{\infty} \frac{1}{m^2} - \sum_{n=1}^{\infty} \frac{e^{-\frac{M_n^2}{r_0^2} Dt}}{M_n^2} \sum_{m=1}^{\infty} \frac{e^{-\frac{m^2 h^2}{z_0^2} Dt}}{m^2} \right] \quad (57)$$

However, the following series are evaluated to be:

$$\sum_{n=1}^{\infty} \frac{1}{M_n^2} = \frac{1}{4} \quad n = 1, 2, 3, 4, \text{ etc.} \quad (58)$$

$$\sum_{m=1}^{\infty} \frac{1}{m^2} = \frac{\pi^2}{8} \quad m = 1, 3, 5, 7, \text{ etc.} \quad (59)$$

From equations (57), (58) and (59)

$$W_a = \pi r_0^2 z_0 (C_{ai} - C_{ao}) \left[ 1 - \frac{32}{\pi^2} \sum_{n=1}^{\infty} \frac{e^{-\frac{M_n^2}{r_0^2} Dt}}{M_n^2} \sum_{m=1}^{\infty} \frac{e^{-\frac{m^2 h^2}{z_0^2} Dt}}{m^2} \right] \quad (60)$$

At  $z = \infty$  the total solvent diffused is  $W_{a\infty}$

$$W_{a\infty} = \pi r_0^2 z_0 (C_{ai} - C_{ao}) \quad (61)$$

The fractional amount of solvent diffused can now be obtained from equations (60) and (61).

$$\frac{W_{i\infty} - W_{i0}}{W_{i\infty}} = \frac{32}{\pi^2} \sum_{n=1}^{\infty} \frac{1}{M_n^2} e^{-\frac{M_n^2}{r_0^2} Dt} \sum_{m=1}^{\infty} \frac{1}{m^2} e^{-\frac{\pi^2 m^2}{L_c^2} Dt} \quad (62)$$

The fractional amount of solvent removed, as described by equation (62), is plotted as a function of the time parameter  $Dt/r_0^2$  or  $4Dt/L_c^2$  as shown by Figure 33. For the case considered the length of the cylinder  $L_c$  was assumed to be equal to the diameter of the cylinder  $2r$  since some choice of dimensions which approximate the actual pellet was required.

As shown, there is initially a very rapid removal of solvent; diffusion begins as soon as the pellet is exposed to the environment of the test cell. However, as the time period lengthens, removal of solvent occurs at an ever decreasing rate and theoretically the solvent is never completely removed because the diffusion gradient also approaches zero.

Test Run #35 was compared with the fractional amount of solvent remaining as derived in this appendix. Good correlation was obtained in the range of operating time of 1 hour to 7 hours or after the propellant reached the operating temperature. Poor correlation between the theoretical equation and test runs was obtained in the

operating time range of zero to 1 hour which is the temperature transient range.

Obviously, the effect of varying temperature has a drastic effect on the diffusion process; for this reason, the diffusion constant is assumed to be a function of temperature. Appendix III assumes that the diffusion process is a function of temperature and that temperature is controlled either as a linear or a parabolic function of time to obtain two new diffusion process differential equations which include the diffusion constants as functions of time. The results obtained in Appendix III will be used to correlate the theoretical diffusion with the actual results of Run #35 in the zero to 1 hour transient temperature range.

### APPENDIX III

#### DIFFUSION OF A SINGLE COMPONENT FROM A FINITE CYLINDER WHEN THE —DIFFUSION CONSTANT IS A FUNCTION OF TEMPERATURE

In Appendix II, a finite cylinder was analyzed in order to determine the diffusion characteristics of such a body when the appropriate boundary conditions are assumed. In the final result, the fractional amount of solvent diffused is obtained as a function of time, cylinder radius, and cylinder length.

The fundamental assumption made in the analysis of Appendix II was that the diffusion constant was a true constant and independent of temperature  $\theta$  and the body coordinates  $r$  and  $z$ . Unsatisfactory correlation of the derived function (Appendix II (equation (62))) at small times  $t$  when the temperature  $\theta$  is undergoing a transient, necessitates a more exact derivation of the mass diffusion relationship.

This appendix proposes to solve this problem.

#### Definition of Parameters:

$r$  = radial coordinate in cylindrical frame of reference - inch

$z$  = axis coordinate in cylindrical frame of reference - inch

$t$  = time - seconds

$\theta$  = temperature

$C_a$  = concentration of solvent "A" - lb/in<sup>3</sup>

$D$  = diffusivity or coefficient of diffusion - in<sup>2</sup>/sec

$A$  = diffusion area - in<sup>2</sup>

$U_a$  = diffusion rate of solvent "A" - lb/sec

$W_a$  = total diffusion of solvent "A" at time - lbs

$W_{\infty}$  = total diffusion of solvent "A" at infinite time - lbs

The diffusion equation which must be solved has been derived in Appendix II and is rewritten as equation (1) here for convenience.

$$\frac{d\bar{C}_a}{dt} = D \left[ \frac{1}{r} \frac{d}{dr} \left( r \frac{d\bar{C}_a}{dr} \right) + \frac{d^2 \bar{C}_a}{dz^2} \right] \quad (1)$$

The diffusion constant "D" will be assumed to be temperature dependent and, according to Rohsenow (Reference 2) the diffusivity varies with the square of the temperature

$$D = K_0 \theta^2 \quad (2)$$

Assume now that the body is heated uniformly by external means and that the temperature is a linear function of time

$$\theta = K_1 t \quad (3)$$

From equations (2) and (3) the diffusivity, for the experiments performed, will vary as a function of the square of the time.

$$D = K_0 K_1^2 t^2 \quad (4)$$

$$D = A_0 t^2 \quad (5)$$

The diffusion equation which must be solved can now be obtained from equations (1) and (5)

$$\frac{1}{t^2} \frac{d\bar{C}_a}{dt} = A_0 \left[ \frac{1}{r} \frac{d}{dr} \left( r \frac{d\bar{C}_a}{dr} \right) + \frac{d^2 \bar{C}_a}{dz^2} \right] \quad (6)$$

An attempt will be made to solve equation (6) by assuming that  $\bar{C}_a$  is a function of three separability conditions which are unique functions of  $r$ ,  $z$ , and  $t$ .

$$\bar{C}_a(r, z, t) = R(r) Z(z) T(t) \quad (7)$$

If equation (7) is appropriately differentiated and the results substituted into equation (6), the following three differential equations are obtained:

$$\frac{dT}{dt} + \alpha^2 t^2 T = 0 \quad (8)$$

$$\frac{d^2 Z}{dz^2} + \left( \frac{\alpha^2}{A_0} - \beta^2 \right) Z = 0 \quad (9)$$

$$\frac{d^2 R}{dr^2} + \frac{1}{r} \frac{dR}{dr} + \beta^2 R = 0 \quad (10)$$

The solution to equation (8) is:

$$T = C_1 e^{-\frac{\alpha^2}{3} t^3} \quad (11)$$

The solution to equation (9) is:

$$Z = C_2 \sin\left(\sqrt{\frac{\alpha^2}{A_0} - \beta^2} z\right) + C_3 \cos\left(\sqrt{\frac{\alpha^2}{A_0} - \beta^2} z\right) \quad (12)$$

Equation (10) is recognized as a zero order Bessel equation and has the following solution:

$$R = C_4 J_0(\beta r) + C_5 Y_0(\beta r) \quad (13)$$

However,  $C_5 = 0$  since  $Y_0(\beta \cdot 0) = \infty$  when  $r = 0$  and this solution doesn't apply. The solution for  $R(r)$  is then:

$$R = C_4 J_0(\beta r) \quad (14)$$

At the boundary  $r = r_0$ ,  $\bar{C}_a = 0$  (since  $C_a = C_{a0}$ ) and the following condition must hold:

$$C_4 J_0(\beta r_0) = 0 \quad (15)$$

The following eigenvalues made  $J_0(\beta r)$  zero.

$$M_n = \beta r_0 \quad (16)$$

The solution for  $R(r)$  is therefore:

$$R = C_4 J_0\left(M_n \frac{r}{r_0}\right) \quad (17)$$

In equation (12), the solution for  $Z(z)$ ,  $C_3 = 0$  since  $\bar{C}_a = 0$  ( $C_a = C_{a0}$ ) at  $Z = 0$ . Then, the solution will be a sine series since  $C_2 \neq 0$  and  $\bar{C}_a = 0$  ( $C_a = C_{a0}$ ) at  $Z = Z_0$ , and the following condition must hold:

$$C_2 \sin\left(\sqrt{\frac{\alpha^2}{A_0} - \beta^2} Z_0\right) = 0 \quad (18)$$

From equation (18)

$$\frac{\alpha^2}{A_0} - \beta^2 = \frac{m^2 \pi^2}{z_0^2} \quad m = 1, 2, 3, 4, \text{ etc.} \quad (19)$$

From equations (16) and (19)  $\alpha^2$  can be determined

$$\alpha^2 = A_0 \left( \frac{m^2 \pi^2}{z_0^2} + \frac{M_n^2}{r_0^2} \right) \quad (20)$$

The total solution for  $\bar{z}(z)$  is:

$$\bar{z} = C_2 \sin \frac{m\pi}{z_0} z \quad (21)$$

It is now possible to obtain the total solution for  $\bar{C}_a$  from equations (7), (11), (17), (20), and (21).

$$\bar{C}_a = \sum_{n=1}^{\infty} C_n e^{-\left(\frac{M_n}{r_0}\right)^2 \frac{A}{3} t^3} J_0\left(M_n \frac{r}{r_0}\right) \sum_{m=1}^{\infty} C_m e^{-\left(\frac{m\pi}{z_0}\right)^2 \frac{A}{3} t^3} \sin \frac{m\pi}{z_0} z \quad (22)$$

The coefficient  $C_m$  is for a Fourier sine series and is:

$$C_m = \frac{2}{z_0} \int_0^{z_0} C_{am}(z) \sin \frac{m\pi}{z_0} z dz \quad (23)$$

Similarly, the coefficient  $C_n$  is for a Bessel series and is:

$$C_n = \frac{2}{r_0^2 [J_0^2(M_n) + J_1^2(M_n)]} \int_0^{r_0} r C_{an}(r) J_0\left(M_n \frac{r}{r_0}\right) dr \quad (24)$$

However,  $J_0(M_n) = 0$  and  $C_n$  becomes:

$$C_n = \frac{2}{r_0^2 J_1^2(M_n)} \int_0^{r_0} r C_{an}(r) J_0\left(M_n \frac{r}{r_0}\right) dr \quad (25)$$

If the initial concentration is uniform, then  $C_{am}$  and  $C_{an}$  are both constants and the following integrals are evaluated to be:

$$\int_0^{r_0} r J_0\left(M_n \frac{r}{r_0}\right) dr = \frac{r_0^2}{M_n} J_1(M_n) \quad n = 1, 2, 3, \text{ etc.} \quad (26)$$

$$\int_0^{z_0} \sin \frac{m\pi z}{z_0} z dz = \frac{2z_0}{m\pi} \quad m = 1, 3, 5, 7, \text{ etc.} \quad (27)$$

The coefficient  $C_m$  for a Fourier sine series is:

$$C_m = \frac{4}{m\pi} C_{0m} \quad m = 1, 3, 5, 7, \text{ etc.} \quad (28)$$

The coefficient  $C_n$  for a Bessel series is:

$$C_n = \frac{2}{M_n J_1(M_n)} C_{0n} \quad (29)$$

The total solution for  $\bar{C}_a$  can now be obtained from equations (23), (28), and (29)

$$\bar{C}_a = C_{0n} C_{0m} \int_{n=1}^{\infty} e^{-\left(\frac{M_n}{r_0}\right)^2 \frac{A_0 t^3}{3}} \frac{2 J_1(M_n \frac{r}{r_0})}{M_n J_1(M_n)} \int_{m=1}^{\infty} e^{-\left(\frac{m\pi}{z_0}\right)^2 \frac{A_0 t^3}{3}} \frac{4}{m\pi} \sin \frac{m\pi z}{z_0} dz \quad (30)$$

Define the following constants:

$$\Theta_r = \frac{A_0}{3} \frac{t^3}{r_0^2} \quad (31)$$

$$\Theta_z = \frac{4A_0}{3} \frac{z^3}{z_0^2} \quad (32)$$

$$C_{0n} C_{0m} = C_{ai} - C_{a0} \quad (33)$$

Where  $C_{ai}$  is the initial concentration and  $C_{a0}$  is the concentration at the boundary after  $t = 0+$ .

$$\frac{\bar{C}_a}{C_{ai} - C_{a0}} = \sum_{n=1}^{\infty} e^{-M_n^2 \theta_r} \frac{2 J_0(M_n r_0)}{M_n J_1(M_n)} \sum_{m=1}^{\infty} e^{-\left(\frac{m\pi}{2}\right)^2 \theta_z} \frac{4}{m\pi} \sin \frac{m\pi}{2} z \quad (34)$$

However,  $\bar{C}_a$  is the differential concentration and is:

$$\bar{C}_a(r, z, t) = C_a(r, z, t) - C_{a0} \quad (35)$$

The % total concentration can now be obtained from equations (34) and (35)

$$\frac{C_a - C_{a0}}{C_{ai} - C_{a0}} = \sum_{n=1}^{\infty} e^{-M_n^2 \theta_r} \frac{2 J_0(M_n r_0)}{M_n J_1(M_n)} \sum_{m=1}^{\infty} e^{-\left(\frac{m\pi}{2}\right)^2 \theta_z} \frac{4}{m\pi} \sin \frac{m\pi}{2} z \quad (36)$$

At  $r=0$  and  $z=z_0/2$ , the central concentration history of a finite cylinder can be obtained from equation (36)

$$\frac{C_a(0, \frac{z_0}{2}, t) - C_{a0}}{C_{ai} - C_{a0}} = \sum_{n=1}^{\infty} \frac{2 e^{-M_n^2 \theta_r}}{M_n J_1(M_n)} \sum_{m=1}^{\infty} \frac{4}{m\pi} e^{-\left(\frac{m\pi}{2}\right)^2 \theta_z} \sin \frac{m\pi}{2} \quad (37)$$

Define the following parameters:

$$P(\theta_z) = \sum_{m=1}^{\infty} \frac{4}{m\pi} e^{-\left(\frac{m\pi}{2}\right)^2 \theta_z} \sin \frac{m\pi}{2} \quad m = 1, 3, 5, 7, \text{ etc.} \quad (38)$$

$$C(\theta_r) = \sum_{n=1}^{\infty} \frac{2 e^{-M_n^2 \theta_r}}{M_n J_1(M_n)} \quad (39)$$

$P(\theta_z)$  and  $C(\theta_r)$  are tabulated in the literature on heat transfer and can be applied to the present problem to obtain the central

concentration history of a cylinder.

$$\frac{C_a\left(C, \frac{z}{2}, t\right) - C_{a0}}{C_{ai} - C_{a0}} = P(\theta_z) C(\theta_r) \quad (40)$$

The instantaneous concentration diffusion rate from the cylinder consists of two components, one of which emanates from the radius  $r=r_0$  and the other which diffuses from the surfaces  $z=0$  and  $z=z_0$ .

At radius  $r=r_0$  the concentration diffusion rate is:

$$W_{ar} = -2\pi r_0 A_0 t^2 \int_0^{z_0} \left. \frac{dC_a}{dr} \right|_{r=r_0} dz \quad (41)$$

At surfaces  $z=0$  and  $z=z_0$ , the concentration diffusion rate is:

$$W_{az} = -4\pi A_0 t^2 \int_0^{r_0} r \left. \frac{dC_a}{dz} \right|_{z=z_0} dr \quad (42)$$

The radial concentration diffusion rate can now be obtained from equations (36) and (41).

$$W_{ar} = \frac{32z_0}{\pi} A_0 (C_{ai} - C_{a0}) t^2 \sum_{n=1}^{\infty} e^{-M_n^2 \theta_r} \sum_{m=1}^{\infty} \frac{1}{m^2} e^{-\left(\frac{m\pi}{2}\right)^2 \theta_z} \quad (43)$$

Similarly, the axial diffusion rate can now be obtained from equations (36) and (42).

$$W_{az} = \frac{32\pi r_0^2}{z_0} A_0 (C_{ai} - C_{a0}) t^2 \sum_{n=1}^{\infty} \frac{1}{M_n^2} e^{-M_n^2 \theta_r} \sum_{m=1}^{\infty} e^{-\left(\frac{m\pi}{2}\right)^2 \theta_z} \quad (44)$$

The cumulative losses in the radial and axial directions will be:

$$W_{ar} = \int_0^t W_{ar} dt \quad (45)$$

$$W_{az} = \int_0^t W_{az} dt \quad (46)$$

From equations (31), (32), (43), and (45) the cumulative radial solvent loss at time  $t$  is:

$$W_{ar} = \frac{32z_0}{\pi} (C_{ai} - C_{ao}) \sum_{n=1}^{\infty} \sum_{m=1}^{\infty} \frac{1/m^2}{\left(\frac{M_n^2}{r_0^2} + \frac{m^2 h^2}{z_0^2}\right)} \left[ 1 - e^{-\left(\frac{M_n^2}{r_0^2} + \frac{m^2 h^2}{z_0^2}\right) \frac{r_0^2}{3} t^3} \right] \quad (47)$$

From equations (31), (32), (44), and (46) the cumulative axial solvent loss at time  $t$  is:

$$W_{az} = \frac{32hr_0^2}{z_0} (C_{ai} - C_{ao}) \sum_{n=1}^{\infty} \sum_{m=1}^{\infty} \frac{1/M_n^2}{\left(\frac{M_n^2}{r_0^2} + \frac{m^2 h^2}{z_0^2}\right)} \left[ 1 - e^{-\left(\frac{M_n^2}{r_0^2} + \frac{m^2 h^2}{z_0^2}\right) \frac{A_0 t^3}{3}} \right] \quad (48)$$

It is now possible to obtain the total loss in solvent by summing the cumulative loss in the radial direction  $W_{ar}$  and the cumulative loss in the axial direction  $W_{az}$ .

The total loss is:

$$W_a = \frac{32z_0 r_0^2}{\pi} (C_{ai} - C_{ao}) \left[ \sum_{n=1}^{\infty} \frac{1}{M_n^2} \sum_{m=1}^{\infty} \frac{1}{m^2} - \sum_{n=1}^{\infty} \frac{e^{-\frac{M_n^2 A_0 t^3}{3}}}{M_n^2} \sum_{m=1}^{\infty} \frac{e^{-\frac{m^2 h^2 A_0 t^3}{z_0^2 3}}}{m^2} \right] \quad (49)$$

However, the following series are evaluated to be:

$$\sum_{n=1}^{\infty} \frac{1}{M_n^2} = 1/4 \quad n = 1, 2, 3, 4, \text{ etc.} \quad (50)$$

$$\sum_{m=1}^{\infty} \frac{1}{m^2} = \frac{\pi^2}{8} \quad m = 1, 3, 5, 7, \text{ etc.} \quad (51)$$

From equations (49), (50), and (51)

$$W_a = \pi r_0^2 z_0 (C_{ai} - C_{ao}) \left[ 1 - \frac{32}{\pi^2} \sum_{n=1}^{\infty} \frac{e^{-\frac{M_n^2 A_0 t^3}{r_0^2 \cdot 3}}}{M_n^2} \sum_{m=1}^{\infty} \frac{e^{-\frac{m^2 h^2 A_0 t^3}{z_0^2 \cdot 3}}}{m^2} \right] \quad (52)$$

At  $t = \infty$  the total solvent diffused is  $W_{a\infty}$ .

$$W_{a\infty} = \pi r_0^2 z_0 (C_{ai} - C_{ao}) \quad (53)$$

The fractional amount of solvent diffused can now be obtained from equations (52) and (53)

$$\frac{W_{a\infty} - W_a}{W_{a\infty}} = \frac{32}{\pi^2} \sum_{n=1}^{\infty} \frac{e^{-\frac{M_n^2 A_0 t^3}{r_0^2 \cdot 3}}}{M_n^2} \sum_{m=1}^{\infty} \frac{e^{-\frac{m^2 h^2 A_0 t^3}{z_0^2 \cdot 3}}}{m^2} \quad (54)$$

Figure 34 is a plot of equation (54) and represents the diffusion of solvent during the initial temperature transient which occurs before the steady state temperature is reached. The diffusion constant for this case has been assumed to be proportional to the temperature squared since a linear increase in temperature with time was an original assumption.

A comparison between the theoretical results and the results from Run #35 showed that better matching was possible when a variable diffusion constant was assumed.

A further improvement in matching test results was obtained when the diffusion constant was assumed to be proportional to temperature. This assumption is realistic since the actual temperature rise with time can be assumed to be parabolic ( $\theta \propto t$ ) and the diffusion constant is proportional to the temperature squared ( $D \propto \theta^2$ ).

Therefore, the following second assumption is made:

$$D = A_1 t^i \quad (55)$$

and the fractional amount of diffusion becomes:

$$\frac{W_{\infty} - W_a}{W_{\infty}} = \frac{32}{\pi^2} \sum_{n=1}^{\infty} \frac{e^{-\frac{M_n^2 A_1 t^i}{r_0^2 2}}}{M_n^2} \sum_{m=1}^{\infty} \frac{e^{-\frac{m^2 n^2 A_1 t^i}{2^2 2}}}{m^2} \quad (56)$$

The fractional amount of diffusion is plotted in Figure 35 and the characteristic of this solvent diffusion curve closely approximates test result #35 when two solvents ether and alcohol are assumed to diffuse at varying rates simultaneously. A comparison between Run #35 and the theoretical curve is shown in Figure 29 where the solid

line represents the test run and the dotted line is a theoretical curve based on the use of Figure 35 for the transient diffusion of ether and alcohol in the initial transient and the use of Figure 33 for the diffusion of alcohol when steady temperature conditions are reached. The ether is assumed to have completely disappeared by the time 180°F has been reached.

Results, although not exact, are satisfactory and indicate that a diffusion process is the controlling mechanism when solvents are removed by dielectric heating from a solid propellant.

Attention is directed to Figure 30 which is of test run #35 and appears to consist of two straight lines when plotted on log paper. This means that the percent volatiles, when curve fitted to an empirical equation of the form  $\%V = K_0 t^{-\gamma}$ , exactly reproduce test run #35 in two regimes from 15 minutes on to seven hours.

The separation time between the two regimes occurs after one hour but no significance can be attached to this fact other than the possibility that ether is essentially completely diffused after one hour. If ether diffusion and alcohol diffusion are separated out of the total percent volatiles diffused, then Figure 31 indicates a possible division of solvent diffusion. Future programs should run special tests to check the diffusion rates of alcohol and ether when each is the only constituent in the solid propellant cylinders.

Unclassified

Security Classification

DOCUMENT CONTROL DATA - R&D		
<i>(Security classification of title, body of abstract and indexing annotation must be entered when the overall report is classified)</i>		
1. ORIGINATING ACTIVITY (Corporate author)		2a. REPORT SECURITY CLASSIFICATION
U. S. Naval Propellant Plant		Unclassified
Indian Head, Md.		2b. GROUP
		-
3. REPORT TITLE		
Industrial Preparedness Measure: Study of Improved Methods of Drying Casting Powder		
4. DESCRIPTIVE NOTES (Type of report and inclusive dates)		
Final report		
5. AUTHOR(S) (Last name, first name, initials)		
Geist, Joseph E.		
6. REPORT DATE	7a. TOTAL NO. OF PAGES	7b. NO. OF REFS
25 March 1965	131	0
8a. CONTRACT OR GRANT NO.		8b. ORIGINATOR'S REPORT NUMBER(S)
a. PROJECT NO. BuWeps Project Order 2-0010 Subhead . 1925		-
c.		8b. OTHER REPORT NO(S) (Any other numbers that may be assigned to report)
d.		-
10. AVAILABILITY/LIMITATION NOTICES		
Qualified requesters may obtain copies of this report direct from DDC		
11. SUPPLEMENTARY NOTES		12. SPONSORING MILITARY ACTIVITY
		Bureau of Naval Weapons Department of the Navy Washington, D. C.
13. ABSTRACT		
<p>Four methods of drying casting powder were studied, namely "sweetie" barrel, bed drying, Roto-louvre, and dielectric. Of the methods studied, the dielectric drying offers the most advantages in regard to safety, adaptability to remote and continuous processing, drying time, and operating cost. Estimated annual savings of \$178,260 may be obtained by using dielectric drying in place of the present dryhouse method.</p>		

DD FORM 1473  
1 JAN 64

Unclassified

Security Classification

Unclassified

Security Classification

14 KEY WORDS	LINK A		LINK B		LINK C	
	ROLE	WT	ROLE	WT	ROLE	WT
Casting Powder - moisture content Casting Powder - drying						

INSTRUCTIONS

1. **ORIGINATING ACTIVITY:** Enter the name and address of the contractor, subcontractor, grantee, Department of Defense activity or other organization (*corporate author*) issuing the report.

2a. **REPORT SECURITY CLASSIFICATION:** Enter the overall security classification of the report. Indicate whether "Restricted Data" is included. Marking is to be in accordance with appropriate security regulations.

2b. **GROUP:** Automatic downgrading is specified in DoD Directive 5200.10 and Armed Forces Industrial Manual. Enter the group number. Also, when applicable, show that optional markings have been used for Group 3 and Group 4 as authorized.

3. **REPORT TITLE:** Enter the complete report title in all capital letters. Titles in all cases should be unclassified. If a meaningful title cannot be selected without classification, show title classification in all capitals in parenthesis immediately following the title.

4. **DESCRIPTIVE NOTES:** If appropriate, enter the type of report, e.g., interim, progress, summary, annual, or final. Give the inclusive dates when a specific reporting period is covered.

5. **AUTHOR(S):** Enter the name(s) of author(s) as shown on or in the report. Enter: last name, first name, middle initial. If military, show rank and branch of service. The name of the principal author is an absolute minimum requirement.

6. **REPORT DATE:** Enter the date of the report as day, month, year, or month, year. If more than one date appears on the report, use date of publication.

7a. **TOTAL NUMBER OF PAGES:** The total page count should follow normal pagination procedures, i.e., enter the number of pages containing information.

7b. **NUMBER OF REFERENCES:** Enter the total number of references cited in the report.

8a. **CONTRACT OR GRANT NUMBER:** If appropriate, enter the applicable number of the contract or grant under which the report was written.

8b, 8c, & 8d. **PROJECT NUMBER:** Enter the appropriate military department identification, such as project number, subproject number, system numbers, task number, etc.

9a. **ORIGINATOR'S REPORT NUMBER(S):** Enter the official report number by which the document will be identified and controlled by the originating activity. This number must be unique to this report.

9b. **OTHER REPORT NUMBER(S):** If the report has been assigned any other report numbers (*either by the originator or by the sponsor*), also enter this number(s).

10. **AVAILABILITY/LIMITATION NOTICES:** Enter any limitations on further dissemination of the report, other than those

imposed by security classification, using standard statements such as:

- (1) "Qualified requesters may obtain copies of this report from DDC."
- (2) "Foreign announcement and dissemination of this report by DDC is not authorized."
- (3) "U. S. Government agencies may obtain copies of this report directly from DDC. Other qualified DDC users shall request through \_\_\_\_\_."
- (4) "U. S. military agencies may obtain copies of this report directly from DDC. Other qualified users shall request through \_\_\_\_\_."
- (5) "All distribution of this report is controlled. Qualified DDC users shall request through \_\_\_\_\_."

If the report has been furnished to the Office of Technical Services, Department of Commerce, for sale to the public, indicate this fact and enter the price, if known.

11. **SUPPLEMENTARY NOTES:** Use for additional explanatory notes.

12. **SPONSORING MILITARY ACTIVITY:** Enter the name of the departmental project office or laboratory sponsoring (*paying for*) the research and development. Include address.

13. **ABSTRACT:** Enter an abstract giving a brief and factual summary of the document indicative of the report, even though it may also appear elsewhere in the body of the technical report. If additional space is required, a continuation sheet shall be attached.

It is highly desirable that the abstract of classified reports be unclassified. Each paragraph of the abstract shall end with an indication of the military security classification of the information in the paragraph, represented as (TS), (S), (C), or (U).

There is no limitation on the length of the abstract. However, the suggested length is from 150 to 225 words.

14. **KEY WORDS:** Key words are technically meaningful terms or short phrases that characterize a report and may be used as index entries for cataloging the report. Key words must be selected so that no security classification is required. Identifiers, such as equipment model designation, trade name, military project code name, geographic location, may be used as key words but will be followed by an indication of technical context. The assignment of links, roles, and weights is optional.

Unclassified

Security Classification

<p>Naval Propellant Plant, Indian Head, Maryland</p> <p>IMPROVEMENT STUDY OF CASTING-POWDER DRYING METHODS - Final Report. By J. E. Geist. 25 March 1965. 136 pp.</p> <p>UNCLASSIFIED</p> <p>Four methods of drying casting powder were studied, namely, "sweetie" barrel, bed drying, Roto-louvre, and dielectric.</p>	<p>Naval Propellant Plant, Indian Head, Maryland</p> <p>IMPROVEMENT STUDY OF CASTING-POWDER DRYING METHODS - Final Report. By J. E. Geist. 25 March 1965. 136 pp.</p> <p>UNCLASSIFIED</p> <p>Four methods of drying casting powder were studied, namely, "sweetie" barrel, bed drying, Roto-louvre, and dielectric.</p>
<p>1. Casting Powder— Moisture Content Safety—Solid Propellants Manufacture</p> <p>2. Propellants— Drying</p> <p>I. Geist, J. E.</p>	<p>1. Casting Powder— Moisture Content Safety—Solid Propellants Manufacture</p> <p>2. Propellants— Drying</p> <p>I. Geist, J. E.</p>
<p>Naval Propellant Plant, Indian Head, Maryland</p> <p>IMPROVEMENT STUDY OF CASTING-POWDER DRYING METHODS - Final Report. By J. E. Geist. 25 March 1965. 136 pp.</p> <p>UNCLASSIFIED</p> <p>Four methods of drying casting powder were studied, namely, "sweetie" barrel, bed drying, Roto-louvre, and dielectric.</p>	<p>Naval Propellant Plant, Indian Head, Maryland</p> <p>IMPROVEMENT STUDY OF CASTING-POWDER DRYING METHODS - Final Report. By J. E. Geist. 25 March 1965. 136 pp.</p> <p>UNCLASSIFIED</p> <p>Four methods of drying casting powder were studied, namely, "sweetie" barrel, bed drying, Roto-louvre, and dielectric.</p>
<p>1. Casting Powder— Moisture Content Safety—Solid Propellant's Manufacture</p> <p>2. Propellants— Drying</p> <p>I. Geist, J. E.</p>	<p>1. Casting Powder— Moisture Content Safety—Solid Propellants Manufacture</p> <p>2. Propellants— Drying</p> <p>I. Geist, J. E.</p>

Of the methods studied, the dielectric drying offers the most advantages in regard to safety, adaptability to remote and continuous processing, drying time, and operating cost. Estimated annual savings of \$178,260 may be obtained by using dielectric drying in place of the present dryhouse method.

Of the methods studied, the dielectric drying offers the most advantages in regard to safety, adaptability to remote and continuous processing, drying time, and operating cost. Estimated annual savings of \$178,260 may be obtained by using dielectric drying in place of the present dryhouse method.

Of the methods studied, the dielectric drying offers the most advantages in regard to safety, adaptability to remote and continuous processing, drying time, and operating cost. Estimated annual savings of \$178,260 may be obtained by using dielectric drying in place of the present dryhouse method.

Of the methods studied, the dielectric drying offers the most advantages in regard to safety, adaptability to remote and continuous processing, drying time and operating cost. Estimated annual savings of \$178,260 may be obtained by using dielectric drying in place of the present dryhouse method.

Of the methods studied, the dielectric drying offers the most advantages in regard to safety, adaptability to remote and continuous processing, drying time, and operating cost. Estimated annual savings of \$178,260 may be obtained by using dielectric drying in place of the present dryhouse method.

Of the methods studied, the dielectric drying offers the most advantages in regard to safety, adaptability to remote and continuous processing, drying time, and operating cost. Estimated annual savings of \$178,260 may be obtained by using dielectric drying in place of the present dryhouse method.

Of the methods studied, the dielectric drying offers the most advantages in regard to safety, adaptability to remote and continuous processing, drying time, and operating cost. Estimated annual savings of \$178,260 may be obtained by using dielectric drying in place of the present dryhouse method.

Of the methods studied, the dielectric drying offers the most advantages in regard to safety, adaptability to remote and continuous processing, drying time and operating cost. Estimated annual savings of \$178,260 may be obtained by using dielectric drying in place of the present dryhouse method.

<p>Naval Propellant Plant, Indian Head, Maryland</p> <p>IMPROVEMENT STUDY OF CASTING-POWDER DRYING METHODS - Final Report. By J. E. Geist. 25 March 1965. 136 pp.</p> <p>UNCLASSIFIED</p> <p>Four methods of drying casting powder were studied, namely, "sweetie" barrel, bed drying, Roto-louvre, and dielectric.</p>	<p>Naval Propellant Plant, Indian Head, Maryland</p> <p>IMPROVEMENT STUDY OF CASTING-POWDER DRYING METHODS - Final Report. By J. E. Geist. 25 March 1965. 136 pp.</p> <p>UNCLASSIFIED</p> <p>Four methods of drying casting powder were studied, namely, "sweetie" barrel, bed drying, Roto-louvre, and dielectric.</p>
<p>Naval Propellant Plant, Indian Head, Maryland</p> <p>IMPROVEMENT STUDY OF CASTING-POWDER DRYING METHODS - Final Report. By J. E. Geist. 25 March 1965. 136 pp.</p> <p>UNCLASSIFIED</p> <p>Four methods of drying casting powder were studied, namely, "sweetie" barrel, bed drying, Roto-louvre, and dielectric.</p>	<p>Naval Propellant Plant, Indian Head, Maryland</p> <p>IMPROVEMENT STUDY OF CASTING-POWDER DRYING METHODS - Final Report. By J. E. Geist. 25 March 1965. 136 pp.</p> <p>UNCLASSIFIED</p> <p>Four methods of drying casting powder were studied, namely, "sweetie" barrel, bed drying, Roto-louvre, and dielectric.</p>

1. Casting Powder—Moisture Content
  2. Safety—Solid Propellants Manufacture
  3. Propellants—Drying
- I. Geist, J. E.

1. Casting Powder—Moisture Content
  2. Safety—Solid Propellants Manufacture
  3. Propellants—Drying
- I. Geist, J. E.